



# DIPLOMARBEIT

Titel der Diplomarbeit

TERRA transcript expression in tumor cell lines and  
establishment of constructs for alteration of this  
expression

Verfasser

Christian Stern

angestrebter akademischer Grad

Magister der Naturwissenschaften (Mag.rer.nat.)

Wien, 2011

Studienkennzahl lt. Studienblatt: A 441

Studienrichtung lt. Studienblatt: Genetik/Mikrobiologie

Betreuerin: Univ.- Prof. Dr. Manuela Baccarini



This diploma thesis was performed at the

Medical University of Vienna  
Department of Internal Medicine I  
Institute of Cancer Research

and supervised by

A.o.Univ.Prof.Dr. Klaus Holzmann



## **Table of contents:**

Zusammenfassung	9
1. Abstract	11
2. Introduction	13
2.1. Telomere	13
2.1.1. Structure	13
2.1.2. Shelterins	16
2.1.3. Functions	17
2.1.4. Dysfunction of telomeres	20
2.1.4.1. Damage response	20
2.2. Cancer and telomeres	22
2.2.1. Telomere maintenance mechanism (TMM)	22
2.3. TERRA	26
2.3.1. TERRA transcription	27
2.3.2. Function of TERRA	27
2.3.2.1. Telomerase inhibition	28
2.3.2.2. Influence on heterochromatin	29
2.3.2.3. TERRA and development	29
2.3.3. Regulation of TERRA	29
2.3.3.1. Nonsense mediated decay (NMD) RNA decay	30
2.3.3.2. RNA interference	30
2.3.3.3. Cell cycle and TERRA	32
2.3.3.4. Mixed lineage leukemia (MLL) protein	32
3. Aims	33
4. Material and methods	34
4.1. Cell culture	34
4.1.1. Cell lines	34
4.1.2. Thawing cells	36

4.1.3. Passaging	37
4.1.4. Freezing cells	37
4.1.5. Cell line transfection	38
4.1.6. Cellcounter	39
4.1.7. Blasticidin dosage determination	40
4.1.8. Neutral red uptake	41
4.1.9. Fluorescent activated cell sorting (FACS)	42
4.1.10. GFP-FACS	42
4.1.11. Cell cycle FACS	43
4.2. Molecular biology	45
4.2.1. Bacteria	45
4.2.1.1. TOP10 Chemically Competent E. coli	45
4.2.1.2. DB3.1. Competent Cells	45
4.2.1.3. Conditions for bacterial growth	45
4.2.2. Cloning Methods	46
4.2.2.1. SEM-Transformation of bacteria	46
4.2.2.1.1. Producing competent cells	46
4.2.2.1.2. Transformation of bacteria	48
4.2.2.2. Plasmid DNA Isolation	49
4.2.2.2.1. STET Boiling Plasmid DNA Miniprep	49
4.2.2.2.2. Wizard® Plus SV Minipreps DNA Purification Systems	50
4.2.2.2.3. S.N.A.P.™ MidiPrep Kit	51
4.2.2.3. Determination of nucleotide concentrations	53
4.2.2.3.1. Nanodrop ND-1000 Spectrophotometer (PqLab)	53
4.2.2.3.2. Qubit® Fluorometer (Invitrogen, Fisher Scientific)	54
4.2.2.4. DNA-restriction	55
4.2.2.5. DNA-Ligation	55
4.2.2.6. Linker preparation	56
4.2.2.6.1. Linker dsDNA annealing	56
4.2.2.6.2. Linker DNA phosphorylation	57
4.2.2.6.3. Linker plus DNA plasmid ligation and transformation	57
4.2.2.7. Fill in and partial fill in of restricted DNA overhangs	58
4.2.2.8. Gel-extraction	59
4.2.2.9. Gateway cloning system	60

4.2.2.10. Plasmid constructs	62
4.2.3. RNA-Isolation by Trizol	63
4.2.4. Genomic DNA-Isolation by Trizol	64
4.2.5. Genomic DNA isolation by Maxwell® DNA Purification Kit	65
4.2.6. Complementary DNA-synthesis	66
4.2.7. Gel-electrophoresis	68
4.2.7.1. Agarose gel-electrophoresis	68
4.2.7.2. Polyacrylamid gel electrophoresis (PAGE)	70
4.2.7.3. RNA-agarose-gel	70
4.2.7.4. Visualisation	72
4.2.7.5. Marker	72
4.2.8. Real time polymerase chain reaction (Real Time-PCR)	73
4.2.8.1. Apparatus and Software for analyses	73
4.2.8.2. Gene expression and telomere length Real Time-PCR	74
4.2.8.3. 2p subtelomeric methylation specific RT-PCR	74
4.2.8.4. Primer design and in-silico validation	76
4.2.8.5. Primer sequences	76
4.2.8.6. Evaluation of Real-Time PCRs	78
4.3. Statistics	78
5. Results	80
5.1. Construction of TERRA expressing vectors	80
5.1.1. Sequencing of pSP73 with telomere fragment	85
5.1.2. Modifying pENTR/D/hH1-shNMP265	89
5.1.2.1. Elimination of SalI restriction site	89
5.1.2.2. Elimination of shNMP265 expression cassette	90
5.1.2.3. Insert new SalI restriction site with a linker into polymerase III expression cassette	91
5.1.3. Cloning the telomere fragment	93
5.1.3.1. pENTR/D/Linker antisense Tel	93
5.1.3.2. pENTR/D/Linker sense Tel	95
5.1.4. Creating promoter-less constructs	99
5.1.4.1. Promoter deletion	99
5.1.4.1.1. Deletion of hH1 in pENTR/D/Linker sense Tel	100

5.1.4.1.2. Deletion of hH1 in pENTR/D/Linker antisense Tel	100
5.1.5. Transfer telomere fragment into viral vectors	102
5.1.5.1. Gateway system	103
5.1.5.1.2. Producing recombinant adenoviral vectors	103
5.1.5.1.2. Producing recombinant lentiviral vectors	104
5.2. Pre-test for production of recombinant adenoviruses using HEK293 FT cells	105
5.2.1. Determining transfection efficiency of HEK293 FT by GFP transfection and FACS analyses	105
5.2.1.1. Optical valuation of transfection	105
5.2.1.2. FACS of GFP-transfection	107
5.2.2. Blasticidin dose determination	108
5.2.2.1. Optical estimation of blasticidin effects	108
5.2.2.2 Neutral-red uptake of blasticidin dosage determination	111
5.3. TERRA expression	112
5.3.1. Cell cycle FACS	112
5.3.1.1. Optical control of confluence	113
5.3.1.2. Cell cycle FACS analyses of cell line with different confluences	114
5.3.2. Confluence dependent total TERRA expression level	121
5.3.2.1. Best Keeper	121
5.3.3. Subtelomer specific TERRA-level	127
5.4. Relative telomere length by Real Time-PCR	131
5.5. Chromosome 2p subtelomeric methylation specific RT-PCR	134
6. Discussion	137
7. Curriculum vitae	142
8. Acknowledgment	145
9. Supplement	146
10. References	158



## **Zusammenfassung:**

Vor kurzem wurde entdeckt, dass Telomere in eine nicht-kodierende RNA genannt telomeric repeat containing RNA (TERRA) oder auch telomerische RNA (telRNA) transkribiert werden. TERRA fungiert als natürlicher Ligand und Hemmstoff für die Telomerase, dem Enzym das von ca. 85% der Tumorzellen verwendet wird, um Telomerlängen aufrecht zu erhalten und damit eine uneingeschränkte Anzahl von Zellteilungen zu ermöglichen. In der Literatur ist bekannt, dass unterschiedliche Promotoren für die Expression zuständig sind und das polyadenylierte und nicht-polyadenylierte TERRAs existieren, wobei nur die Nicht-polyadenylierte an den Chromosomenenden lokalisiert ist.

Der Transkriptionsstartpunkt von TERRA Transkripten ist in der subtelomerischen Region lokalisiert. Aus diesem Grund besteht auch ein Teil der TERRA Transkripte aus subtelomerischen Sequenzen.

Der Methylierungsgrad der subtelomerischen Regionen unterscheidet sich in verschiedenen Tumor Zelllinien. In einer unserer vorangegangenen Studien wurde der Methylierungsgrad der CpG Inseln der Chromosomenenden 2p TERRA Promoter Regionen von Saos-2 und T98-G mittels aufwendiger Bisulfit Konvertierung untersucht. Wir fanden eine CpG Position in dieser Promoter Region die sich in der Erkennungssequenz und Schnittstelle eines Restriktionsenzym befindet.

In meiner Studie wurden pENTR-Vektoren und anschließend adenovirale Vektoren mit Promotoren für verschieden RNA-Polymerasen, mit einem 0,8kb Telomer-Fragment in sense und antisense Orientierung produziert. Diese Vektoren dienen zukünftigen Expressions- und Inhibitorstudien.

Zell-Zyklus-FACS Analysen zeigten den Einfluss der Konfluenz auf den Zell-Zyklus Status und Real-Time PCRs den Einfluss der Konfluenz auf das TERRA Expressionslevel. Die untersuchten Telomerase negativen Zelllinien die ALT (Alternative lengthening of telomeres) assoziiert sind, zeigten im Vergleich mit den Telomerase positiven Zelllinien allgemein höhere TERRA-Werte. Ausserdem konnte bei allen Zelllinien ein Trend von erhöhter TERRA-Expression mit steigender Konfluenz ermittelt werden.

Chromosomenenden spezifische 2p, 18p, 10p und 10q TERRA Expression wurde mit spezifischen Primern gemessen und es wurden unterschiedliche Expressionslevels in den untersuchten Zelllinien gefunden.

Der neu entwickelte methylierungsspezifische Real-Time PCR Assay ermöglicht die Berechnung des Methylierungsgrades einer CpG-Insel im Chromosomenende 2p TERRA

Promoter. Wenn es möglich ist andere Loci wie diesen in anderen subtelomerischen TERRA Promoter Regionen zu finden, könnten weitere Assays entwickelt werden.

Die Erkenntnisse dieser Studie werden als Startpunkt für zukünftige Studien und Untersuchungen dienen. Die erstellten Konstrukte spielen eine wichtige Rolle um neue Erkenntnisse über TERRA-Expression, -Regulierung und -Funktion zu gewinnen und dienen vielleicht dazu neue Mechanismen der Telomerase Inhibierung und damit auch der Tumordinhibierung zu entwickeln.

## **1. Abstract:**

Recently it was discovered that telomeres are transcribed into a non-coding RNA called telomeric repeat-containing RNA (TERRA) or telomeric RNA (telRNA). TERRA acts as a natural ligand and inhibitor of telomerase, the enzyme that is used by about 85% of tumor cells to maintain telomere length, which allows an unlimited number of cell divisions. In the literature it is known that different promoters are responsible for TERRA-expression and that non-polyadenylated and polyadenylated TERRAs exist, but only non-polyadenylated is localized at chromosome ends.

The transcription start point of TERRA transcripts is localized in the subtelomeric region. For this reason, parts of TERRA transcripts are subtelomeric derivation.

The methylation levels of subtelomeric regions differ in several tumor cell lines. In our previous study, methylation levels of CpG islands of chromosome end 2p TERRA promoter region of Saos-2 and T98-G were examined, by the laborious technique of bisulfite conversion. We found a CpG position in this promoter region, located in the recognition and cutting site of a restriction enzyme.

In my study, pENTR vectors and then adenoviral vectors were produced with promoters for different RNA polymerases and with a 0.8kb telomere fragment in sense and antisense orientation. These vectors serve for future expression and inhibitor studies.

Cell cycle FACS analysis showed the influence of confluence on cell cycle state and Real-time PCR the effect of confluence on TERRA expression level. The investigated telomerase negative cell lines which are associated to ALT (alternative lengthening of telomeres), showed, in comparison to telomerase positive cell line generally higher TERRA levels. Also in all cell lines a trend of increasing TERRA expression by increasing confluence could be determined.

Chromosome end specific 2p, 18p, 10p and 10q TERRA expression levels were measured using specific primers and determined levels differ in the examined cell lines.

The newly developed methylation-specific Real-time PCR assay allows calculations of methylation grade of a CpG island of chromosome end 2p TERRA promoter. Perhaps it is possible to find other loci such as those in other subtelomeric TERRA promoter regions and to develop additional assays.

The findings from this study will serve as a starting point for future studies and investigations. The generated constructs play an important role to new insights into TERRA-expression,

regulation and function and perhaps serve to develop new mechanism of telomerase inhibition and hence tumor inhibition.

## **2. Introduction:**

### **2.1 Telomere:**

Telomeres are the physical ends of chromosomes (Figure 2.1.). First proclaimed and named by Herman Muller 1938[1], who described them in *Drosophila melanogaster*. He already knew that a chromosome cannot exist without telomeres. The structure and function of telomeres are highly conserved in eukaryotes [2].

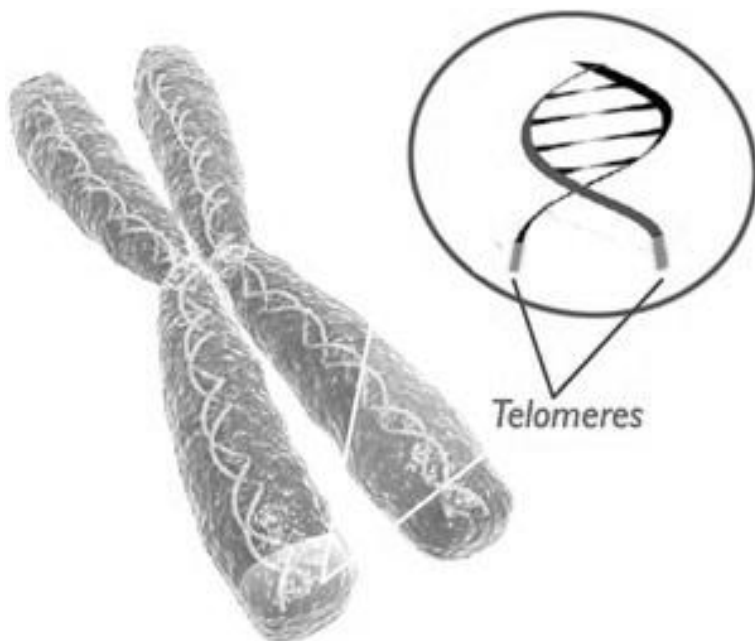


**Figure 2.1.: Telomeres:** Schematic representation of karyotype chromosomes with shown localization of telomeres. Scheme taken from [3].

#### **2.1.1. Structure:**

Telomeres consist of DNA-repeat sequences which are the same in all vertebrates. In vertebrates this exists as a repeated sequence of 6 nucleotides 5'-TTAGGG-3' built up as a double strand (ds) DNA with a length of a few thousand base pairs (bp) (Figure 2.2.) [4].

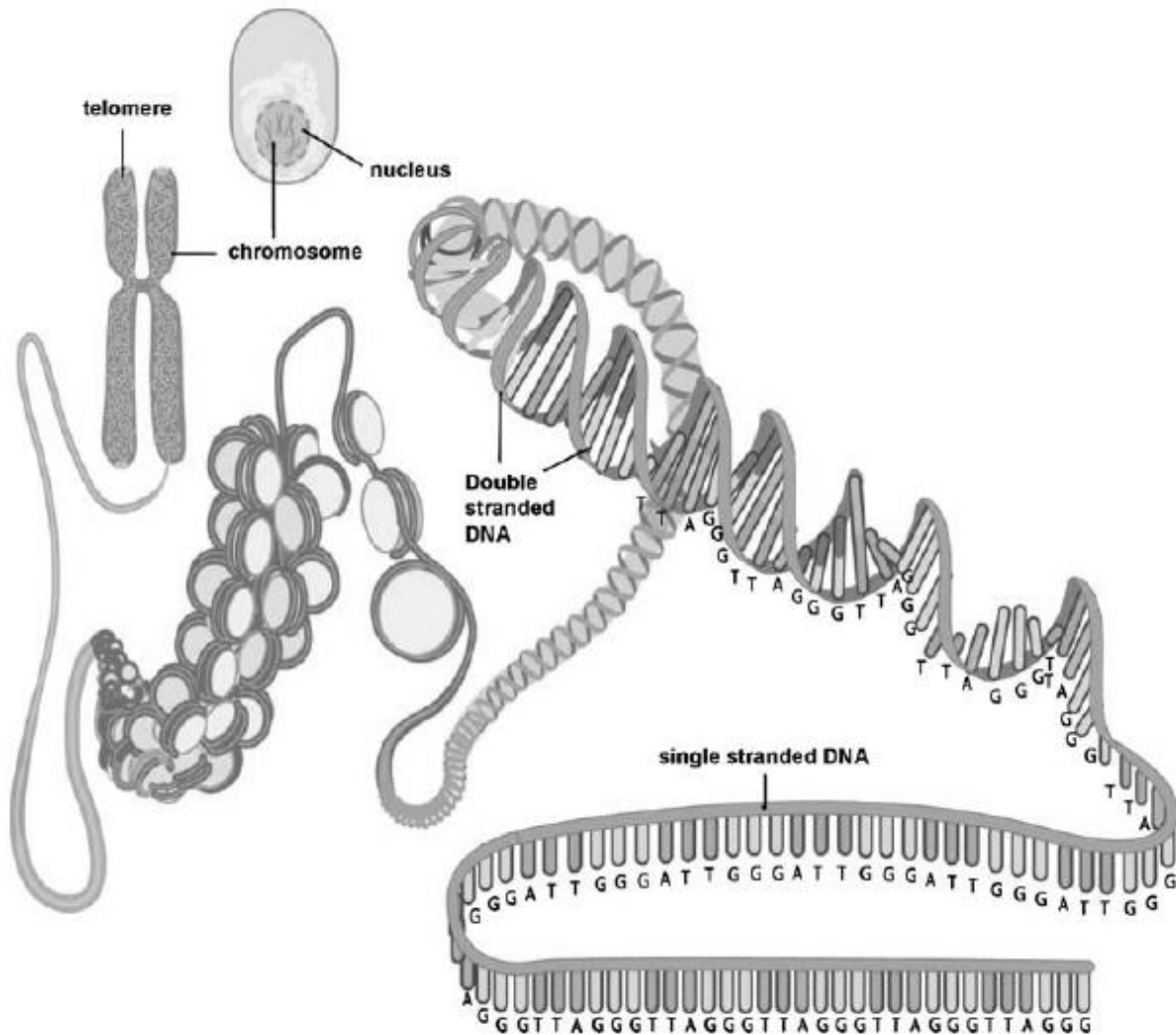
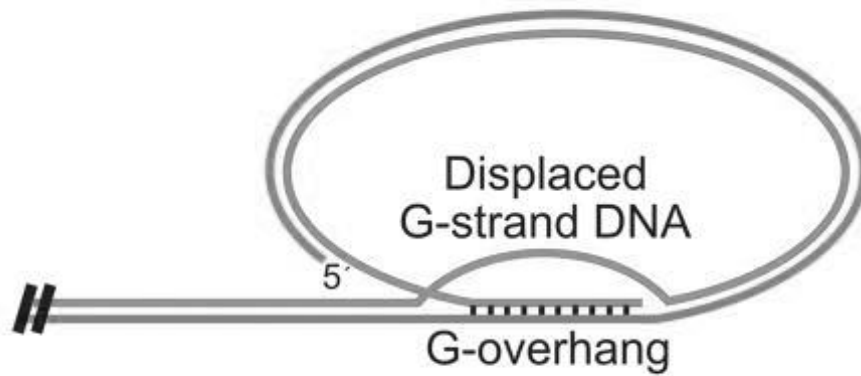


**Figure 2.2.: Telomeres are located at the ends of the linear chromosomes and consists of TTAGGG repeats in human:** Schematic representation of chromosomal and telomere assembly. Chromosomes which are located in the nucleus are dsDNA which get their constitution by wrapping around histones. At the end of chromosomes (telomeres) the DNA are only single stranded. Schema taken from [5].

The two telomeric DNA strands called G-rich strand for the one with 5'-TTAGGG-3' repeats and C-rich strand for the one with the reverse complement 5'-CCCTAA-3' repeats. Structurally important, the telomeric dsDNA ends with a telomeric single strand (ss) DNA sequence (Figure 2.2.) The G-rich strand has a 3' overhang, the so called G-tail which forms a loop called telomere loop (t-loop). The ssDNA G-tail strand invades the dsDNA and binds to complementary sequences of C-rich strand (Figure 2.3.). The displaced former dsDNA forms a loop called displacement loop (d-loop) [6, 7]. These loops have an important function for

protecting chromosome ends because they enable two possible conformations of telomere ends (Figure 2.3.).

### A. Closed T-loop conformation



### B. Open conformation

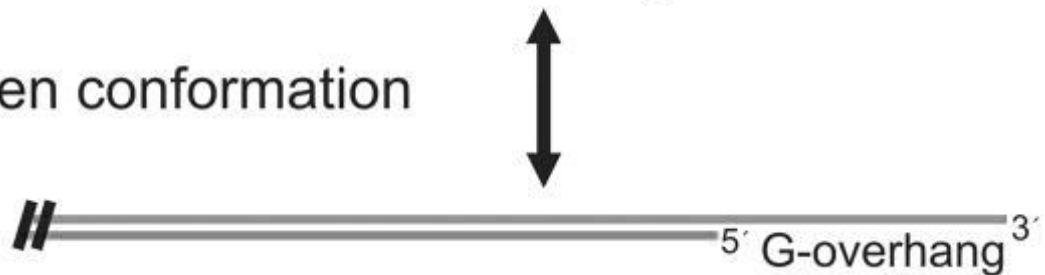


**Figure 2.3.: Telomere cycling between (A) closed and (B) open conformations.**

A: Closed T-loop conformation: G-overhang invades double stranded telomeric DNA and builds T-loop (telomeric loop) and D-loop (displacement loop)

B: Open conformation with 3' G-overhang

Schema taken from [8].

Human telomeric DNA is not presented as classical linear dsDNA with helix structure. The telomeric repeats form hybrid-type intramolecular G-quadruplex structures with mixed parallel/antiparallel strands (Figure 2.4.) [9]. This special structure stabilizes telomeric DNA and blocks telomerase activity [10].

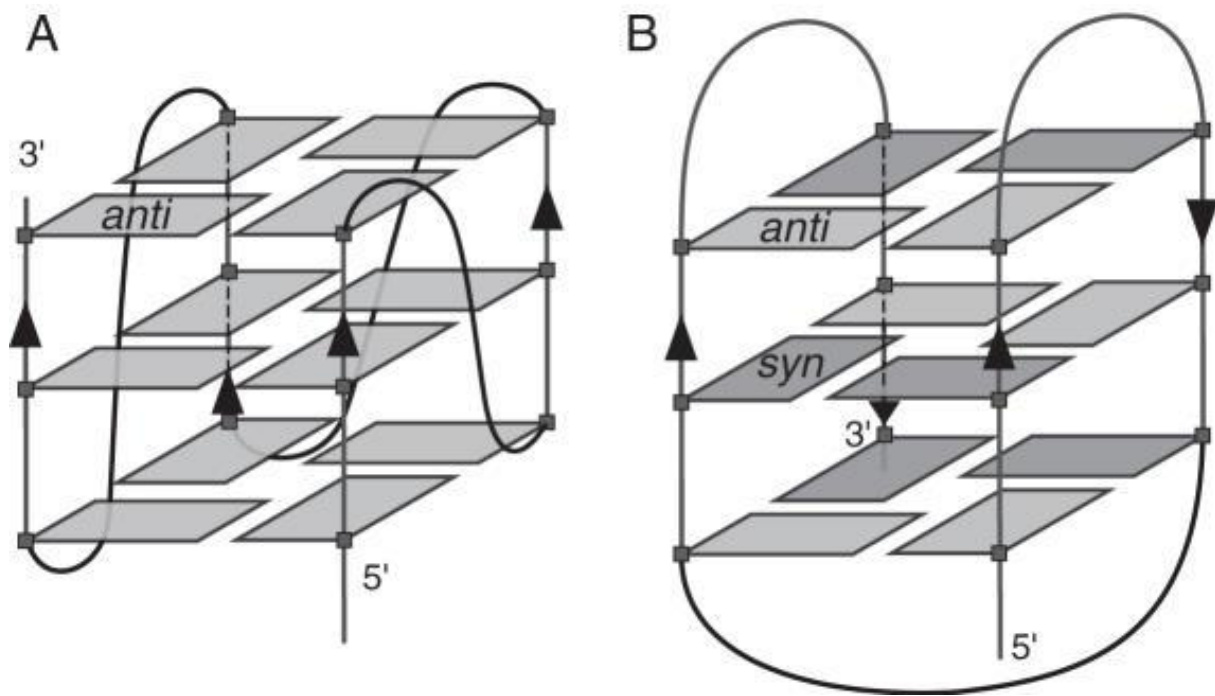


**Figure 2.4.: Schema of hybrid-type intramolecular G-quadruplex structures with mixed parallel/antiparallel strands:**

(A): Telomere forms propeller-type parallel-stranded intramolecular G-quadruplex with anti-parallel (anti) strands found in the presence of potassium in crystalline state.

(B): Telomere forms second Basket-type with both parallel (syn)/antiparallel (anti) strands. This intramolecular G-quadruplex structure was reached in sodium solution determined by NMR (nuclear magnetic resonance) spectroscopy.

Arrows show direction of DNA (5' to 3'). Schema taken from [9].

The telomeres within cells consist not only of telomeric DNA, but also of proteins that are capable to bind and are found associated with telomeres. Biochemical purification of the telomeric proteome mentioned 210 proteins that interacts with telomeric structure and also may influence them [11]. The most important proteins in mammalian are 6 proteins, which together are called shelterins.

### **2.1.2. Shelterins:**

The whole telomere is coated by a multiprotein complex called shelterins which protects and stabilizes mammalian telomeres, as described in the following text [12]. It consists of six proteins, TRF1 (Telomeric Repeat binding Factor 1), TRF2, RAP1 (Repressor/Activator



Protein 1), TIN2 (TRF1 INteracting protein 1), TPP1 (TINT1/PIP1/PTOP 1) and POT 1 (Protection Of Telomeres 1) (Figure 2.5.).

TRF1 and TRF2 bind constitutively at dsDNA telomeric repeats and recruit the other four shelterin proteins [12]. It was also shown, that TRF1 has DNA remodeling activity [13, 14] and promote efficient replication of telomeres [15]. TRF2 plays a role at t-loop formation [16] and chromosome end protection [17]. A recent study proclaimed that there is also an influence on chromatin formation [18].

RAP1 is not well characterized but it's an important factor for telomere protection and could be necessary for TRF2 telomeric localization and stability [19].

TIN2 functions as bridge between TRF1, TRF2 and TPP1 and has no DNA binding domain. It's important for stabilizing the whole shelterin complex [20, 21].

Another connecting function has TPP1 that produces a bridge between POT1 and TIN2 [22]. TPP1 forms a heterodimer with POT1 and interacts with telomerase and might influences recruitment or regulation [23, 24]. High affinity of POT1 to the single stranded overhang leads to the assumption, that it might bind to the displaced G-strand and stabilize loop structure.

The shelterin complex has a very important function for building the t-loop and thereby for capping the ends of chromosomes (Figure 2.5.). Uncapping of telomeres leads to double strand breaks, non-homologous end-joining (NHEJ) and erosion of telomeres. This may inactivate different pathways like ATM, p53, and p21CIP1 and may result in senescence or/and apoptosis. p16/INK4 could also play a role, but this hypothesis has not yet been fully investigated [25-27].

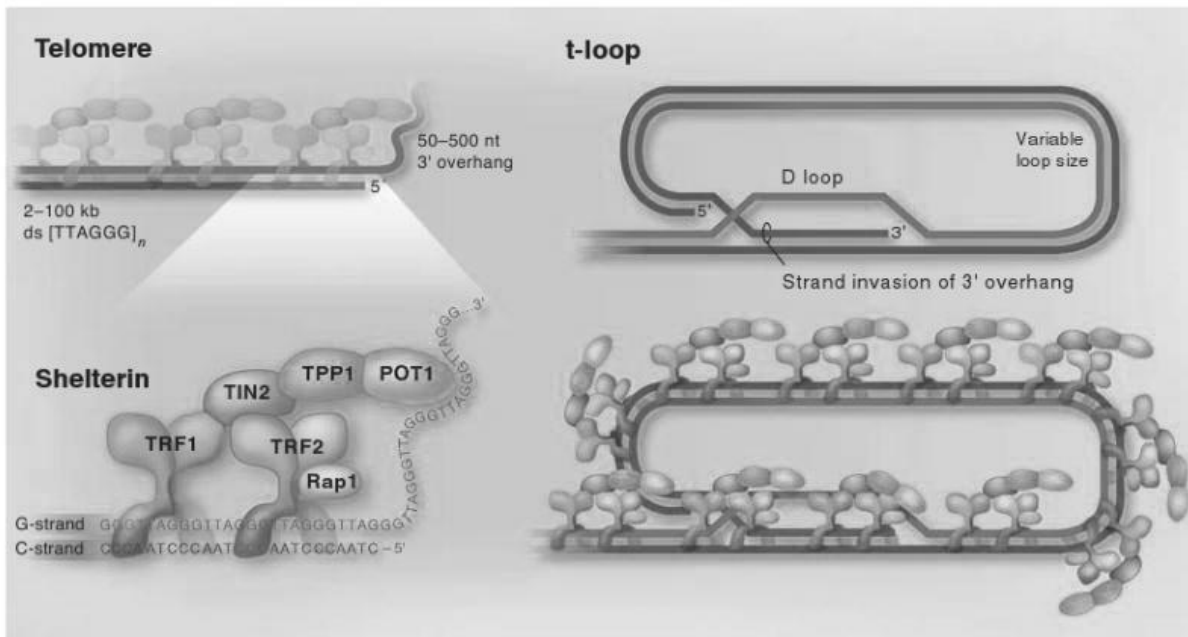


**Figure 2.5.: Telomere Structure:** Mammalian telomeres are long repeats of 5'-TTAGGG-3' repeats and telomere associated proteins, the 6 most important are called shelterins (upper left). The shelterin complex binds specific to telomeric DNA (lower left) and is composed of TRF1 and TRF2 which bind double stranded telomeric DNA, POT1 which binds to single stranded telomeric sequence. Rap1 binds to TRF2 and TIN2 and TPP1 connect TRF1 and TRF2. Telomeres build a loop which is called t-loop and a loop which is called d-loop (upper right). By invasion of single stranded telomere overhang into double stranded telomeric DNA these two loops are formed. This whole structure is associated which shlelterins (lower right). Schema taken from [28].

### 2.1.3. Functions:

Telomeres play an important role for chromosome stability [25]. They protect the end of chromosomes from erosion, recombination and recognition as damaged DNA and end-to-end fusion with other chromosomes. Due to the end-replication problem every cell cycle chromosomes get shorten 50-100 bp. This shortening was first discovered by James Watson [29] and already before he developed his hypothesis Hayflick investigated that human cells derived from embryonic tissues are not able to divide infinitely. He suggested a dividing potential of 50 times and this became known as Hayflick limit [30]. The reason for this shortening is the DNA polymerase, which is not able to synthesis a full, new strand (Figure 2.6.). The strand which is not constantly synthesized is called lagging strand. The replication starts a few times and these parts become connected. For every start a new start point is

necessary which is created by primase. This start point is an RNA fragment and has to be eliminated by RNase H. The occurring cavity gets filled up and connected by the enzyme ligase. At the 3' end of the newly synthesized strand there is no possibility to fill this cavity, which results in the DNA becoming shorter with every replication. Telomeres function, so to say, as buffer to save important coding genomic DNA sequences [31, 32].

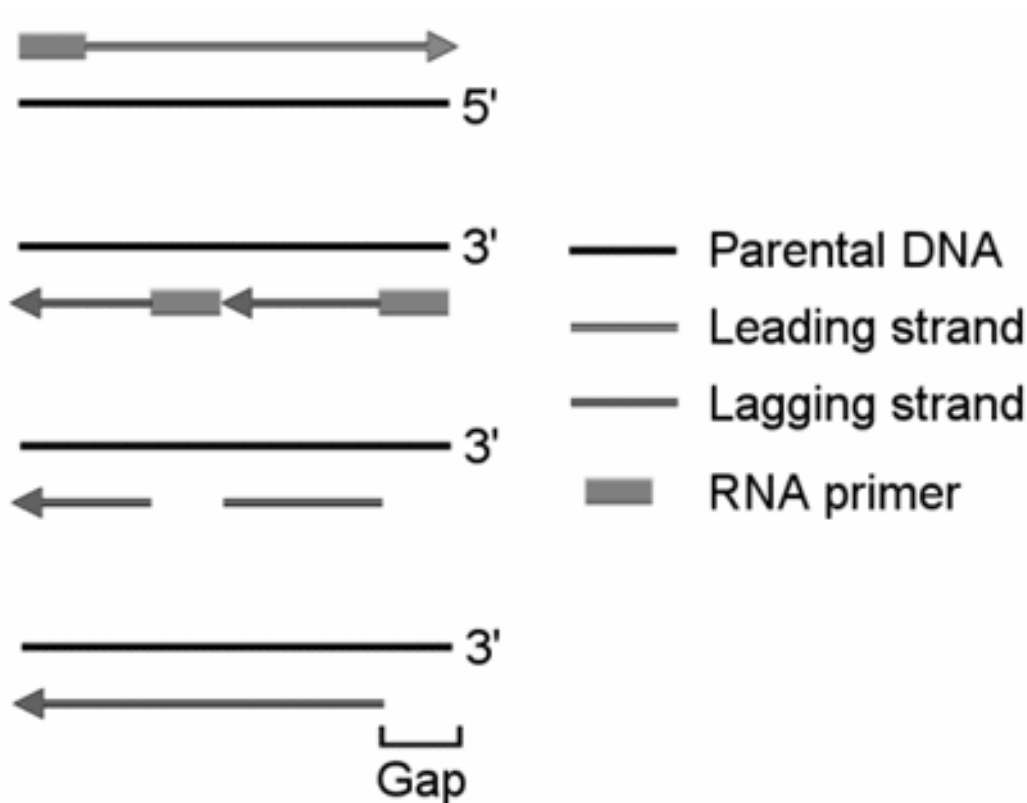


**Figure 2.6.: End-replication problem:** At DNA replication two new strands are synthesized in 5'-3' direction. One new strand could be synthesized without an intermission (leading strand). The other synthesis has to start a few times and these synthesized DNA parts are called Okazaki fragments and have to be connected. DNA polymerase needs for every synthesis start an RNA primer which is depleted after synthesis initiation. This leads to the end-replication problem. As synthesis is only possible in the 5'-3' direction the last part of a 5' end of new strands where RNA primer binds were not able to be synthesized. Schema taken from [33].

#### **2.1.4. Dysfunction of telomeres:**

If telomeres can no longer exert end protective functions they are called dysfunctional. One of the most important dysfunctions of telomeres is the end-replication problem, which leads to the shortening of telomeres. If a critical length is reached, this results into replicative senescence or apoptosis [31, 32]. Senescence or apoptosis is not initiated because of the short length, but rather because of the altered structure [34].

Also direct damage of telomeres can affect the function of telomeres. Mainly direct damages are produced by cellular stress, for instance oxidative stress which is the major source of DNA damages or by mutations of genes related to telomere associated proteins [35, 36]. These damages influence telomere length and integrity and can lead to senescence and/or apoptosis.

##### **2.1.4.1. Damage response:**

Dysfunctional telomeres are examined like DNA damages and, consequentially, like DNA double strand breaks (DSB). The reaction to these damages is a DNA damage response.

Telomeres become marked with phosphorylated H2AX ( $\gamma$ -H2AX), a variant of histone H2A that localize to sites of DNA damage. A method for detecting dysfunctional telomeres is based on fluorescence called telomere-dysfunction induced foci (TIF) [37]. Also other proteins are located at dysfunctional telomeres like DNA damage inducible kinases ataxia telangiectasia mutated (ATM), ataxia telangiectasia- and Rad3-related (ATR), DNA-dependent protein kinase DNA-PK, CHK1 and CHK2 also the RMN complex and the BRCT motif proteins MDC1/NFBD1 and 53BP1 [26, 38-41]. This composition is similar to that at DNA double strand breaks.

Dysfunctional telomeres are a high risk factor for organism. Like irreparable DNA damages they can enhance developing of tumors. Because of this such cells go into senescence or apoptosis as tumor suppression mechanism. Cells which go into apoptosis die and cells which go into senescence stay into a G1 cell cycle arrest and stop proliferating [42].

To enforce this ways of self-protection for the organism p53 and p16 plays an important role. Both of them suppress the cancer genesis and can induce senescence or apoptosis [43-45] (Figure 2.7., p16 not shown in figure). p53 is a transcriptional regulator which influences cell

cycle and is able to activate or represses genes in response to stress [45]. These genes induce a DNA repair mechanism, which leads to senescence or programmed cell death. Which mechanism is enhanced depends on cell type, degree and type of damage [46]. Under normal conditions p53 is bound to the negative regulator Mdm2. which under cellular stress p53 becomes phosphorylated and active [47]. p16 which acts through the p16/Ink4a RB pathway is also a cell cycle regulator and stabilize p53 [42].

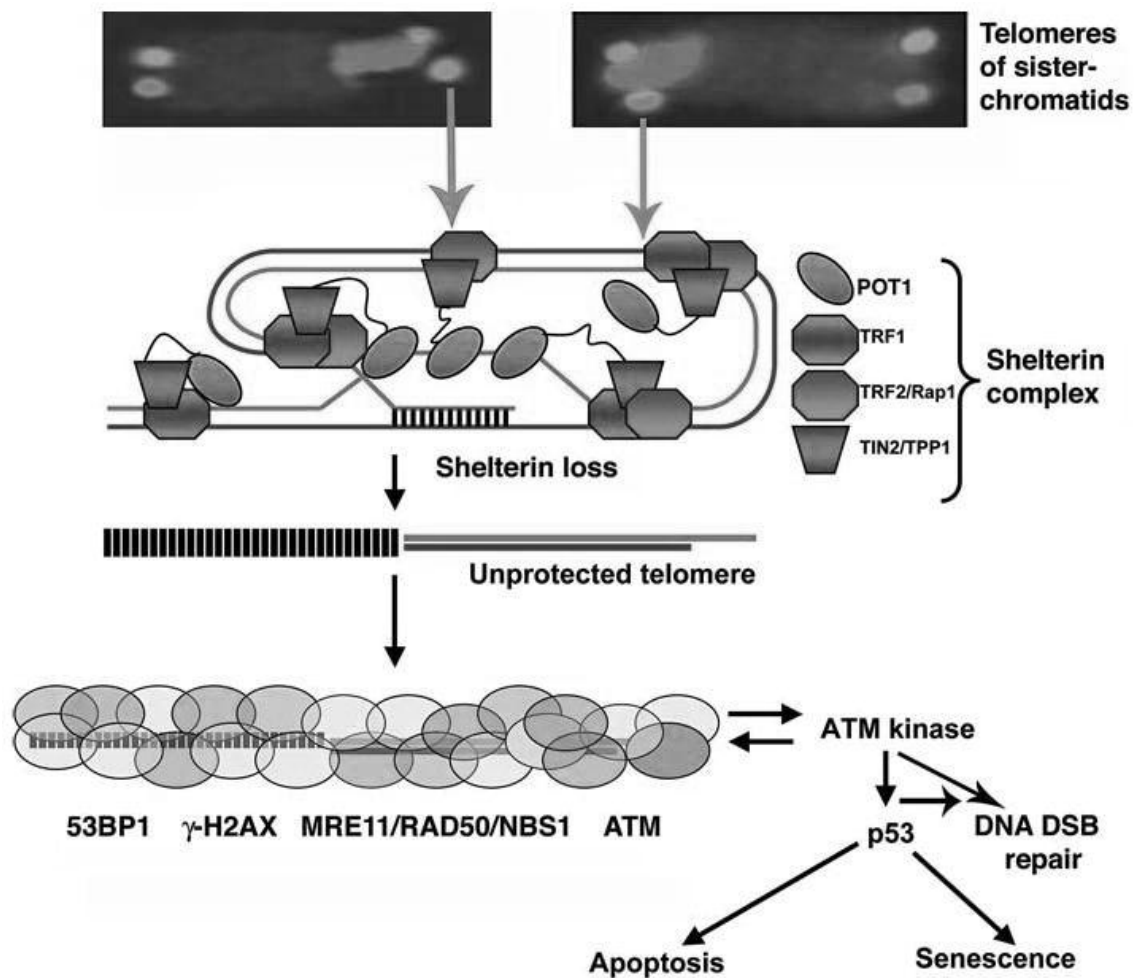


**Figure 2.7.: DNA damage response at dysfunctional telomeres:** The shelterin complex covers and protects telomeres. This complex is composed of 6 subunits (TRF1. TRF2. POT1. Tin2. TPP1 and Rap1). Cause for loss of these proteins is not wholly clear, however it leads to unprotected telomeres and in a row to DNA damage response signaling. This includes p53 binding protein 1 (53BP1) which acts as a transcriptional co-activator of the p53 tumor suppression [48],  $\gamma$ -H2AX a phosphorylated H2AX variant of histone 2A [37], MRN complex (MRE11/RAD50/NBS1) [49] which acts as activator for ATM (in absence of ATM, ATR kinase is activated) [26]. ATM kinase leads to DNA double stand break repair or with p53 to senescence or apoptosis. Schema taken from [50].

## **2.2. Cancer and telomeres:**

The potential of dysfunctional telomeres to initiate cancer development are inhibited by p53 and p16 function [42, 44, 45]. Tumor cells have to overcome this suppressing mechanism. Even p53 and/or p16 are eliminated by mutations or suppressing mechanism, tumor cells have to protect and maintain their telomeres. Otherwise the unregulated and advanced proliferation of tumor cells would lead to shortening of chromosomes and, as consequence, to the loss of genetic information. To prevent this, tumor cells have to develop a telomere maintenance mechanism.

### **2.2.1. Telomere Maintenance Mechanism (TMM):**

Tumor cells need the ability to maintain their telomeres, otherwise they would not be able to reach a state of immortality with unlimited proliferation. Today, two mechanisms in tumor cells are known.

About 80-85% of tumor cells use the function of telomerase [51]. Telomerase is a ribonucleoprotein complex which acts as reverse transcriptase and adds TTAGGG repeats at the end of chromosomes [52] (Figure 2.8.). The catalytic subunit called TERT (telomerase reverse transcriptase) forms a dimer, which is connected with a RNA component called TR or TERC (telomerase RNA) which acts as template for the ssDNA TTAGGG repeats. The complementary strand is then synthesized by DNA polymerases. Another part of telomerase is dyskerin which binds and stabilizes TERC [53].

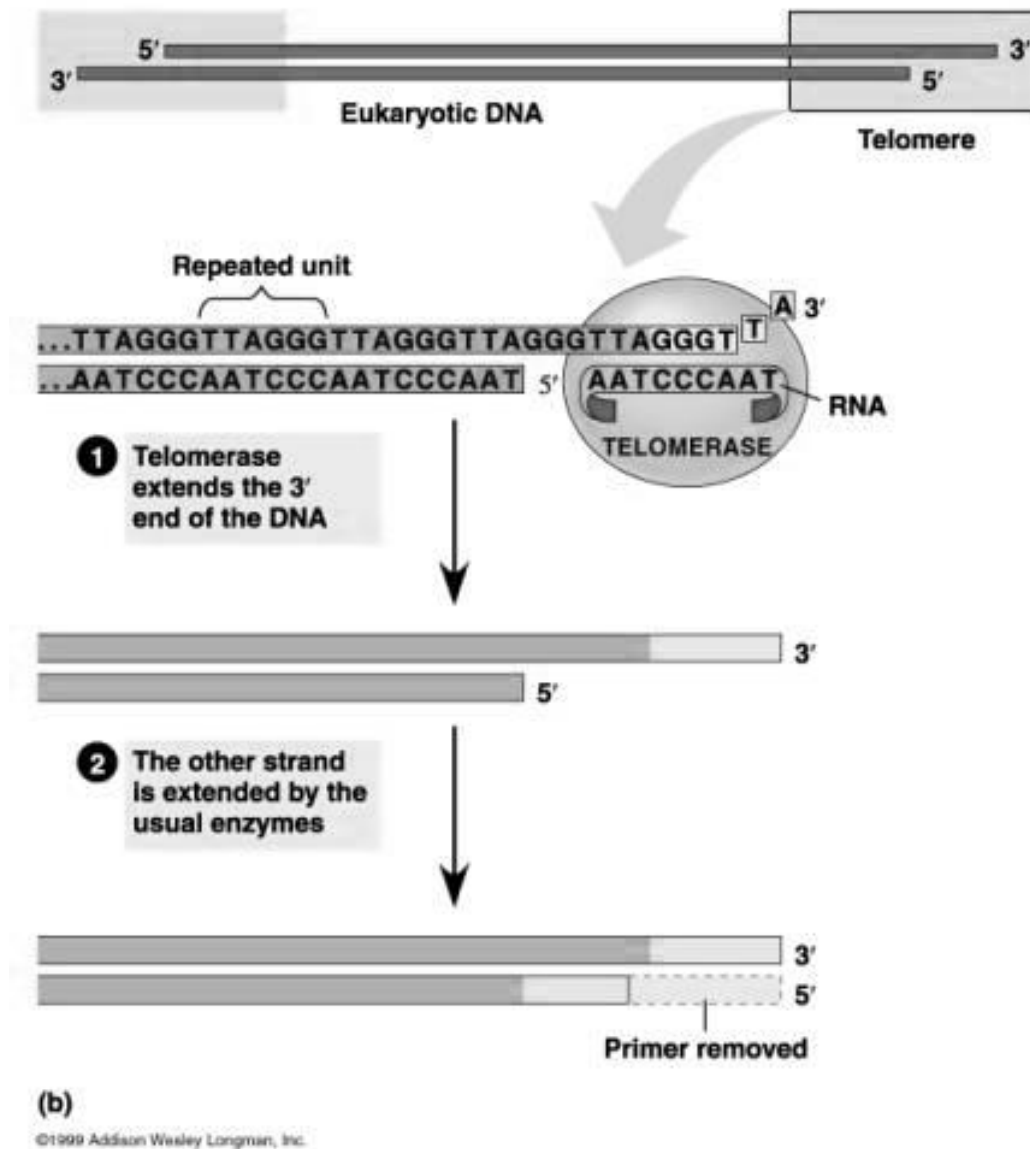


**Figure 2.8.: Action of telomerase:** Chromosome ends have a 3' end overhang on the leading strand. Telomerase bind to the overhang, the RNA component TERC binds to the complementary sequence of the single strand. Part of TERC acts as template and the catalytic subunit (TERT) adds bases to the 3' end. The complementary strand is synthesized by DNA polymerases. Schema taken from [54].

At least 15% of tumor cells express and use no telomerase for telomere maintenance but rather a mechanism called Alternative Lengthening of Telomeres (ALT) [55]. ALT shows some special features that are not present in telomerase positive cells or normal somatic cells.

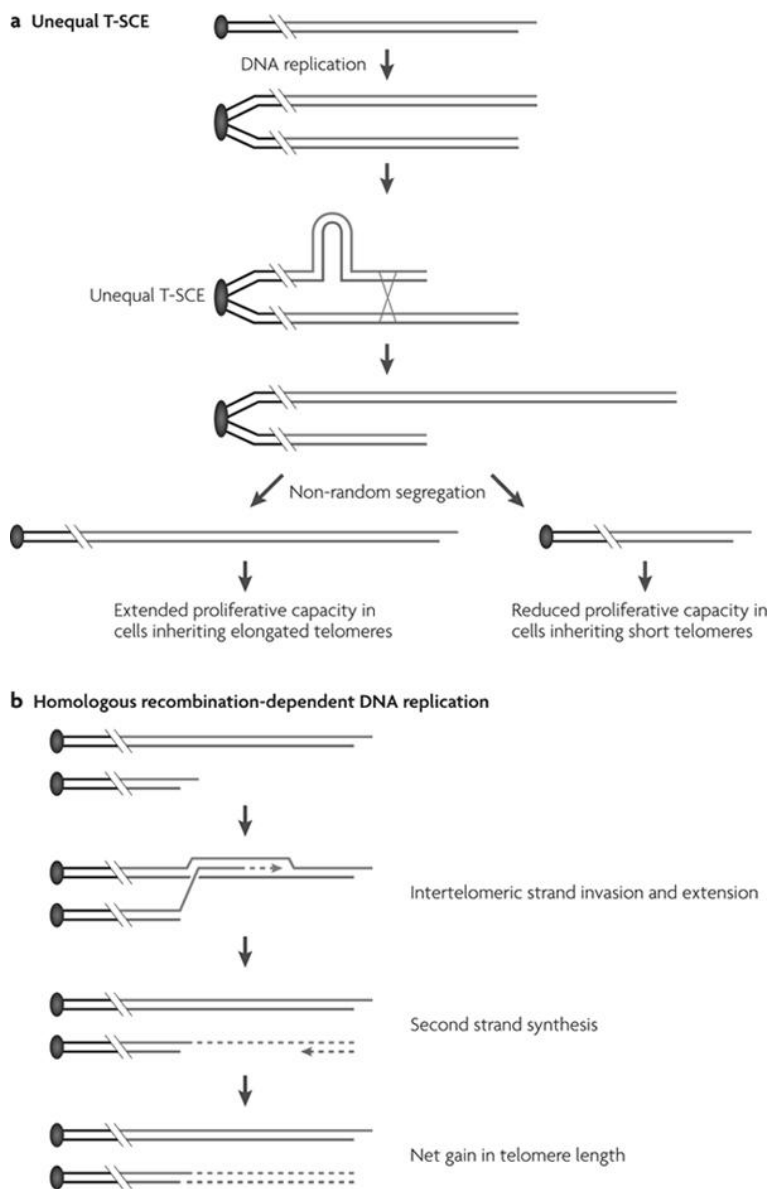
Extrachromosomal telomeric DNA is present in the forms of double stranded telomeric circles (T-circles) and single stranded C-circles, depending on C-rich strand [56, 57]. T-circles, which are derived from recombinations, are also detectable in telomerase positive cells if telomeres are elongated [58, 59]. Unique features are the C-circles, the derivation of which is unclear, but they seem to be markers for ALT positive tumor cells [60]. Telomeric DNA and associated binding proteins are found in promyelocytic leukaemia nuclear bodies (PML nuclear bodies). PML nuclear bodies are spherical structures which are associated with several functions, including DNA repair, senescence, apoptosis, viral defense, proteolysis and stress response, and which is named after one of its constitutive components, promyelocytic leukaemia (PML) protein. If these bodies include telomeric DNA they are called ALT-associated PML bodies (APBs) [61]. ALT positive cells also show a very heterogeneous telomere length that ranges from undetectable to over 50kb, perhaps due to recombination events [62].

The mechanism of telomere elongation is uncertain. Two models are proposed today, the unequal telomere sister chromatid exchange (T-SCE) model and the homologous recombination-dependent DNA replication model (Figure 2.9.). These models are not mutually exclusive.

T-SCEs occur much more frequently in ALT cells than in telomerase-positive cell lines or normal cells [63]. This strengthens the hypothesis that one daughter cell with a lengthened telomere and one with a shortened telomere can arise provided there is a mechanism for segregating chromosomes with lengthened telomere into one and chromosomes with shortened telomere into the other cell [64].

The second and more favored model, the homologous recombination-dependent DNA replication model new telomeric DNA is synthesized by an existing telomeric sequence from an adjacent chromosomal telomere as a copy template. The template has not to be the telomere of another chromosome. Possibilities include copying itself via t-loop formation, sister chromatid as template, linear extrachromosomal DNA as template or rolling circle mechanism with c-circles as template [65].





Nature Reviews | Genetics

**Figure 2.9.: Models of ALT mechanism:** Two models of ALT are proposed. a) Unequal T-SCE (telomere sister chromatid exchange): After DNA replication re-combination between sister chromatids happens and results in two different daughter cells. One with elongated telomeres with an increased proliferation capacity and the second one with shortened telomeres and decreased proliferation capacity. To reach an unlimited proliferation of the cell population it is necessary that a mechanism segregate longer elongated telomeres into one cell and shortened in the other cell. This mechanism is not yet known. b) Homologous recombination-dependent DNA replication: The second proposed mechanism hypothesizes the existing telomeric DNA is used with a recombination-mediated synthesis to add telomeric DNA at telomeres. The donor of this telomeric DNA can either be sister chromatids, linear extrachromosomal DNAs, rolling circle mechanism with c-circles or the DNA itself via t-loop formation. Schema taken from [66].

Telomerase activity and ALT do not have to be exclusive. Evidences for activity of both mechanisms in the same cells exist and also small numbers of tumors express telomerase and simultaneously show markers for ALT [67].

### **2.3. TERRA:**

For a long time telomeres were seen as heterochromatic region because of heterochromatic marks as trimethylation at lysine 9 on histone H3. trimethylation at lysine 20 on Histone H4. histone hypoacetylation, association of heterochromatinprotein 1 (HP1) and hypermethylation of cytosines of CpG islands present in the subtelomeric region [68, 69]. A position effect was also noticeable by the fact that genes nearby can be transcriptional silenced [43]. Because of these heterochromatic marks and the geneless nature of telomeres, telomeres were seen as transcriptional silence.

A few years ago it was found that mammalian telomeres are transcriptional active. A non-coding RNA is transcribed called TERRA (telomeric repeat containing RNA) or telRNA [70, 71].

TERRA consists of UUAGGG- repeats of the telomeric DNA, but it also contains a part of subtelomeric DNA that becomes transcribed. Promoters for TERRA could be identified in the subtelomeric region and seem to be located not more than 1kb upstream of telomeric sequence [72]. In-silico analyze with these promoter elements predicts that half of the subtelomeres may be transcriptional active and express chromosome specific TERRA (see supplement information of [72]).

The length of TERRA transcripts is seen as very heterogeneous with size up to some thousand nucleotides (nts) [70, 71]. A new study has shown that the length of telomeric repeat of TERRA, the UUAGGG-repeats, is only about 200 nts [73]. This indicates that most of TERRA sequences originate from the subtelomeric parts of individual chromosomes.

Telomeric RNA is highly conserved. It not only exists in human, it was also found in several eukaryotes, including yeasts, birds, fishes, plants and mammals [70, 71, 74, 75].

### **2.3.1. TERRA transcription:**

Investigation has shown that many subtelomeres exhibit a conserved repetitive region in a centromere to telomere direction. This repetitive region includes a 61bp repeat, a 29 bp repeat and a 37bp repeat, together called 61-29-37 repeats. Two of them, the 29bp and the 37bp repeats form a CpG dinucleotide rich DNA island. Such CpG islands are associated with many mammalian RNA polymerase II promoter sequences. In silico analysis and in situ hybridizations detecting at least 20 human chromosome ends with this 61-29-37 repeats and so on potential start points for TERRA transcription [72]. These promoters are heavily methylated by DNA-methyltransferases (DNMTs). Studies showed double knock out of DNMT1 and DNMT3b in human tumor cells leads to hypomethylation of TERRA promoter and in succession to increased TERRA levels [76].

Because the starting point is located in the subtelomeric region, the longest part of TERRA molecules may consists of subtelomeric sequences [72, 73]. TERRA is largely transcribed by RNA polymerase II. Experiments showed that RNA polymerase II is associated with human telomeres and with TRF1 [71]. About 7% of TERRA transcripts are 3'end polyadenylated like most of RNA polymerase II transcripts. Treatment with  $\alpha$ -amanitin, a specific RNA polymerase II inhibitor reduces TERRA level extremely. But actinomycin D treatment, which is a general transcription inhibitor, reduces TERRA level more than  $\alpha$ -amanitin. This may be an indicator that another polymerase (RNA polymerase I or RNA polymeras III) is also used to transcribe TERRA [70, 71]. The 5' end of TERRA contain 7-methylguanosine cap structures which together with the poly(A) tail contributes to their stability. A very interesting discovery was that only not polyadenylated TERRA is associated with chromatin [73]. The reason for the different distribution is unclear, maybe different localization signals exist at the end of polyadenylated and not polyadenylated TERRA.

### **2.3.2. Function of TERRA:**

TERRA was discovered recently and only a limited amount of original research reports are available. Therefore, functions and effects of TERRA are not fully identified.

### **2.3.2.1. Telomerase inhibition:**

The amount of TERRA is very low at telomerase positive tumor cells. Normal somatic cells and ALT tumor cells however possess a high TERRA expression level [77]. In vitro reconstituted telomerase and synthetic TERRA molecules showed the inhibitory function of TERRA on telomerase. A new study showed that TERRA binds to enzymatic subunit TERT and acts as a natural ligand and inhibitor of human telomerase [78]. How this exactly occurs has not yet been investigated, but there are currently three models suggested (Figure 2.10.).

The first model states that TERRA prevents access of telomerase to telomeres by binding telomere-proximal telomerase molecules. The second model states that TERRA is bound to telomeric heterochromatin and sequesters telomerase and inhibits possibility to access 3' end of telomere. The third model states that TERRA binds to telomerase which is then bound to telomeric chromatin and inhibits the possibility of telomerase to access 3' end of telomere.

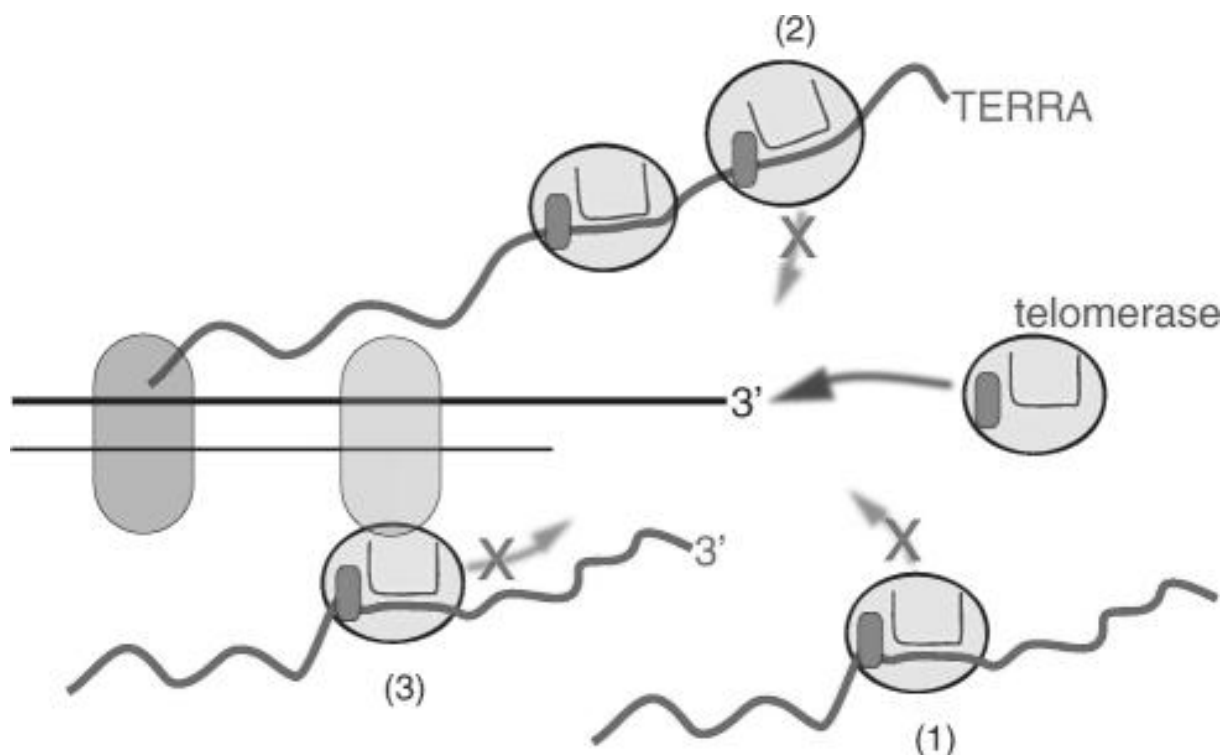


**Figure 2.10.: Possible actions of telomerase inhibiting by TERRA:** TERRA interacts with TERT and also base pairs with the RNA TERC. Today there are three possible models of interaction. (1) TERRA binds telomerase without connection to telomeres. (2) TERRA, binds to telomeric chromatin (gray oval) and then binds and sequesters telomerase. Access and action of telomerase telomere end is inhibited. (3) TERRA interacts with telomere-bound telomerase (gray oval) and inhibits access to 3' end. Schema taken from [78].

### **2.3.2.2. Influence on heterochromatin:**

Large non-coding RNAs (ncRNAs) have the ability to influence heterochromatic state by recruiting chromatin remodeling complexes. One example is Xist which is necessary for X chromosome inactivation in females during embryogenesis. Similarities between Xist and TERRA implicate a possible function of TERRA in maintaining a heterochromatic state at chromosome ends.

TERRA is also co-localized at the distal telomere of the inactivated X chromosome in female mouse embryos [79]. It seems that this localization does not correlate directly, as the localization of TERRA does not depend on Xist expression.

### **2.3.2.3. TERRA and development:**

TERRA may be regulated developmentally, which induces the assumption that it plays a role during development and for chromosomal transactions occurring during cellular differentiation [71, 79, 80]. It also can be found in undifferentiated embryonic stem cells (ES cells). There it's been associated with X and Y chromosome of males and both X chromosomes of females. During differentiation this changes as only inactivated X chromosome of females and Y chromosomes of males are connected with TERRA [79]. Another analogy of TERRA and Xist is that both are controlled by nonsense mediated RNA decay [81, 82].

TERRA also occurs during reprogramming. Experiments with differentiated fibroblasts which are induced to become pluripotent stem cells with the reprogramming factors Sox 2, c-myc, Klf 4, and Oct 3/4 showed an increase in TERRA [80, 83]. Why this increase in TERRA levels occurs is not yet clear. It is speculated by the authors that one or few of the reprogramming factor acts as transcriptional regulator or that some other mechanism during differentiation and reprogramming enhance TERRA expression.

### **2.3.3. Regulation of TERRA:**

The whole, complex regulation mechanism of TERRA expression and maintenance is not fully understood today. Some correlations have been investigated and have given a brief insight into the TERRA regulation mechanism.

### **2.3.3.1. Nonsense mediated decay (NMD) RNA decay:**

Nonsense mediated decay is a highly conserved cellular mechanism in eukaryotes [84]. After transcription, pre-mRNA is marked by ribonucleoprotein components and then processed. Introns get cut out and exons get connected to mRNA which is called splicing. The exon-exon-border stay marked with protein complexes, called exon-junction-complex. During first translation round (pioneer round) these protein complexes are removed and a stop-codon terminates translation and activates termination factors. Because of mutation stop-codons could arise somewhere in the open reading frame at which point the pioneer round stops. If this happens, downstream of this stop codon existing exon-junction-complex with still remained associated protein complexes. Following these complexes recruiting decapping enzymes and it resulted into degradation. This is only possible if the pre-mature stop codon is not located more than 50-55bp upstream of the last exon-junction-complex, due to the size of this complex and if it is not in the last intron [84].

NMD RNA decay also influences TERRA at telomeres. TERRA sequences contain stop codon sequences in the repeating sequence. Studies have shown that depletion of NMD factors increases TERRA locally at telomeres [70, 81]. An important fact is that whole TERRA levels are not effected, therefore the half-life of TERRA molecules is not reduced. Two possibilities of interacting between TERRA and NMD machinery exist. NMD proteins could be involved into local degradation of TERRA at telomeres or they are involved into displacement of TERRA from telomeres.

### **2.3.3.2. RNA interference:**

RNA interference (RNAi) is also a highly conserved mechanism in many different organisms [85]. Normal functions of this mechanism include defense against viruses, regulation of gene expressions and control of transposons. Double stranded RNA is recognized by ribonuclease proteins droscha and/or dicer and cut into small RNA molecules with 20-25bp length called small interfering RNAs (siRNAs) (Figure 2.11.). After that siRNA is separated into single strands and one of the strands (guide strand) is integrated into a RNA-induced silencing complex (RISC). There it is bound to the argonaute proteins which are endonucleases and every time a complementary RNA is present they destroy it [86].

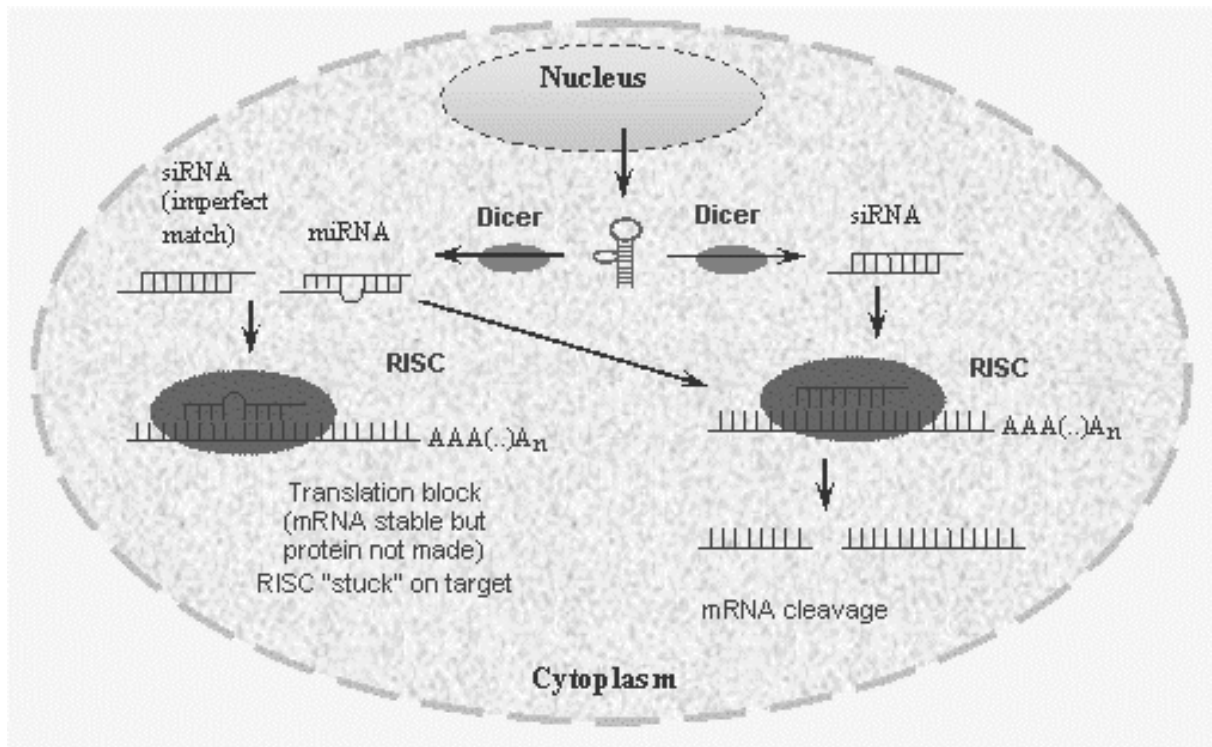


**Figure 2.11.: A simple model of RNAi pathway:** dsRNA or miRNA primary transcripts are detected and cut into small dsRNAs with 20-25bp length by RNaseII enzymes (Dicer and Drosha). They are called small interfering RNAs (siRNAs). The effector complex RNA-induced silencing complex (RISC) recognizes siRNAs and during assembly double strands get separated and one of the single strands binds to RISC. This RNA acts as a template for RNAs which is cleaved by the RNaseH enzyme Argonaute that is bound to RISC. If RISC bound siRNA and target mRNA have mismatches, the RISC complex stays bound but mRNA will not be cleaved. This results in a translation block. Schema taken from [87].

RNAi may be directly involved in heterochromatin formation of telomeres in yeast [88]. The possibility exists that TERRA triggers heterochromatinization of telomeres by RNAi as precursor to generate siRNA. It has also been shown that in mouse cells transfected with synthetic RNAi an increased association of Argonaute1 with telomeres is noticeable and TERRA is overproduced [89]. It was also shown that mouse embryonic stem (ES) cells with a knock-out of Dicer showed a decreased in TERRA levels when compared with wildtype (wt) counterparts [71].

### **2.3.3.3. Cell cycle and TERRA:**

A new study proclaimed different TERRA level during cell cycle [78]. They investigated that TERRA accumulates in early G1. during S phase TERRA level decreases continuously and reaches lowest expression levels at the transition between late S and G2. A reason for this could be because low TERRA level during S-phase allows telomerase to extend telomeres. Another argument is that it plays a role for replication of chromosome ends by the canonical DNA replication machinery [78].

Different TERRA levels during cell cycle may also be important for chromosome stability. TERRA, together with heterogeneous nuclear ribonucleoprotein A1 (hnRNPA1) and POT1, seems to regulate replication protein A (RPA) displacing after DNA replication. This is important for telomere capping after DNA replication in order to maintain chromosome integrity [90].

### **2.3.3.4. Mixed lineage leukemia (MLL) protein:**

The MLL protein is a histone methyltransferase, which acts as positive global regulator of gene expression [91]. The MLL protein is normally cleaved into a N-terminal fragment and a C-terminal fragment. N-terminal is associated with chromosomal sites, C-terminal contains a SET (Suvar3-9. enhancer-of-zeste, Trithorax) domain that manifests H3/K4 histone methyltransferase activity. It has been shown, that MLL binds to telomeres and affects the epigenetic status [91]. MLL was also seen to interact with p53 which increased the TERRA expression in response to progressive telomere uncapping. The conclusion of this discovery was that MLL dependent TERRA expression could be a cellular response by reason of telomere uncapping. Possible features could be preventing DNA damage response and the induction of cellular senescence [91].



### **3. Aims of this study:**

Establishment of methods for determination and influence of TERRA expression in tumor cells:

- In silico construction of vectors for TERRA sense and antisense expression for TERRA inhibition and elevation and telomerase inhibition.
- Cloning of telomere fragment into pENTR gateway vector with hH1 promoter and terminator as donor vector. Deletion of hH1 promoter within the pENTR vectors for using RNA polymerase II promoter expression vectors.
- Transfer telomere fragment expression cassettes of pENTR vectors into lentiviral and adenoviral vectors to result ectopic expression vectors for TERRA sense and antisense expression under control of hH1, CMV and Ubc6 promoters.
- Cell cycle dependent TERRA level, subtelomere specific TERRA levels and telomere length screening of different tumor cell lines via Real-Time PCR to determine endogenous basis level.
- Establishing methylation dependent Real-Time PCR assay for subtelomeric region of chromosome 2p.

## **4. Material and Methods:**

### **4.1. Cell culture:**

#### **4.1.1. Cell Lines:**

All cell lines were grown under specified cell culture conditions (Table 4.1.) for a few months in T25 tissue culture flasks (25cm<sup>2</sup>) from Sarstedt (#83.1810.002).

**Table 4.1.: Used cell lines which were grown under cell culture conditions:**

<b>Cell line:</b>	<b>Origin:</b>	<b>Medium:</b>	<b>Notes:</b>	<b>Passage:</b>
T98-G (CRL-1690)	ATCC	Minimum essential medium (MEM) + 10% FCS (both Sigma Aldrich, #56419C, #12238C)	T98G is a glioblastoma multiforme cell line from a 61 years old male Caucasian	412
U-2 OS (HTB-96)	ATCC	Iscove's Modified Dulbecco's medium (IMDM) + 10% FCS (both Sigma-Aldrich, #I3390)	U-2 OS is an osteosarcoma cell line from a 15 years old female Caucasian	21
Saos-2 (HTB-85)	ATCC	McCoy's 5A medium + 10% FCS (both Sigma-Aldrich, #M4892)	Saos-2 is an osteosarcoma cell line from an 11 years old female Caucasian	54
SW-480 (CCL-228)	ATCC	RPMI-1640 medium + 10% FCS (both Sigma-Aldrich, #M3817)	SW-480 is a colorectal adenocarcinoma cell line from a 50 years old male Caucasian	SW480R: 110. SW480B unknown, Passage 10 after genome analyses
Fibroblasts	Dr. Shehata	$\alpha$ -MEM + 20% FCS (both Sigma-Aldrich, #M8042)	The fibroblast cells were isolated from a patient by courtesy of Dr. Medhat Shehata (Medical University Vienna, Internal Medicine I)	8
HEK293 FT	ATCC	DNP + 10%FCS (both Sigma-Aldrich)	HEK293 FT is an embryonic kidney cell line which can be used for lentiviral infections as production cell line.	24
HEK293	ATCC	DMEM (Dulbecco's Modified Eagle's Medium - high glucose) + 10% FCS (both Sigma-Aldrich, #D5796)	HEK293 is an embryonic kidney cell line transformed with adenovirus 5 DNA and can be used as adenoviral production cell line.	42
YTBO	Patient	RPMI-1640 + 10% FCS	Established from patient astrocytoma at the institution	85

During long time passaging (at least 20 years cell culture) of SW-480 cells at the labor of Prof. Brigitte Marian (Division of Cancer, Department of Medicine I, Comprehensive Cancer Center, Medical University Vienna) some isolate of those cultures created a new phenotype. Sandra Sampl discovered that new phenotype represented decreased cell doubling time as compared to initial SW-480 culture and much longer telomeres (unpublished).

We hypothesized the presence of ALT in those cells. This new cell line is called SW480 B, and the other original, with shorter telomeres, is called SW480 R.

Cell lines in table 4.2. were not cultivated by myself. RNAs and DNAs of these cell lines which used for experiments were originally isolated by Monika Hunjadi (diploma thesis in progress).

**Table 4.2.: Cell lines used by Monika Hunjadi**

<b>Cell line:</b>	<b>Notes:</b>
Caco-2	Caco-2 is a colorectal adenocarcinoma cell line isolated from a 72 years old male Caucasian
Vaco235	Vaco235 is a adenoma cell line
HCT 116	HCT 116 is a colorectal carcinoma cell line
LT97	LT97 is a premalignant cell line established out of small colorectal polyps of a patient with familial polyposis coli
HT-29	HT-29 is a primary tumor colorectal adenocarcinoma cell line isolated from a 44 years old female Caucasian
SW-620	SW-620 is a metastasis of the same tumor SW480 originates

#### **4.1.2. Thawing cells:**

Most of the cell lines are frozen in cryo-vials in liquid nitrogen. Before use they had to be thawed. This was done according to protocol group holzmann laboratory (“Auftauen von Zellen”)

#### **Material:**

Required medium for the cell line

#### **Procedure:**

- Thaw cells in a water bath
- Carry over cells into 15ml tube
- Centrifuge 800g, 10’
- Discard supernatant

- Resuspend pellet in 3ml medium
- Carry over into tissue culture flask
- 37°C

#### **4.1.3. Passaging:**

Passaging was done at confluences between 70 – 100% with a ratio of 1:5 according to protocol group holzmann laboratory (“Splitten und Einfrieren von Zellen”).

##### Material:

Medium

Trypsin/EDTA (Invitrogen, #15400054)

PBS (Invitrogen, #AM9624)

##### Procedure:

- Suck of medium
- Add 2ml PBS
- Suck of PBS
- Add 1ml Trypsin/EDTA
- 37°C, ~5'
- Control if cells detach via microscope
- Add 2ml medium
- Discard solution depending on splitting ratio
- Add medium to 3ml

#### **4.1.4. Freezing cells:**

This was done according to protocol group holzmann laboratory (“Splitten und Einfrieren von Zellen”)

##### Material:

FCS + 10% DMSO (both Sigma Aldrich, #D2650)

Trypsin/EDTA

PBS

Procedure:

- Suck of medium
- Add 2ml PBS
- Suck of PBS
- Add 1ml Trypsin/EDTA
- 37°C, ~5'
- Control if cells detach via microscope
- Carry over into 15ml tube
- Centrifuge 1.000g, 5'
- Discard medium
- Resuspend pellet in 1.5ml FCS + 10% DMSO
- Carry over into cryo vial
- On dry ice, 30'
- At -80°C, 24h
- Stored in liquid nitrogen

**4.1.5. Cell line transfection:**

Cells can uptake nutrient and other substances via vesicles. This capability is used to transfer DNA into cells. Desired DNA is packaged into vesicles and put in front of them so they can take it up.

For transfection of cell lines Lipofectamine™ 2000 Transfection reagent (Invitrogen, # 11668019) was used.

Material:

Lipofectamine™ 2000

Serum free medium

Procedure:

- Cells were settled into 6wells so the next a confluence of about 50% was present
- 1µg Plasmid mixed with 250µl serum free medium into 1.5ml tube

- 4µl Lipofectamine™ 2000 mixed with 250µl serum free medium into 1.5ml tube
- RT, 5'
- Mixing of the two tubes
- RT, 20'
- Dripping the 500µl on cells
- 37°C, 6h
- Medium change
- After three days RNA can be isolated

#### **4.1.6. Cellcounter:**

Cells were counted with Casy Cellcounter (Schärfe System GmbH). This is necessary for transfections and antibiotic-dosage-determinations.

#### **Material:**

PBS

Trypsin

100% EtOH

Casyton

Casy clean

#### **Procedure:**

- Medium of attached cells was sucked off
- Add 2ml PBS
- Suck of PBS
- Add 1ml trypsin at cells
- 37°C, ~5'
- Control of detaching via microscope
- 100µl for cells counting into 1.5ml tube
- Casy Cellcounter has to be clean, so measuring with clean Casyton was done to ensure this
- If it was found to not be clean, cleaning with Casy clean was done
- Mix 50µl with 400µl 100% EtOH
- Invert a few times

- Mix 50µl of this with Casyton
- Measuring at Casy Cellcounter

These peaks show the area of death cells. This could be stored for every cell line and for following measures only the right adjustments are necessary.

- Mix 50µl of cells with Casyton
- Measuring at Casy Cellcounter
- Number of cells is announced

#### **4.1.7. Blasticidin dosage determination:**

Blasticidin (PAA, #P05-017) is a eukaryote antibiotic which inhibits peptide-bond formation in the ribosomal machinery and can be used for selection of lentiviral constructs from Invitrogen.

#### **Material:**

Medium

Blasticidin stock solution (5mg/ml)

#### **Procedure:**

- Settling  $10^4$  cells/well into a 96 well plate with 100µl medium.
- Used cell lines: U2OS, SW480-B, Saos2. SW480-R
- 37°C, o.n.
- 100µl of medium mixed with blasticidin with different concentrations with fivefold repetitions
- 37°C for one week
- Daily control of cytotoxic effects with microscope
- Neutral-red-uptake



**Table 4.3.: Schema of 96well plate for blasticidin dosage determination:**

	0	0	0	0	0	<b>0</b>	<b>0</b>	<b>0</b>	<b>0</b>	<b>0</b>	
	3	3	3	3	3	<b>3</b>	<b>3</b>	<b>3</b>	<b>3</b>	<b>3</b>	
	5	5	5	5	5	<b>5</b>	<b>5</b>	<b>5</b>	<b>5</b>	<b>5</b>	
	6	6	6	6	6	<b>6</b>	<b>6</b>	<b>6</b>	<b>6</b>	<b>6</b>	
	8	8	8	8	8	<b>8</b>	<b>8</b>	<b>8</b>	<b>8</b>	<b>8</b>	
	10	10	10	10	10	<b>10</b>	<b>10</b>	<b>10</b>	<b>10</b>	<b>10</b>	

Number deals with used Blasticidin concentration. Unit was  $\mu\text{g/ml}$ . External wells were left blank. Two cell lines could be tested per 96well plate. First and second cell line (bold) had the same conditions, every row had the same blasticidin concentration, in every well of a cell line the same account of cells were settled.

#### **4.1.8. Neutral red uptake:**

Neutralred (Invitrogen, #N3246) are uncharged at neutral pH. It diffuses into lysozymes and because of the acidic pH it becomes an ion and cannot move out. Dead or hardly tattered cells do not have intact lysozymes and so they do not become red.

For determination of effects of antibiotics neutral red uptake was done to count living cells according to protocol of laboratory of Brigitte Marian (Division of Cancer, Department of Medicine I, Comprehensive Cancer Center, Medical University Vienna).

#### **Material:**

Neutral red solution:

- 1mg neutral red
- 20ml serum free medium
- 37°C, 1h
- Filtering

PBS

NR-fix:

- 5ml glacial acetic acid
- 365ml 96% EtOH
- 130ml ddH<sub>2</sub>O

Procedure:

- Suck off medium
- Add 0.2ml/96well neutral red solution
- 37°C, 2h
- Suck off neutral red solution
- Add 200µl/96well PBS
- Shake gently
- Suck of PBS
- Add 100µl/96well NR-fix
- Shaking gently, 5'
- Measuring at photometer at 562nm and 620nm (as reference)

#### **4.1.9. Fluorescence activated cell sorting (FACS):**

FACS is a method for counting and examining cells and cellular particles. A stream of fluid with cells passing an electronic detection apparatus allows the analysis of light scattering and the associated fluorescent characteristics.

Two different FACS-analyses were conducted. A GFP-FACS and a cell cycle FACS. FACS analyses were conducted by Dr. Irene Herbacek (Division of Cancer, Department of Medicine I, Comprehensive Cancer Center, Medical University Vienna).

#### **4.1.10. GFP-FACS:**

With GFP-vectors transient transfected cells were counted.

Material:

PBS

Procedure:

- Suck of medium
- Add 2ml PBS
- Scratch
- Carry over into FACS tube
- FACS analyses were conducted by Dr. Irene Herbacek (Division of Cancer, Department of Medicine I, Comprehensive Cancer Center, Medical University Vienna)

**4.1.11. Cell cycle FACS:**

Cell cycle state of cells was determined by FACS analysis.

Material:

Trypsin/EDTA

PBS

10%FCS-MEM

Nuclear isolation buffer:

- 10.5g citric acid (0.5M)
- 0.5ml TWEEN
- ddH<sub>2</sub>O to 100ml

RNase A:

- Mix RNase A with PBS with a concentration of 1mg/ml
- Aliquots in 1.5ml tubes
- 100°C, 15'
- On ice
- Stored at -20°C

Propidium iodide:

- Mix propidium iodide with PBS with a concentration of 0.5mg/ml
- Stored away from light

Staining solution:

- 0.05ml RNase A
- 0.05ml propidium iodide
- 0.5ml PBS

Procedure:

Trypsinized:

- Suck of medium
- Add 2ml PBS
- Suck of PBS
- Add 2ml PBS
- Suck of PBS
- Add 500µl Trypsin/EDTA
- 37°C, 5'
- 5ml 10% FCS-MEM
- Carry over into 15ml tube

Scatched:

- Suck of medium
- Add 2ml PBS
- Scratch
- Carry over into 15ml tube

Following steps were the same for both experimental approaches.

- Centrifuge 1.000g, 5'
- Discard supernatant
- Resuspend pellet in 1ml PBS
- Centrifuge 1.000g, 2'
- Every further work has to be done on ice
- Add 1ml cold Nuclear isolation buffer
- Mix well
- On ice, 5'
- Mix with pipette
- Quality of nuclear disposal is visible via microscope

- Centrifuge 2.000g, 5', 4°C
- Resuspend nuclear pellet in 0.5ml staining solution
- Carry over into FACS-tube
- Protect with aluminum foil
- Measurements were conducted by Dr. Irene Herbacek

## **4.2. Molecular Biology:**

### **4.2.1. Bacteria:**

Plasmid uptake of normal bacteria is not very efficient. Due to this bacteria have to become competent. This procedure destabilizes the bacterial membrane and enhances plasmid uptake.

#### **4.2.1.1. TOP10 Chemically Competent E. coli:**

The One Shot® TOP10 Chemically Competent E. coli strain (Invitrogen, #C404010) was highly competent (about  $10^8$  per  $\mu\text{g}$  plasmid DNA) used for transformations if needed.

#### **4.2.1.2. DB3.1 Competent Cells:**

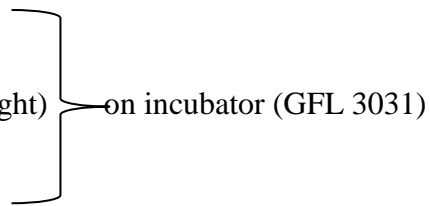
LIBRARY EFFICIENCY DB3.1 Competent Cells (Invitrogen, #11782-018) contains the gyrA462 allele which renders the strain resistance to the toxic effect of the ccdB gene which is present in destination-vectors for gateway reactions.

#### **4.2.1.3. Conditions for bacterial growth:**

LB Broth (Sigma-Aldrich Chemie GmbH, #L3022) were used as growing medium and if necessary antibiotics were added (kanamycin 50 $\mu\text{g}/\text{ml}$ , ampicillin 100 $\mu\text{g}/\text{ml}$ , chloramphenicol 30 $\mu\text{g}/\text{ml}$  all Sigma-Aldrich Chemie GmbH #K1876. #A9393. #C0378).

Growth at:

37°C  
o.n. (overnight)  
200rpm



on incubator (GFL 3031)

If plates were used:

- LB Broth with select agar (Sigma-Aldrich Chemie GmbH, #A5054) were mixed
- Heated at microwave until select agar was dissolved
- After this cooled down, the antibiotics were added (a temperature which is too high would destroy the antibiotics)
- 5-10 ml per plate were used

#### **4.2.2. Cloning Methods:**

##### **4.2.2.1. SEM-Transformation of bacteria:**

SEM-transformation was done for transforming plasmids into competent E. coli TOP10 and DB3.1 cells as described [92].

##### **4.2.2.1.1. Producing competent cells:**

Self-produced competent cells transformation efficiency was about  $10^6$  transformants per  $\mu\text{g}$  plasmid DNA as tested with pUC19.

### Materials:

10x TB-Buffer:

- 100mM Pipes
- 150mM CaCl<sub>2</sub>
- 2.5M KCl
- With KOH at pH 6.7 regulated
- Autoclaved

550mM MnCl<sub>2</sub> (sterile filtered, stored at +4°C, light protected)

1x TB:

- 320ml ddH<sub>2</sub>O
- 40ml 10xTB
- 40ml 550mM MnCl<sub>2</sub>

### Procedure:

- Single streak of competent cell on LB plate with antibiotics (Streptomycin, Sigma-Aldrich, #S6501)
- Picking colony
- Overnight culture (LB with antibiotics)
- 2x 20-50µl of the o.n. culture in 2x 200ml LB without antibiotics (in two 1l bulb)
- o.n. , ~200rpm, RT until an OD<sub>600</sub> of 0.6
- Cool down on ice
- LB in 8x 50ml falcons, 20' on ice
- 15', 2.500g, 4°C
- Supernatant is discarded
- Every pellet is re-suspended with 5ml 1xTB
- Merge into two falcons
- 10' on ice
- 10', 2.500g, 4°C
- Supernatant is discarded
- Every pellet is re-suspended into 5ml 1xTB
- Merge into one falcon
- DMSO (7 Vol%)
- 10' on ice
- Portion every 700µl into 1.5ml tubes

- Quick-freeze with N<sub>2</sub>
- Storing at -80°C

#### **4.2.2.1.2. Transformation of bacteria:**

##### Materials:

##### SOB-medium:

- 20g Trypton/Pepton out of casein (Roth, #8952.1)
- 5g Select yeast extract (Sigma-Aldrich, #Y0500)
- 0.5g NaCl
- 10ml 250mM KCl
- ddH<sub>2</sub>O to 1L
- with NaOH to pH 7
- autoclave

##### SOC-medium:

- SOB-medium
- 1/100 volume 1M MgCl<sub>2</sub>
- 1/100 volume 2M glucose

##### Procedure:

- Thaw competent cells on ice
- Plasmid in 1.5ml tube on ice
- Adding 200µl competent cells (blue tip with chopped end), mixing VERY carefully
- 20', on ice
- Heatshock, 35'', 42°C (waterbath)
- Adding 800µl SOC-medium
- Inverting 2x
- Transferred into overnight culture tube
- 1h, 37°C, 200rpm
- Transfer in 1.5ml tube
- Centrifuge 1.000g, 3', RT
- Discard large part of supernatant



- Resuspend pellet
- Transfer on LB-plate (if necessary with antibiotics)
- Dunk Trigalski spattle into EtOH, burn off
- Plate bacterias with spittle
- O.n. into incubator at 37°C

#### **4.2.2.2. Plasmid DNA isolation:**

##### **4.2.2.2.1. STET Boiling Plasmid DNA Miniprep:**

The DNA isolation with a shortened protocol of the original STET Boiling Plasmid DNA Miniprep [93] does contain remaining proteins and other compounds potentially hindering cloning, so it was only used for screening of resulting transformants after cloning steps.

#### **Materials:**

STET-buffer:

- 8% Saccharose (Sigma-Aldrich, #84097)
- 0.5% Triton X-100 (Sigma-Aldrich, #T8787)
- 50mM Tris pH8 (Sigma-Aldrich, #T87602)
- 50mM EDTA (Sigma-Aldrich, #431788)
- ddH<sub>2</sub>O to 1l and autoclaved
- stored at +4°C

Lysozyme: 50mg/ml stock (stored at -20°C, Invitrogen, #GIC207)

RNase A: 100mg/ml stock (in 10mM Tris-HCL pH 7.5 and 15mm NaCl heat to 100°C and cool it to room temperature, stored -20°C)

Isopropanol

EtOH 75%

#### **Procedure:**

- 1.5 ml of an overnight E.coli culture is transferred into 1.5ml tubes
- Centrifuge 3', 10.000g
- Supernatant is discarded

- This steps can be repeated (2-4x) to increase the plasmid yield
- For each isolation mix 100µl STET buffer and 10µl Lysozyme
- This 110µl are added, re-suspend pellet
- 5', RT
- 1', 95°C
- Centrifuge 10.000g, 10', 4°C
- Pellet carefully discard with a tooth peak prior soaked with RNase A solution
- 110µl isopropanol, mix
- Centrifuge 10.000g, 15', 4°C
- Supernatant is discarded
- 200µl EtOH 75% (4°C), not resolving
- Supernatant is discarded
- Pellet dry about 15' at RT
- Pellet is re-suspended in 50µl 1xTE
- Stored at -20°C

#### **4.2.2.2.2. Wizard® Plus SV Minipreps DNA Purification Systems:**

The kit was used according to Promegas manufacturer's recommendations. All Materials required are contained in the kit (Promega, #A1460).

#### **Materials:**

Cell Re-suspension Solution

Cell Lysis Solution

Alkaline Protease

Neutralization Solution

Column Wash Solution

Wizard SV Minicolumns

Collection tubes

#### **Procedure:**

- Transferring 1.5 ml of an overnight E.coli culture into 1.5ml tubes
- Centrifuge 2', 10.000g
- Supernatant is discarded

- This steps was repeated (2-4x) to increase the plasmid yield
- Re-suspend in 250µl Resuspension solution
- 250µl Lysis solution
- Mix, incubate for 3'
- 10µl alkaline protease solution
- Mix, incubate for 5'
- 350µl neutralization solution
- 10', 14.000g
- Supernatant is transferred into spin column which is plugged into a collection tube
- 1', 14.000g
- Flow-through is discarded
- 750µl wash solution
- 1', 14.000g
- Flow-through is discarded
- 250µl wash solution
- 1', 14.000g
- Flow-through is discarded
- 2', 14.000g
- Put column on new clean 1.5ml tube
- 30µl nuclease free water
- Incubation for 2' at room temperature
- 1', 14 000g
- The flow-through is transferred on the spin column again (this increases the plasmid yield)
- Incubation for 2' at room temperature
- 1', 14.000g
- DNA stored at -20°C

#### **4.2.2.2.3. S.N.A.P.<sup>TM</sup> MidiPrep Kit:**

This kit was used for isolate destination vectors for gateway reactions. It is necessary, because gateway reactions aren't work if other isolation kits are used (#K191001).

Material:

S.N.A.P.<sup>TM</sup> MidiPrep Column A (Filtering)

S.N.A.P.<sup>TM</sup> MidiPrep Column B (Binding)

Resuspension Buffer with RNase A

Lysis Buffer

Precipitation Salt

Binding Buffer

Wash Buffer

1x Final Wash Buffer

Procedure:

- Transfer bacterial culture into 50ml tubes
- Centrifuge at 4°C with 4.000g, 10'
- Discard supernatant
- Transfer bacterial culture into 50ml tubes
- Centrifuge at 4°C with 4.000g, 10'
- Re-suspend with 4ml Resuspension Buffer
- Add 4ml Lysis Buffer
- Invert 3-5 times
- 3', RT
- Add 4ml Precipitation Salt
- Invert 6-8 times
- 5' on ice, inverting twice during incubation
- Transfer into Column A which is into a 50ml tube
- Centrifuged 3.000g, 5'
- Discard Column A
- Add 12ml Binding Buffer to filtrate
- Inverting twice
- Transfer into Column B which is into a 50ml tube
- Centrifuge 1.000g, 2'
- Discard flow through
- Add 5ml Wash buffer
- Centrifuge 2.000g, 1'
- Discard flow through

- Add 5ml 1x Final Wash Buffer
- Centrifuge 2000g, 2'
- Add 10ml 1x Final Wash Buffer
- Centrifuge 2.000g, 2'
- Discard flow through
- Centrifuge 4.000g, 5'
- Transfer column into a new 50ml tube
- Add 750µl ddH<sub>2</sub>O
- 3', RT
- Centrifuge 4.000g, 5'
- Stored at -20°C

#### **4.2.2.3. Determination of nucleotide concentrations:**

Two different methods were used to determine the concentration of DNAs and RNAs, the Nanodrop ND-1000 Spectrophotometer (Peqlab) and the Qubit® Fluorometer (Invitrogen, Fisher Scientific). Both instruments were used according to the manufacturer's recommendations. Nanodrop measures optical density based on nucleotides and calculates their concentrations with a special formula. Qubit measures a dye that becomes fluorescent if it binds to DNA or RNA.

Advantage of the Nanodrop: very quick, cheap

Advantage of the Qubit: Only intact molecules are detected

#### **4.2.2.3.1. Nanodrop ND-1000 Spectrophotometer (Peqlab):**

##### Material:

Solvent of nucleotide probe

##### Procedure:

- Starting program on PC
- 2µl ddH<sub>2</sub>O or 1xTE (depending on the solvent) to blank

- For every measurement 1-2µl sample
- The instrument connected with a computer shows concentrations of the DNA or RNA and also purity (260/280 and 230/280 values shows containing salt, alcohol, proteins and other factors which absorb light at 260 or 230nm)

#### **4.2.2.3.2. Qubit® Fluorometer (Invitrogen, Fisher Scientific):**

All Materials are contained in the kit. Different kits for dsDNA, dsRNA, ssDNA and ssRNA are useable. For dsDNA Qubit® dsDNA BR Assay Kit (Invitrogen, #Q32850) was used.

##### Materials:

Quant-iT™ buffer  
 Quant-iT™ reagent  
 Quant-iT™ Standard #1  
 Quant-iT™ Standard #2  
 Qubit™ assay tubes

##### Procedure:

- All reagents should be at room temperature
- Qubit™ assay tubes were used to mix the samples
- Mix 199µl Quant-iT™ buffer with 1µl Quant-iT™ reagent for every sample plus two for the standards. That's the Quant-iT™ working solution
- Mix Quant-iT™ Standard #1 and Quant-iT™ Standard #2 with ever 190µl working solution
- 1µl of every sample get mixed with 199µl working solution (if bigger amounts are needed more sample and in return less working solution can be used)
- Vortex
- 2', RT
- Starting program on PC
- Calibrate with standards

The formula to calculate the concentration is:

$$\text{Concentration of DNA} = \text{QF value} \times (200)/\mu\text{l of sample}$$

#### **4.2.2.4. DNA-restriction:**

To cut DNA restriction endonucleases can be used. These enzymes detect special nucleotide sequences and cut at a determined position.

DNAs were cut with restriction endonucleases from Fermentas. All of them were used with the recommended buffers of Roche and at 37°C for 90 minutes if not other mentioned.

#### **4.2.2.5. DNA-Ligation:**

To link DNA fragments ligation is necessary. Under ATP consumption 5' end and 3' of DNA are connected. Only phosphorylated nucleotides can be connected at this way.

For ligations Fast-Link™ DNA Ligation Kit (Epicentre biotechnology, #LK11025) was used. All Materials are contained in the kit.

#### **Material:**

10x Fast-Link buffer

ATP (10mM)

Fast-Link DNA ligase (2u/μl)

#### **Procedure:**

For blunt end ligations:

- 1.5μl Fast-Link buffer into 1.5ml tube
- Add 0.75μl ATP
- Add vector DNA (1)
- Add insert DNA (5)
- Add ddH<sub>2</sub>O to 14.5μl
- Add 0.5ml Fast-Link DNA ligase
- RT, 15'
- Heat inactivation, 70°C, 15'

For cohesive ends ligation:

- 1.5μl Fast-Link buffer into 1.5ml tube
- Add 1.5μl ATP
- Add vector DNA (1)

- Add insert DNA (2)
- Add ddH<sub>2</sub>O to 14.5μl
- Add 0.5ml Fast-Link DNA ligase
- RT, 5'
- Heat inactivation, 70°C, 15'

#### **4.2.2.6. Linker preparation:**

Before use the linker that is necessary for the cloning strategy had to be perpetrated.

The linker had to be annealed, phosphorylated and into the pENTR/D/hH1 vector ligated. The sequence was: AATTGTCGAC. This includes a SalI restriction site and EcoRI recognition sites at the ends. A self-annealing was so possible and a new SalI restriction site was included into pENTR/D/hH1 vector.

##### **4.2.2.6.1. Linker dsDNA annealing:**

Procedure from <http://strucutre.biochem.queensu.ca/protocols/linkerligation.pdf>

##### **Material:**

1M NaCl

##### **Procedure:**

- 18μl Linker (5.4μg) into PCR-tube
- Add 2μl 1M NaCl
- 95°C, 2'
- 52°C, 10'
- 4°C

Before ligation nucleotide phosphorylation was necessary.



#### **4.2.2.6.2. Linker DNA phosphorylation:**

The phosphorylation step adds a phosphate at the 5' end of the linker. T4 Polynucleotide Kinase (Fermentas, #EK0031) was used. All Materials required are contained in the kit.

##### Material:

10x Reaction Buffer A

ATP (10mM)

T4 Polynucleotide Kinase (10u/μl)

##### Procedure:

- 2μl Linker (546ng) into 1.5ml tube
- Add 2μl 10x Buffer A
- Add 1μl ATP
- Add 14μl ddH<sub>2</sub>O
- Add 1μl T4 Polynucleotide Kinase
- 37°C, 30'
- 65°C, 15'
- 4°C

#### **4.2.2.6.3. Linker plus DNA plasmid ligation and transformation:**

After phosphorylation linker was integrated into pENTR/D/hH1 via ligation. Materials like described at point 4.2.2.6.2.

##### Procedure:

- 1μl Linker (27ng) into 1.5ml tube
- Add 2μl Ligation Buffer
- Add 2μl ATP
- Add 10μl Plasmid DNA (pENTR/D/hH1. 223ng) cut with EcoRI
- Add 3μl ddH<sub>2</sub>O
- Add 2μl Ligase
- 16°C, o.n.
- Heat inactivation, 65°C, 20'

Before transformation EcoRI recut was conducted.

Procedure:

- 10µl of ligation solution into 1.5ml tube
- Add 3µl H-Buffer (Roche)
- Add 16µl ddH<sub>2</sub>O
- Add 1µl EcoRI (10U/µl)
- 37°C, 60'
- Heat inactivation, 65°C, 20'
- Transformation like described 4.2.2.1.

**4.2.2.7. Fill in and partial fill in of restricted DNA overhangs:**

As Klenow fragment the bigger protein part of DNA polymerase I from E.coli is called after cleavage with subtilisin. This fragment has the ability for 5' → 3' polymerase activity and 3' → 5' exonuclease activity (proof reading). 5' → 3' exonuclease activity is not available any more.

Klenow fragment kit (Fermentas, #EP0051) was used. The kit was used according to the manufacturer's recommendations for partial and complete fill in in different steps during the establishment of the plasmid construct. For partial fill in the dNTP Mix wasn't used. Instead single dNTPs at the same concentration as for dNTPs were used. All Materials are contained in the kit.

Material:

10x Reaction Buffer for Klenow fragment

dNTP Mix (2nM each)

Klenow fragment (10u/µl)

Procedure:

- DNA (100-400ng) into 1.5ml tube
- Add 2µl 10x Reaction Buffer
- Add 0.5µl dNTP Mix (final concentration of 0.05mM)
- Add ddH<sub>2</sub>O to 19.5µl

- Add 0.5µl Klenow fragment (10u/µl)
- 37°C, 10'
- Heat inactivation, 75°C, 10'

For partial fill in:

For psp73 with telomere fragment after BglII and BamHI cut, dGTP and dATP were used.  
For pENTR/D/hH1 Linker after SalI cut, dTTP and dCTP were used.

For promoter deletion: Deletion of hH1 promoter of pENTR/D/hH1 Antisense Tel only required a fill in after BamHI and ClaI cut. Deletion of hH1 promoter of pENTR/D/hH1 Sense Tel after BamHI and SacI cut, exonucleolytic activity of Klenow fragment was used to create blunt ends. At this reaction solution without dNTP Mix was incubated 10' on 37°C, the dNTP Mix were added and 10' at 37°C incubated.

#### **4.2.2.8. Gel-extraction:**

For gel-extraction QIAEX II Gel Extraction Kit (Qiagen, #20021) were used. The kit was used according to the manufacture's recommendations and all materials are contained in the kit.

#### Material:

Buffer QX1  
QIAEX II  
Buffer PE

#### Procedure:

- DNA was cut out from gel with a scalpel
- Transfer into 1.5ml tube
- Weight the out cut gel
- Add 3 volumes of Buffer QX1 (for instance: 100mg sample = 300µl Buffer QX1)
- Vortex QIAEX II
- Add 10µl QIAEX II (if more than 2µg DNA is present, than more QIAEX II is necessary)
- 50°C, 10', shaking with 600rpm

- Centrifuge 13.000rpm, 30sec.
- Discard supernatant
- Add 500µl Buffer QX1. vortex
- Centrifuge 13.000rpm, 30sec.
- Discard supernatant
- Add 500µl Buffer PE, vortex
- Centrifuge 13.000rpm, 30sec.
- Discard supernatant
- Add 500µl Buffer PE, vortex
- Centrifuge 13.000rpm, 30sec.
- Discard supernatant
- Air-dry pellet
- Add 10µl ddH<sub>2</sub>O and re-suspend
- Centrifuge 13.000rpm, 30sec.
- Pipet supernatant into clean tube
- Stored at -20°C

#### **4.2.2.9. Gateway cloning system:**

Gateway® Cloning of Invitrogen gives the ability to transfer DNA fragments directly without cutting steps and searching for compatible restriction enzyme sites. It based on the recombination system of viruses which are able to transfer their DNA without the cutting of genomic DNA. DNA fragment has to be in the rfb-cassette of an ENTR-vector. This cassette is flanked by att R sites, which serve as recognition sites for exchange. With a LR-reaction the fragment is exchanged with the fragment of a Destination-vector that is flanked by att L sites. If necessary the reaction is reversible with a BP-reaction. Advantages are that easy transfer of DNA is possible and selection is very easy (Figure 4.1.). ENTR-vectors of Invitrogen always have gene coding for kanamycin resistance and Destination-vectors always have a gene coding for ampicillin resistance. Destination vector cassettes also include a gene for chloramphenicol resistance and a ccd B gene which has lethal effects except of some bacterial strains which contain gyrA462 allele. Gateway® LR Clonase® enzyme mix (Invitrogen, #11791019) was used.

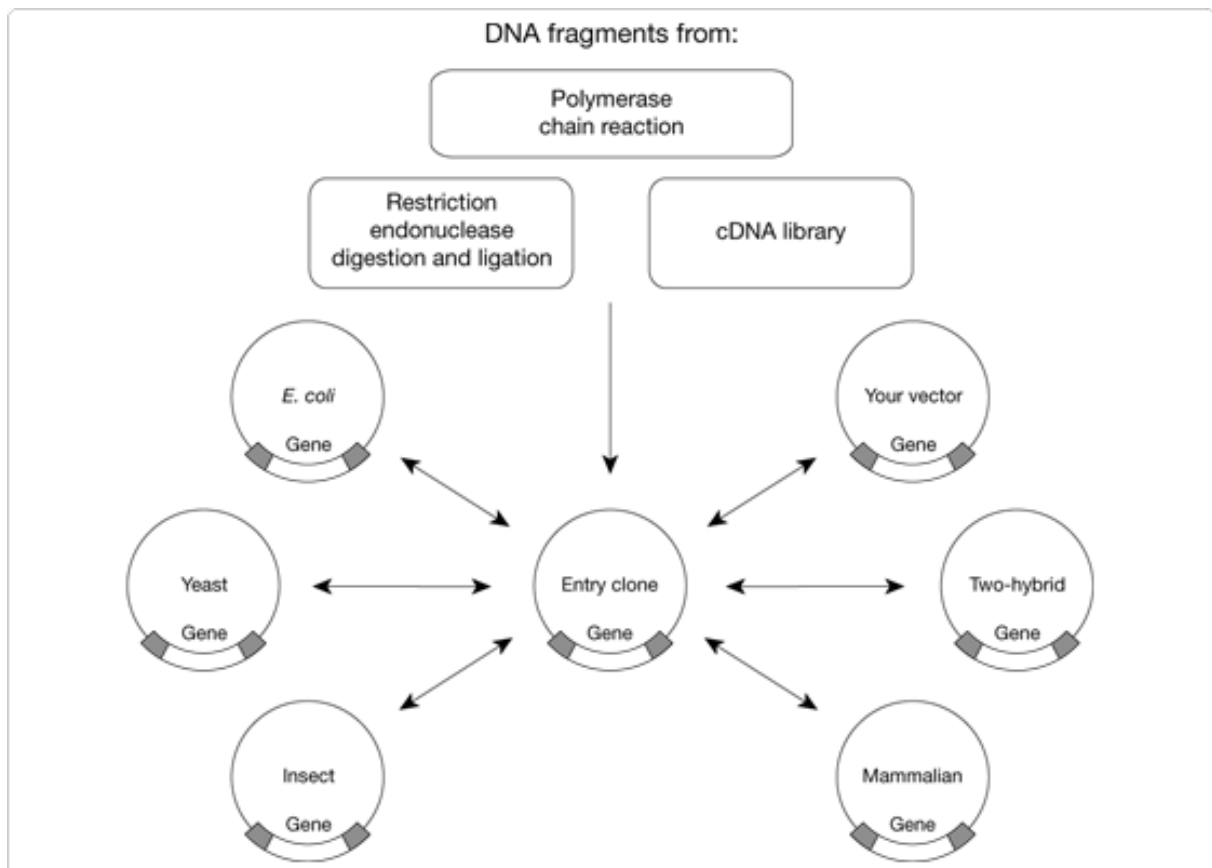


**Figure 4.1.: Gateway® technology:** If the gene of interest is cloned into an ENTR-vector (middle circle) it's possible to transfer it into every destination vectors of interest (other circles) via site specific recombination. Also it's possible to transfer the gene back from destination vectors into an ENTR-vector. Schema taken from [94].

Material:

1x TE Buffer

- 10mM Tris, pH 7.4
- 1mM EDTA, pH 8.0

LR Clonase™ II enzyme mix

Proteinase K

Procedure:

- pENTR-vector (10fmol) into a 1.5ml tube
- Add Destination-vector (20fmol)
- Add 1x TE buffer to 4µl
- Add 1µl LR Clonase™ II enzyme mix
- Vortex

- 25°C, o.n.
- Add 1µl Proteinase K
- 37°C, 10'
- Transformation

#### **4.2.2.10. Plasmid constructs:**

**Table 4.4.: Plasmids used and/or constructed in this study:** pAd means Adenoviralvectors, Kan = Kanamycin, Amp = Ampicilin

<b>Plasmid:</b>	<b>Origin/Construction:</b>	<b>Resistance:</b>
pENTR/D/hH1-shNMP265	pENTR/D/hH1 vector with an shNMP265 insert	Kan
pENTR/D/hH1-shNMP265 ΔSall	Elimination of Sall restriction site by cutting and fill in (5.1.2.1.)	Kan
pENTR/D/hH1 ΔshNMP265 ΔSall	Elimination of shNMP265 by EcoRI cut end religation (5.1.2.2.)	Kan
pENTR/D/hH1 Linker	Insert of Linker (5.1.2.3.)	Kan
pENTR/D/hH1 Sense Tel	Insert of telomere fragment in sense orientation (5.1.3.2.)	Kan
pENTR/D/hH1 Antisense Tel	Insert of telomere fragment in antisense orientation (5.1.3.1.)	Kan
pENTR/D/Sense Tel ΔhH1	Elimination of hH1 promoter of pENTR/D/hH1 Sense Tel (5.1.4.1.1.)	Kan
pENTR/D/Antisense Tel ΔhH1	Elimination of hH1 promoter of pENTR/D/hH1 Antisense Tel (5.1.4.1.2.)	Kan
psp73 Tel	psp73 vector with an integrated 800bp telomere repeat (TTAGGG), Received from Dr. Yasuhiko Kiyozuka M.D., PH.D., Department of Pathology II, Kansai Medical University Osaka	Amp
pAd/PL-DEST™ Gateway® Vector	Invitrogen, #V494-20. adenoviral promoterless gateway vector	Amp
pAd/pl Sense Tel	Gateway reaction of pENTR/D/hH1 Sense with pAd/pl (5.1.5.1.2.)	Amp
pAd/pl Antisense Tel	Gateway reaction of pENTR/D/hH1 Antisense with pAd/pl (5.1.5.1.2.)	Amp
pAd/CMV/V5-DEST™ Gateway® Vector	Invitrogen, #V493-20. adenoviral gateway vector with CMV promoter	Amp
pAd/CMV Sense –hH1 Tel	Gateway reaction of pENTR/D/Sense ΔhH1 with pAd/CMV (5.1.5.1.2.)	Amp
pEGFP-C1	Used as efficiency control for transfection experiments (Clontech)	Kan
pLenti6/Block-it™-DEST	Lentiviral promoterless expression vector from Invitrogen (#K4943-00)	Amp
pLenti6/UbC/V5-DEST	Lentiviral expression vector with UbC promoter from Invitrogen (#V499-10)	Amp

### **4.2.3. RNA-Isolation by Trizol:**

RNAs isolated from cell lines were used for expression study experiments.

#### **Materials:**

TRIZOL® Reagent (Invitrogen, #15596026)

Chloroform

Isopropanol

Ethanol 75%

RNasin Plus RNase Inhibitor (Promega, 40u/μl, #N2611)

1x TE as solvent

#### **Procedure:**

- Cell lines of 6wells or T25 were pelletized, shock frozen in liquid nitrogen and stored at -80°C
- Frozen pellets were immediately mixed with Trizol (depending on cell count 250-1000μl) to save RNA from degradation as good as possible
- Mixed
- For expression studies cells under culture conditions were directly, after suction of medium sheeted with Trizol (depending on cell count 250-1000μl) and scrapped to dissociate from bottom
- This cells were transferred into a 1.5ml tube

Now the following procedures were the same.

- 5', RT
- Add chloroform (100μl/500μl trizol)
- Vortex 15''
- 2-3', RT
- Centrifuge 12.000g, 15', +2-8°C
- 3 phases (bottom red organic phase, middle interphase, above clear aqueous phase)
- Aqueous phase in new tube (RNase free!)
- Rest storing for DNA and protein isolation
- Add Isopropanol (250μl/500μl trizol) => precipitation
- Mix
- 10', RT

- Centrifuge 12.000g, 10', +2-8°C
- Discard supernatant
- Add 75% Ethanol (500µl/500µl trizol)
- Short vortexing
- Centrifuge 7.600g, 5', 4°C
- Discard supernatant
- Dry pellets at RT
- Resolve pellets in 30µl RNase free ddH<sub>2</sub>O with 1/100 volume heat stable RNasin Plus (Promega 40U/µl)
- Store at -80°C

After thawing and before measuring RNA has to be heat to 55-60°C for 10' to prevent accumulation of RNA-aggregates.

#### **4.2.4. Genomic DNA-Isolation by Trizol:**

Remains of RNA-Isolation by Trizol used for genomic DNA-Isolation.

##### Material:

100% EtOH

0.1M Na-Citrat in 10% EtOH

75% EtOH

8mM NaOH (pH 9)

0.1M HEPES (Invitrogen, #15630049)

15mM EDTA

##### Procedure:

- Remains of RNA Isolation at RT
- Centrifuge 12.000g, 10', 4°C
- If part of aqueous phase is already there, removing
- Add 100% EtOH (150µl/500µl Trizol)
- Inverting a few times
- RT, 2-3'
- Centrifuge 2.000g, 5', 4°C



- Pellet should be visible
- Upper one (phenol-ethanol phase) discarded (could be used for protein isolation, but wasn't used in this study)
- Add 0.1M Na-citrat in 10% EtOH (500µl/500µl Trizol)
- Mix
- RT, 30'
- Centrifuge 2.000g, 5', 4°C
- Discard supernatant
- Add 0.1M Na-citrat in 10% EtOH (500µl/500µl Trizol)
- Mix
- RT, 30'
- Centrifuge 2.000g, 5', 4°C
- Discard supernatant
- Add 0.1M Na-citrat in 10% EtOH (500µl/500µl Trizol)
- Mix
- RT, 30'
- Centrifuge 2.000g, 5', 4°C
- Discard supernatant
- Re-suspend pellet in 75% EtOH (1ml/500µl Trizol)
- RT, 15'
- Centrifuge 2.000g, 5', 4°C
- Discard supernatant
- Air-dry
- Add 50µl 8mM NaOH
- 30' dissolving
- Add 7µl 0.1M HEPES
- Add 4µl 15mM EDTA
- Stored at -20°C

#### **4.2.5. Genomic DNA isolation by Maxwell® DNA Purification Kit:**

Genomic DNA isolated with (Promega) leads to a higher purification than with Trizol isolated gDNA. DNAs isolated with Trizol also aren't able to be cut by restriction enzymes (reference diploma thesis of Sandra Sampl). DNA is isolated automatically as shown in Figure 4.2.

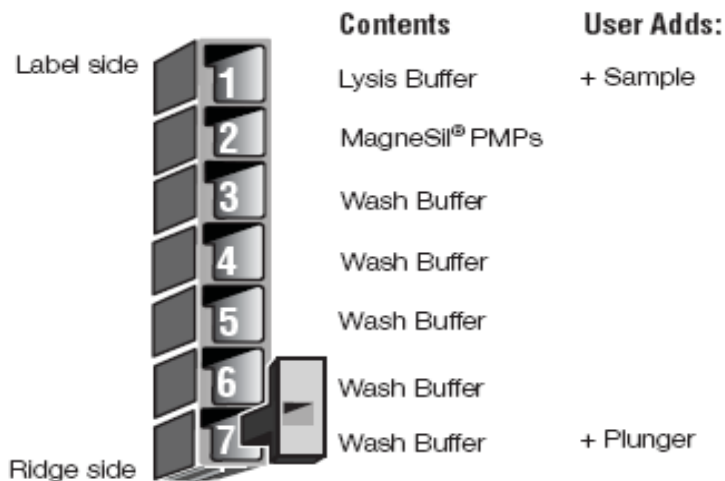


**Figure 4.2.: Maxwell® DNA Purification Kit cartridge:** Sample is loaded into well 1 containing lysis buffer. In Maxwell Purification System sample is automatically transferred from well to well. At the end clean genomic DNA is eluted in elution buffer into elution tube (not shown). Schema taken from [95].

Material:

- Cartridge
- Plunger
- Elution Tube
- Elution Buffer

Procedure:

- 300µl Elution buffer is added into elution tube
- Sample is added into well 1 containing lysis buffer
- Cartridge is put into Maxwell®16 instrument
- Program Tissue is used
- After procedure DNA is contained in elution buffer
- Transferred into 1.5ml tube
- Stored at -20°C

**4.2.6. Complementary DNA-synthesis:**

RNA is very sensitive for depletion and degradation and PCR systems are optimized for DNAs. So RNA get converted to so called complementary DNA (cDNA) via reverse

transcriptase activity of RNA-viruses which use them to transcribe their RNA genome into DNA to integrate it into host cells.

cDNA-synthesis was used for gene expression experiments with real-time PCR. RNAs used for cDNA-synthesis were reverse transcribed with RevertAid™ Premium First Strand cDNA Synthesis Kit (Fermentas Molecular Biology Tools, #K1621).

Material:

5x RT-buffer

dNTP mix (10nM)

Random hexamer primer

RevertAid™ Premium Enzyme Mix (containing RevertAid™ M-MuLV Reverse Transcriptase, 200u/μl)

RNase Inhibitor (20u/μl)

Procedure:

- 500ng RNA into PCR tube
- Add 0.5μl Random hexamer primer
- Add nuclease free H<sub>2</sub>O to 6μl
- 70°C, 5'
- On ice
- Add 4μl Mastermix
  - 2μl 5x RT-buffer
  - 0.5μl RNase Inhibitor
  - 1μl dNTP mix
  - 0.5μl RevertAid™ Premium Enzyme Mix
- Mix
- Tubes into PCR-cycler
- 28°C, 15'
- 42°C, 60'
- 70°C, 10'
- On ice, 5'
- Fill up with ddH<sub>2</sub>O at 250μl (resulting concentration: 2ng/μl)

#### **4.2.7. Gel-electrophoresis:**

Gel-electrophoresis is used to separate DNA fragments according to size and conformation. Two different types of gel-electrophoreses were used, agarose-gel-electrophoresis and polyacrylamide gel electrophoresis (PAGE) essentially performed as described in 4.2.7.1. and 4.2.7.2. Longer DNA fragments (over 500bp) were identified with agarose-gel-electrophoresis, shorter or short differences were identified with PAGE. Also a denaturing RNA-agarose-gel was done to check up RNA quality.

#### **4.2.7.1. Agarose gel-electrophoresis:**

Agarose gel-electrophoresis as a standard molecular biological method was very often used normally under the same conditions.

#### **Material:**

SeaKem® LE agarose (Boizym, #849001)

50x TAE Buffer:

- 242g Tris base
- 57.1ml glacial acetic acid
- 100ml 0.5M EDTA (pH 8)
- ddH<sub>2</sub>O to 1l
- autoclave

6x Loading Buffer:

- 60mM EDTA
- 10mM Tris HCl (pH 7.6)
- 0.03% Bromophenol blue
- 0.03% Xylen blue
- 60% glycerol

$\lambda$ -Marker III:

- 50 $\mu$ g  $\lambda$ -DNA
- 42 $\mu$ l buffer B (Roche)
- 4 $\mu$ l HindIII
- 4 $\mu$ l EcoRI
- ddH<sub>2</sub>O to 417 $\mu$ l
- 37°C, o.n.
- 83 $\mu$ l 6x loading buffer

Mass Ruler<sup>TM</sup> High Range DNA Ladder, ready to use (Fermentas, #SM0393)

Procedure:

- Weigh Agarose powder and fill up with water (normally 1% agarose-gels were used, 1g at 100ml)
- Solution heated at microwave until powder was dissolved
- Add 50x TAE Buffer (2ml at 100ml)
- Agarose cooled and then fuelled into gel chamber
- Putting a ridge in the gel and the whole gel cooled until agarose becomes solid
- Removing ridge
- Putting gel with chamber into gel apparatus
- Filling gel apparatus with 1x TAE Buffer
- Adding 6x Loading Buffer to each sample
- Samples are loaded into slots
- Adding also a marker (Mass Ruler<sup>TM</sup> High Range DNA Ladder and/or  $\lambda$ -Marker III) into s slot
- Running gel with 80V, 120' (power supply: BioRad Power Pac Basic)

#### **4.2.7.2. Polyacrylamid gel electrophoresis (PAGE):**

##### Material:

40 x TAE:

- 96.8 g Tris base
- 22.8 ml glacial acetic acid
- 40ml EDTA (pH 8. 0.5 M) and fill to 1000 ml with ddH<sub>2</sub>O and autoclave

Acrylamide/Bis 19:1 Solution (Biorad, # 161-0144)

25% APS (Ammoniumperoxodisulfate, Sigma-Aldrich, #A3678)

TEMED (N,N,N',N'-Tetramethylethylenediamine, Sigma-Aldrich, #T9281)

GeneRuler™ 50bp DNA Ladder Mix, ready to use (Fermentas, #SM0333)

##### Procedure:

- 12.6ml ddH<sub>2</sub>O
- Add 375µl 40x TAE
- Add 1.95ml Acrylamide/Bis 19:1 Solution (Biorad)
- Add 20.8µl 25% APS (Ammoniumperoxodisulfate, MERCK, Germany)
- Add 20.8µl TEMED (N,N,N',N'-Tetramethylethylenediamine, Sigma, USA)
- Mix
- Poor in prepared trays for gels (BioRAd PAGE system3)
- Put ridge in gel
- Wait until gel is solid
- Remove ridge
- Add 6x Loading Buffer to each sample
- Loading sample into slots
- Loading GeneRuler™ 50bp DNA Ladder in one slot
- Running gel with 80V, 1h, with a power supply (Power Pac 3.000. Biorad, USA)

#### **4.2.7.3. RNA-agarose-gel:**

Denaturing RNA-agarose-gel was done to check up RNA quality before cDNA synthesis. Ratio of 28S to 18S RNA bands shows the status of RNA degradation. Procedure as described in Atlas® Pure Total RNA Labeling System [96].

Material:

SeaKem® LE agarose

10x MOPS Buffer:

- 41.85g MOPS (Sigma-Aldrich, #M3183)
- 3.68g NaOAc\*3H<sub>2</sub>O
- 1.86g EDTA
- ddH<sub>2</sub>O to 200ml
- 5N NaOH
- pH 7
- ddH<sub>2</sub>O to 250ml
- Autoclave

12.3M formaldehyde

Loading solution:

- 45µl formamide
- 45µl 12.3M formaldehyde
- 10µl 10x MOPS Buffer
- 3.5µl Ethidium bromide (10mg/ml)
- 1.5µl 0.1M EDTA (pH 7.5)
- 8µl bromphenol blue dye and xylene dye (in 50% glycerol)

Procedure:

- 1g agarose
- 82.5ml ddH<sub>2</sub>O
- Add magnetic stir bar
- Heating at microwave until agarose is dissolved
- Cool down on magnetic stir-plate
- Add 10ml 10x MOPS
- Add 7.5ml 12.3M formaldehyde
- Pour onto gel tray
- Put ridge into gel
- Waiting until gel is solid
- Remove ridge
- Fill gel apparatus with 1x MOPS as running buffer

- Before use RNA-samples is heated to 56°C, 10' to prevent accumulation of RNA-aggregates
- 1µg RNA into 1.5ml tube
- Add 10µl Loading solution
- 70°C, 15'
- Cool on ice
- Load on gel
- Run gel with 80V until lower band reach last third of gel

#### **4.2.7.4. Visualisation:**

To visualize DNA on agarose-gel or PAGE, gels were stained by Ethidium Bromide (1:10.000 dilution, Sigma-Aldrich, #160539) for 10' and UV irradiated with GelDoc System (BioRad) or Typhoon TRO Variable Mode Imager (GE Healthcare).

#### **4.2.7.5. Marker:**

Used markers for length determination of nucleotides after gel electrophoresis (Figure 4.3.).

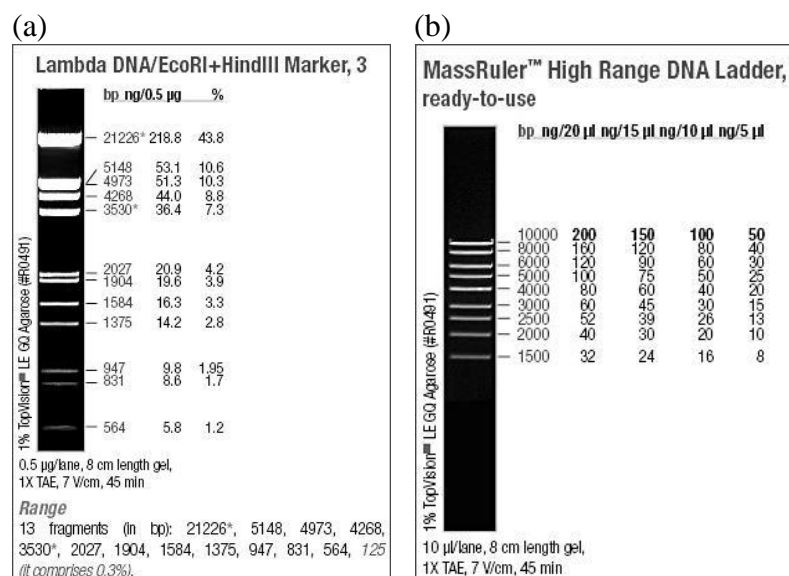


**Figure 4.3.: Used length markers**

(a): λ-marker map

(b): Mass Ruler map



#### **4.2.8. Real time polymerase chain reaction (Real Time-PCR):**

PCR is a molecular biological assay that allows amplifying specific DNA sequences. This method, invented by Kary Mullis, is today one of the most used techniques in molecular biological laboratories.

Primers, which are short oligonucleotides which bind to complementary sequences at template DNA, define amplifying part. Normally they have a length of 15 – 30 nucleotides. DNA-polymerase produces with free dNTPs (deoxy-nucleo-triphosphates) a new DNA. They are regulated by different steps. Polymerase derived from *thermus aquaticus*, a bacterium that, lives in geysers. This polymerase, called taq-polymerase survives high temperatures like appear in PCR-steps.

PCR-steps:

❖ Denaturation:

DNA-strands are separated by heating to 95°C

❖ Annealing:

Primers bind to complementary sequence at single strand template DNA. Temperature is primer dependent. Primer has to be in molar excess over DNA to force binding.

❖ Extension:

Polymerase recognizes free 3' of primer and adds nucleotides. A new DNA strand is produced. Polymerase works as long as temperature permits it or until template ends.

These steps are repeated 40 times to produce billions of requested DNA fragments. Often annealing step and extension step are combined to reduce time.

Real Time-PCR was used to investigate expression of TERRA, telomere length and for determination of 2p subtelomeric methylation.

#### **4.2.8.1. Apparatus and Software for analyses:**

All measurements were done at the same apparatus, 7500 Fast Real Time PCR System (Applied Biosystem) and analysed with 7500 software v2.0.3.

#### **4.2.8.2. Gene expression and telomere length Real Time-PCR:**

Real Time-PCRs were done with GoTaq® qPCR Master Mix (Promega, #A6001). Telomere length measuring based onto O'Callaghan et al. [97].

##### Material:

2x GoTaq® qPCR Master Mix

100x CRX Reference Dye

Tel1b primer

Tel2b primer

##### Procedure:

- For telomere length 30ng/96well were used
- For TERRA expression analyses 8ng/96well were used
- Before use of 2x GoTaq® qPCR Master Mix it had to be mixed with 100x CRX Reference Dye (1µl 100x CRX Reference Dye with 99µl 2x GoTaq® qPCR Master Mix)
- Mix Tel1b and Tel2b as forward and reverse primer
- Add 0.16µl primer mix (200nM) with 4µl 2x GoTaq® qPCR Master Mix with 100x CRX Reference Dye per sample
- Mix
- Pipetting 4µl master mix/96well with a low retention tip
- Pipetting 4µl sample/96well
- Sealing plate
- PCR-Program:
  - 95°C, 5' initial denaturation
  - 95°C, 30'' denaturation
  - 60°C, 1' annealing/extension
  - 60°C, 5' final extension
  - Melt curve

} 40 cycles

#### **4.2.8.3. 2p subtelomeric methylation specific RT-PCR:**

Based on recent publication of Kanel et al. (2010) [98].

FastDigest® MspI and FastDigest® HpaII (Fermentas, #FD0544. #FD0514) were used as restriction enzymes. RT-PCRs were done with Maxima® SYBR Green/ROX qPCR Master Mix (Fermentas, #K0251).

Sequence of 2p TERRA promoter region:

CTGCATAAGCGCACAGTCGCAAGCCGCCAGGCGCGGAGCGTGGGGGTGGCGGGG TGCAGGCGCAGAGACGGACGTCC <u>CCGG</u> GGGCGCGGCACAGAGACAGGTGGAAC CTCAATAATCCGAAAAGCCGGGCTC
---

**Figure 4.4.: Sequence of amplified 2p TERRA promoter region by 2p(new) primer (Table 4.7.):** Bold and underlined nucleotides show recognition sequence for restriction enzymes MspI and HpaII.

Material:

Sham-buffer:

- 10mM Tris
- 100mM NaCl
- 1mM dithiothreitol (Sigma-Aldrich, #43817)
- 0.1nM EDTA
- 200g/L BSA (Sigma-Aldrich, #A2153)
- 500ml/L glycerol

MspI, non-methylation sensitive restriction enzyme

HspII, methylation sensitive restriction enzyme with the same recognition sequence as MspI

Procedure:

- For 2p subtelomeric methylation specific RT-PCR 30ng/96well were used
- Mix CFTR as forward and reverse primer for housekeeping control MP\_HC2 forward and reverse for 2p subtelomeric region
- Add 0.16µl primer mix (200nM) with 4µl Master Mix per sample
- Pipetting 4µl master mix/96well with a low retention tip
- Pipetting 4µl sample/96well
- Short before PCR-start 0.3µl of restriction enzyme was added or sham buffer as control
- Sealing plate

- PCR-Program:
  - 37°C, 10' restriction enzymes cuts
  - 95°C, 2' initial denaturation
  - 95°C, 15'' denaturation
  - 60°C, 1' annealing/extension
  - 60°C, 5' final extension
  - Melt curve

} 40 cycles

For determination of methylation percentage following formula was used [98]:

$$\text{Methylation percentage} = 2^{(CT_{\text{uncut}} - CT_{\text{HpaII}})} * 100$$

Also percentage of successful cut was determined as control by a self developed formula:

$$\text{Cut percentage} = (1 - 2^{(CT_{\text{uncut}} - CT_{\text{MspI}})}) * 100$$

#### **4.2.8.4. Primer design and in-silico validation:**

Primers for RT-PCR were designed with the program CloneManager 9 (Scientific & Educational Software). Primers and target sequences were validated for product size and melting properties. DNA sequences were obtained from public database at the National Center Of Biotechnology Information (<http://www.ncbi.nlm.nih.gov>).

#### **4.2.8.5. Primer sequences:**

Primer for housekeeping gene 36B4 and  $\beta$ -actin were self-designed. Primers for TERRA and telomere length were also taken from literature [97] and have some special properties:

- ❖ The polymerase can start at the 3'-end, but only if primers are bound to telomeric sequence. If two primers bind themselves and produce a dimer polymerase it is not able to work, because every fifth and sixth base pair will give a mismatch. So the base on the 3' end remains unpaired and polymerase cannot start elongation.
- ❖ These primers have six bases on their 5' end, which do not pair, when the rest of the primers are annealed to telomeric sequence. The counterpart for these six bases is built on the 3' end of each produced amplicon and should inhibit binding of primers somewhere in the middle of the amplicon.

Subtelomeric TERRA specific primers were self-designed or taken from literature. 10q [73] and 10p [72] were from literature, 18p and 2p self-designed with Clonemanager 9 (Table 4.5., 4.6. and 4.7.).

**Table 4.5.: Primers for housekeeping genes:** Optimal Tm and GC-content were determined by Clonemanager9

Gene:	Primer:	Sequence:	optimal Tm:	GC-content:
36B4	36B4-fwd	5'-CAG CAA GTG GGA AGG TGT AAT CC-3'	65°C	52%
	36B4-rev	5'-CCC ATT CTA TCA TCA ACG GGT ACA A-3'	64°C	44%
β-actin:	β-actin-fwd	5'-GGA TGC AGA AGG AGA TCA CTG-3'	62°C	52%
	β-actin-rev	5'-CGA TCC ACA CGG AGT ACT TG-3'	62°C	55%

**Table 4.6.: Primers for telomere length and TERRA:** Optimal Tm and GC-content were determined by Clonemanager9

Gene:	Primer:	Sequence:	optimal Tm:	GC-content:
TERRA/telomere length	tel1b	5'-CGG TTT GTT TGG GTT TGG GTT TGG GTT TGG GTT TGG GGT-3'	78°C	51%
	tel2b	5'-GGC TTG CCT TAC CCT TAC CCT TAC CCT TAC CCT TAC CCT-3'	77°C	53%
Chromosome 2p:	chr2_590	5'-TAA GCC GAA GCC TAA CTC GTG TC-3'	66°C	52%
	chr2_738	5'-GTA AAG GCG AAG CAG CAT TCT CC-3'	66°C	52%
Chromosome 18p:	chr18_617	5'-CCT AAC CCT CAC CCT TCT AAC-3'	61°C	52%
	chr18_725	5'-ACC AGC CAC CAC TTT CTG ATA GG-3'	66°C	52%
Chromosome 10p:	chr10p_fwd	5'-TAA AAA TGT TTC CCG GTT GC-3'	59°C	40%
	chr10p_rev	5'-CAC CCT CAC CCT AAG CAC AT-3'	63°C	59%
Chromosome 10q:	chr10q_fwd	5'-GAA TCC TGC GCA CCG AGA T-3'	64°C	40%
	chr10q_rev	5'-CTG CAC TTG AAC CCT GCA ATA C-3'	64°C	50%

**Table 4.7.: Primers for 2p subtelomeric methylation specific Real time-PCR:** Optimal Tm and GC-content were determined by Clonemanager9

Gene:	Primer:	Sequence:	optimal Tm:	GC-content:
CFTR:	CFTR fwd	5'-TTC CAG GTC CGT GTC CTT A-3'	62°C	51%
	CFTR rev	5'-GAA GGA GGG TCT AGG AAG C-3'	60°C	57%
2p (new):	HC2_fwd	5'-CTG CAT AAG CGC ACA GTC-3'	60°C	55%
	HC2_rev	5'-GAG CCC GGC TTT TCG GAT-3'	64°C	61%

#### **4.2.8.6. Evaluation of Real-Time PCRs:**

Efficiency (E) of  $\beta$ -actin, 36B4 and TERRA were measured prior.  $\beta$ -actin has an efficiency of 0.93 (93%), 36B4 of 0.97 (97%) and TERRA of 0.83 (83%).

Analyse with BestKeeper calculates and evaluates the performance of the housekeeping genes. Geometric and arithmetic means of CT values, then all possible pair combinations between the candidates are calculated and the correlated with Pearson correlation. This results in Pearson correlation coefficients (r) and error probability (p-value). In addition the Best Keeper index (BK) is formed and the individual Housekeeping genes are then ultimately correlated with the BK-index. Correlation coefficients (r), coefficient of determination (R<sup>2</sup>) and error probability (p) are calculated. The coefficient of determination (R<sup>2</sup>) specifies how exact statements about the correlation coefficient (r) could be made.

Validations of results were determined by standard deviation of cycle-thresholds. Standard deviations below 0.5 were esteemed as valid.

Relative quantitation showed the difference between the amounts of a sample in comparison with a reference sample.

$$RQ = (E_{\text{target}} + 1)^{\Delta C_{\text{t target (sample-reference sample)}}} / (E_{\text{Housekeeping}} + 1)^{\Delta C_{\text{t housekeeping (sample-reference sample)}}$$

#### **4.3. Statistics:**

Statistics calculations were done with GraphPad Prism 5.02. One-way Anova to determine if differences between RQs are significant different and Post-test to determine if TERRA expressions and confluences show a linear trend were done. P-values below 5% (0.0500) were

assessed as significant different and also for linear trend analysis, P-value of 5% (0.0500) was used as threshold.

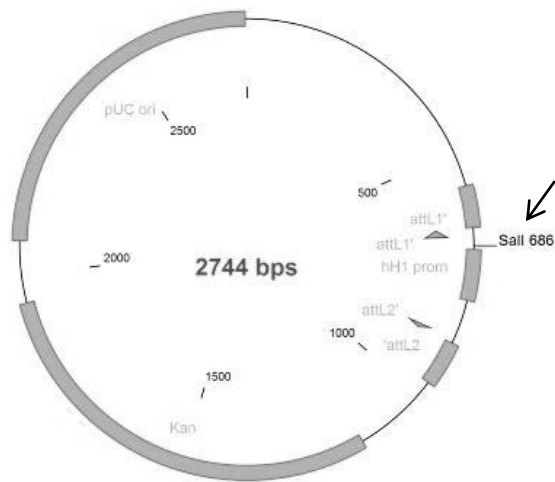
## **5. Results:**

### **5.1. Construction of TERRA expressing vectors:**

The cloning-strategy was a multistep process which started from two vectors, pSP73 with the telomere fragment and the pENTR/D/hH1-shNMP265. At the end the telomere fragment should be in viral vectors, pAd/L-DEST<sup>TM</sup>, pAd/CMV/V5-DEST<sup>TM</sup>, pLenti6/UbC/V5-DEST and pLenti6/BLOCK-iT<sup>TM</sup>-DEST. Plasmid-DNA were isolated with Wizard<sup>®</sup> *Plus* SV Minipreps DNA Purification Systems like described in material and methods, otherwise it is mentioned. Figure 5.1. shows a schematic presentation of the cloning strategy which are described at the next chapters.



pENTR/D/hH1 shRNA NMP265



pENTR/D/hH1 shNMP265 Delta SalI

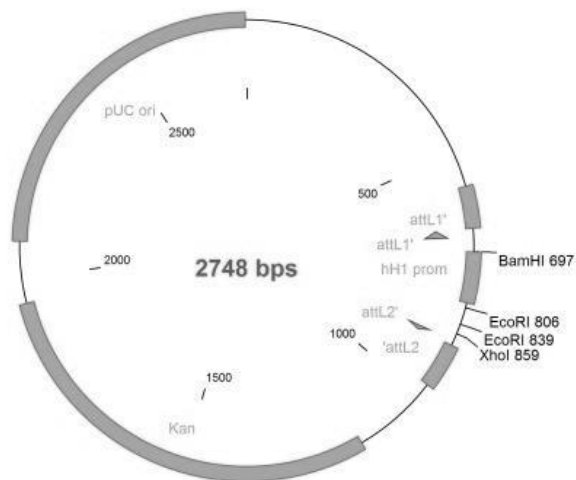
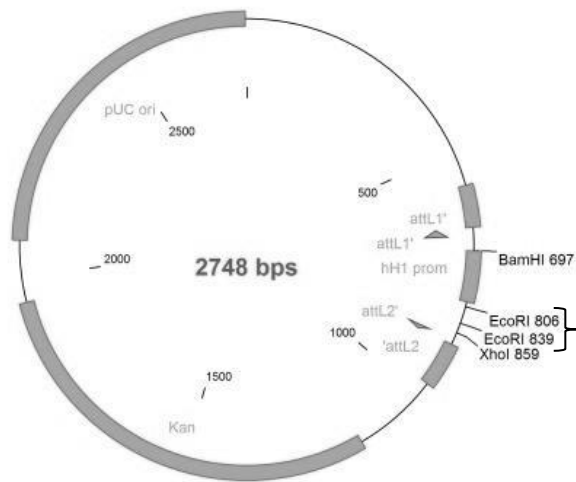


**Figure 5.1.: Schema of cloning strategy:**

Deletion of SalI restriction site (marked with arrow) from pENTR/D/hH1 shRNA NMP265 (Chapter 5.1.2.1.)

pENTR/D/hH1 shNMP265 Delta Sall



pENTR/D/hH1 delta shNMP265

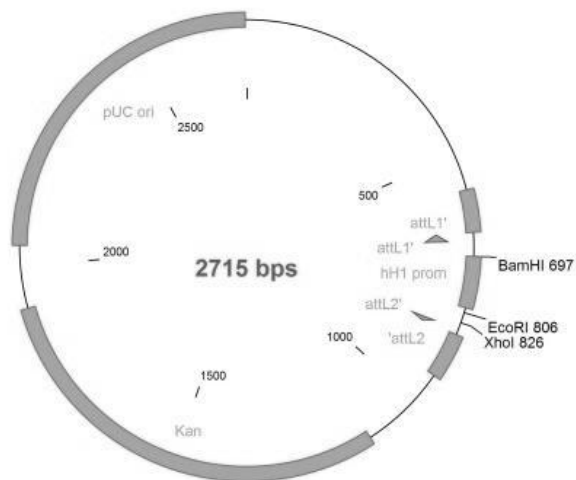
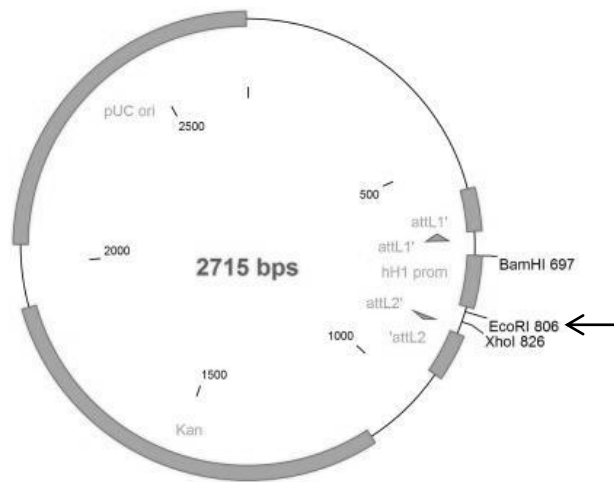


**Figure 5.1. (continued):** Schematic vector maps of shRNA NMP265 deletion. Clamp shows removed part (Chapter 5.1.2.2.).

pENTR/D/hH1 delta shNMP265



pENTR/D/hH1 Linker

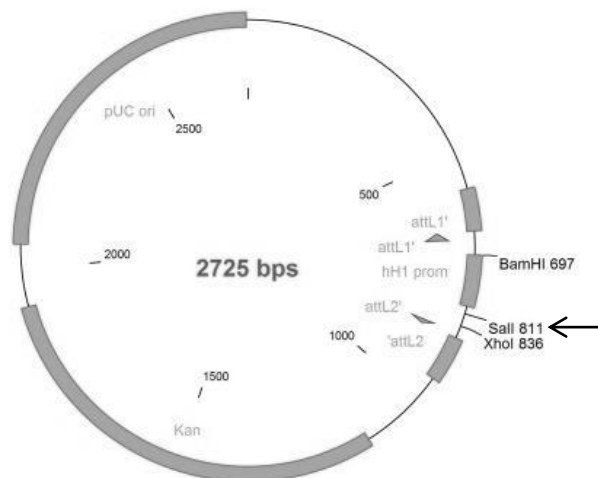


**Figure 5.1. (continued):** Schema of linker insertion. Cut at EcoRI restriction site (marked with arrow), integration of Linker and formation of new SalI restriction site (marked with arrow) (Chapter 5.1.2.3.).

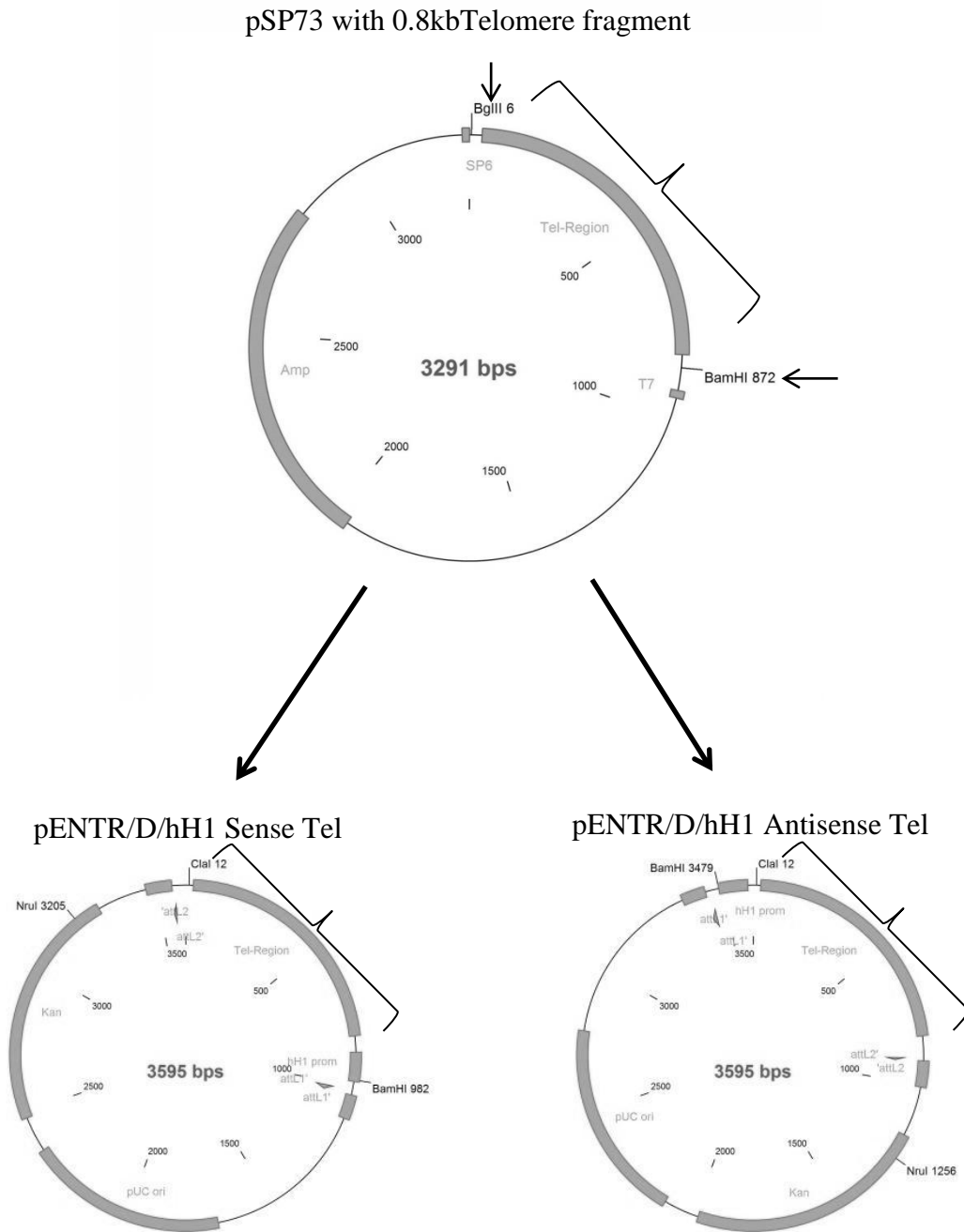


**Figure 5.1. (continued):** Cut of Vector pSP73 with telomere fragment (marked with clamp) with BamHI and BglII (marked with arrows), partial fill-in and transfer into pENTR/D/hH1 Linker cutted with SalI and following partial fill-in. Two vectors with different telomere fragment orientation were produced, sense and antisense orientation (Chapter 5.1.3.).

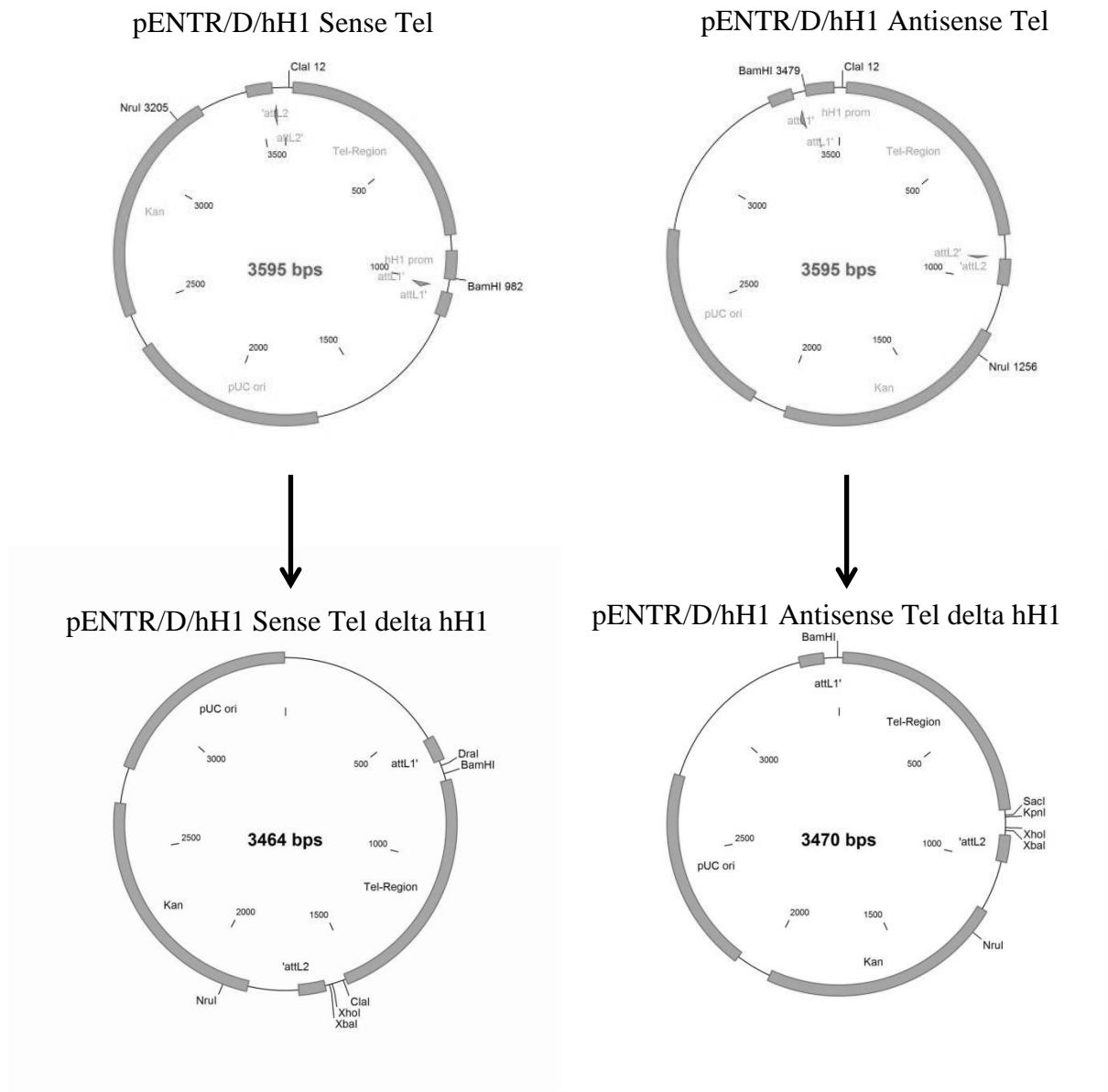


**Figure 5.1. (continued):** Deletion of hH1 promoter regions of pENTR/D/hH1 Sense Tel and pENTR/D/hH1 Antisense Tel (Chapter 5.1.4.).

### **5.1.1. Sequencing of pSP73 with telomere fragment:**

First sequencing of pSP73 with the telomere fragment was carried out. For this the plasmid was sent to VBC genomics and was sequenced from both sites of the inserted fragment. From one site it was sequenced from T7 promoter and from the other from SP6 promoter (Figure 5.2.). This displayed that the telomere sequence is contained in the vector and also showed the orientation.











termed pENTR/D/hH1 deltaSalI (supplement Figure 10.2.) and was used for further cloning steps.

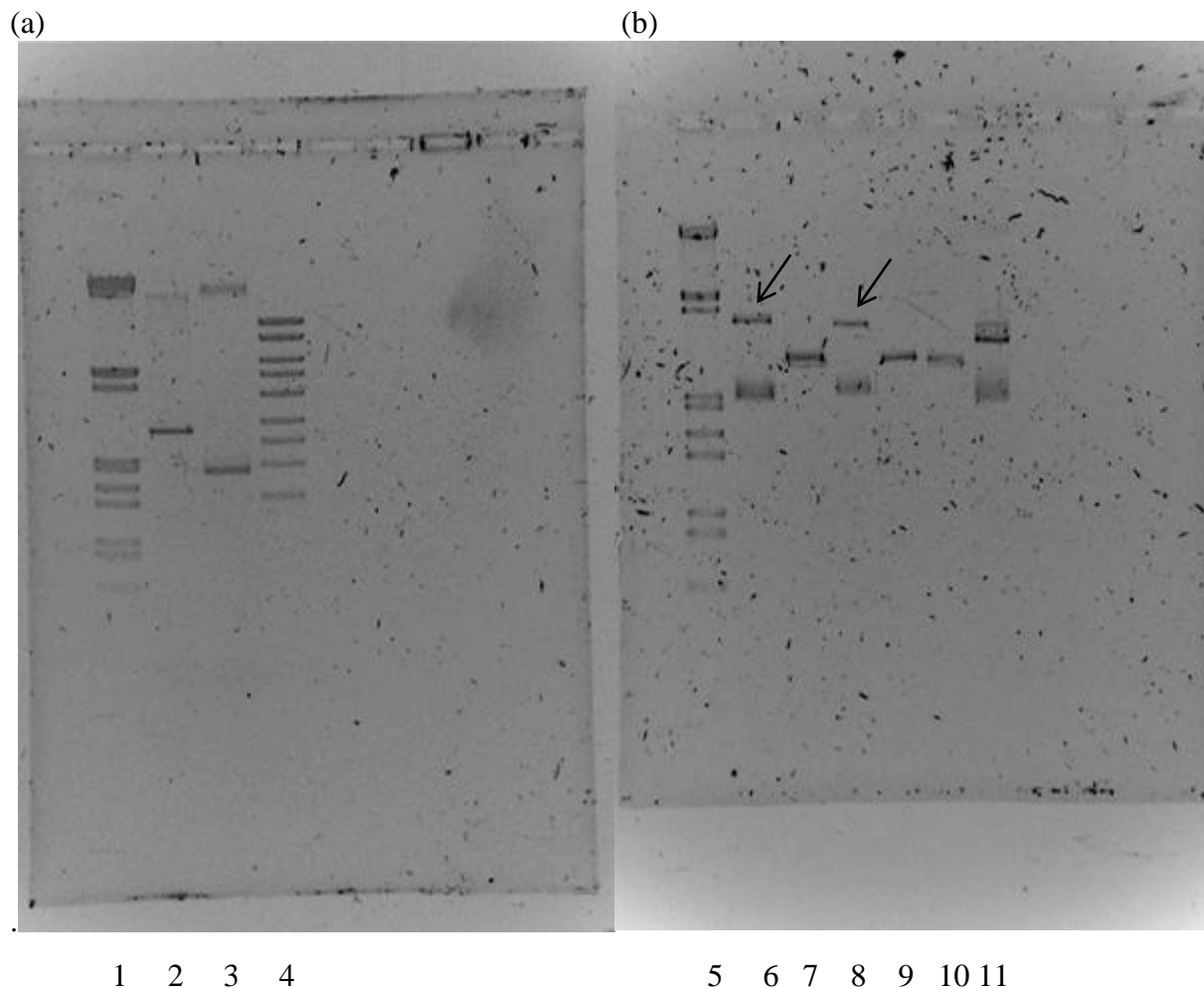


**Figure 5.3.: 1% agarose-gel of SalI restriction site elimination of pENTR/D/hH1 shNMP265:**

(a) pENTR/D/hH1 shNMP265 before SalI restriction site elimination: (1)  $\lambda$ -marker, (2) pENTR/D/hH1 shNMP265 uncut, (3) pENTR/D/hH1 shNMP265 digested with SalI resulted 2744bps, (4) Mass ruler

(b) Analysed clones (5)  $\lambda$ -marker, (6) clone 1 SalI cut, (7) clone 1 BamHI cut, (8) clone 1 uncut, (9) clone 2 SalI cut, (10) clone 2 BamHI cut, (11) clone 2 uncut. Arrows show uncut and clone with SalI cut with no SalI restriction site (Clone 1. lane 6 - 8)

#### **5.1.2.2. Elimination of shNMP265 expression cassette:**

With EcoRI the shNMP265 expression cassette was cut out and after the vector was ligated. This led in regulatory elements for polymerase III expression, like the start nucleotide

position and the poly-T sequence, as stop signal. Transformation, picking four clones and DNA-isolation followed. Vector was controlled with XhoI and BamHI cuts on 5% PAGE gel (Figure 5.4). Clone C showed a shift of banding patterns (33bps) and was so identified as correct clone, termed pENTR/D/hH1 delta shNMP265 (supplement Figure 10.3.) and was used for further cloning steps.

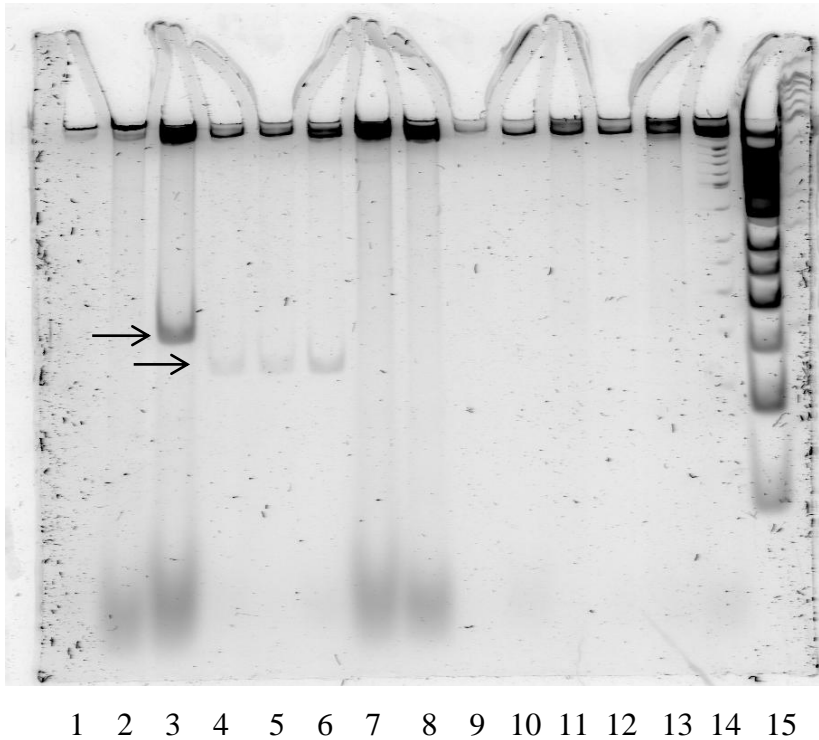


**Figure 5.4.: Removing shNMP265 expression cassette of pENTR/D/hH1 NMP265-shRNA:**

5% PAGE-gel: (1) clone C uncut, (2) pENTR NMP265-shRNA uncut, (3) pENTR NMP265-shRNA XhoI + BamHI cut, (4) clone C XhoI + BamHI cut, (5) clone B XhoI + BamHI cut, (6) clone A XhoI + BamHI cut, (7) pENTR NMP265-shRNA BamHI cut, (8) pENTR NMP265-shRNA XhoI cut, (9) clone C BamHI cut, (10) clone C XhoI cut, (11) clone B BamHI cut, (12) clone B XhoI cut, (13) clone A BamHI cut, (14) clone A XhoI, (15) 50bp marker. Shift of about 33bps is visible (marked with arrows)

**5.1.2.3. Insert new SalI restriction site with a linker into polymerase III expression cassette:**

To insert a new SalI restriction site on a desired position a linker was ordered from VBC genomics. This linker had a SalI restriction site and EcoRI recognition sites (Figure 5.5. b).

Before use, the linker had to be phosphorylated and annealed as described in material and methods. With EcoRI cut and ligation the linker was infixed. Before transformation EcoRI recut was conducted to cut vectors without an integrated linker. After transformation two clones were picked and plasmid-DNA was isolated for restriction analyses. Clone II showed the existence of a SalI restriction site and with a double cut using SalI and MluI which showed fragments of 1212bps, 932bps and 581bps, the correct position within the expression cassette was determined (Figure 5.5.a). The clone was termed pENTR/D/hH1 Linker (supplement Figure 10.4.)

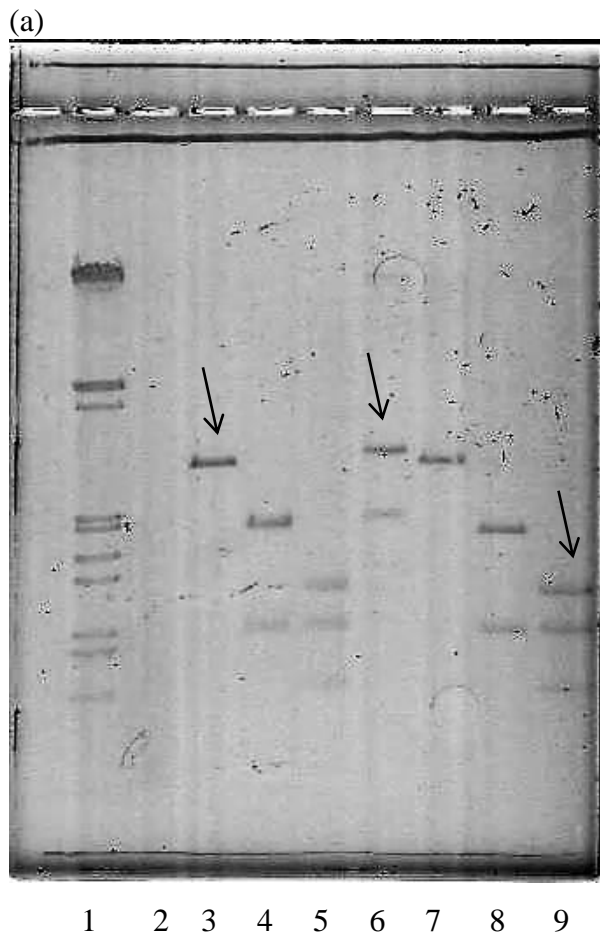


**Figure 5.5.: Linker integration into pENTR/D/hH1 expression cassette:**

(a) 1% agarose-gel, pENTR/D/hH1 with linker integrated, (1)  $\lambda$ -marker, (2) clone I uncut (not visible), (3) clone I SalI cut, (4) clone I MluI cut, (5) clone I SalI and MluI cut, (6) clone II uncut, (7) clone II SalI cut resulted 2725bps, (8) clone II MluI cut resulted 1793bps and 932bps, (9) clone II SalI and MluI cut resulted 1212bps, 932bps and 581bps. Plasmid fragments of predicted sizes are marked with arrows

(b)

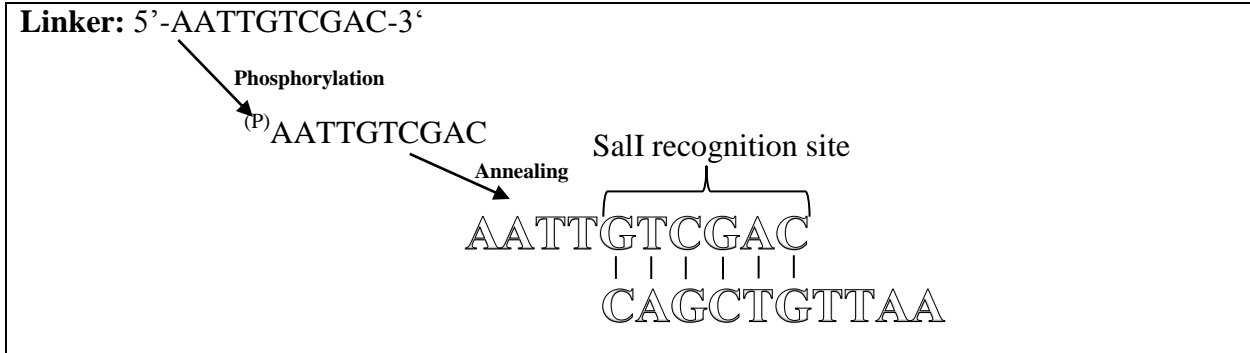


**Figure 5.5. (continued):**

(b) Schematic demonstration of linker preconditioning before cloning into the EcoRI site of plasmid DNA to insert new SalI restriction site

### **5.1.3. Cloning the telomere fragment:**

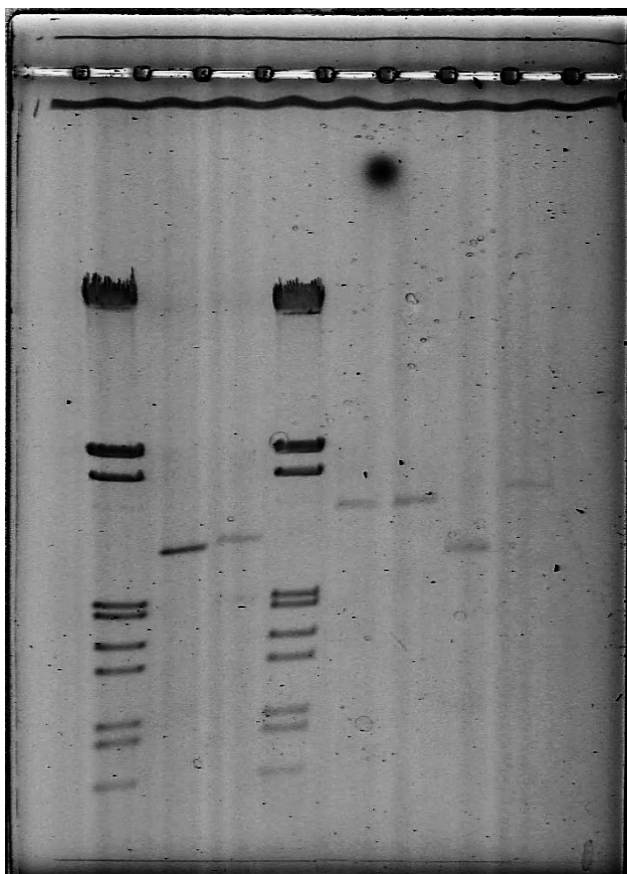
The telomere fragment was cloned from pSP73 to pENTR/D/hH1 and in addition transferred into gateway compatible pDEST viral expression vectors.

#### **5.1.3.1. pENTR/D/Linker antisense Tel:**

Plasmid DNA pSP73 with telomere fragment (supplement Figure 10.5.) was restricted with BamHI and BglII, this produced a predicted 866bps telomere fragment and a 2435bps remaining vector backbone with ampicillin resistance (Figure 5.6). After gel-purification of the telomere fragment, partial fill in with Klenow-fragment and dGTP and dATP followed as described in material and methods.

Plasmid DNA pENTR/D/hH1 Linker was restricted with SalI (Figure 5.6.) and a partial fill in with Klenow-fragment and dTTP and dCTP resulted into a complementary overhang for the inserting-step of the telomere fragment.

After the ligation before transformation, SalI recut was done to get rid of vectors without telomere fragment.



1 2 3 4 5 6 7 8

**Figure 5.6.: pSP73 and pENTR/D/hH1 Linker restriction:**

1% agarose-gel, (1)  $\lambda$ -marker, (2) pENTR/D/hH1 Linker SalI cut resulted predicted and seen 3kb fragment, (3) pENTR/D/ Linker uncut differs to fragment of lane 2. (4)  $\lambda$ -marker, (5) pSP73 Tel BamHI cut resulted 3291bps, (6) pSP73 Tel BglII cut resulted 3291bps, (7) pSP73 Tel BamHI and BglII cut resulted 2425bps and 866bps, (8) pSP73 Tel uncut differs to single (lane 5 and 6) and double cuts (lane 7) .

Efficiency of transformation was very low, although control transformation with pUC19 DNA reaches  $10^6$  transformants per  $\mu\text{g}$  plasmid (data not shown). Few transformations had to be done to obtain one E.coli colony with a correct insert. Plasmid DNA from colony was checked with EcoRI cut which showed the telomere fragment with the expected size of about 817bps and fragments with 2769 bps and 10bps. Orientation was checked by a double restriction cut with ClaI and NruI (Figure 5.7). NruI cut outside of the inserted fragment, ClaI cut inside and showed bands of 2350bps and 1245bps which were predicted. So pENTR/D/Linker with a telomere fragment with an antisense orientation was identified and termed pENTR/D/hH1 Antisense Tel (supplement Figure 10.6.).

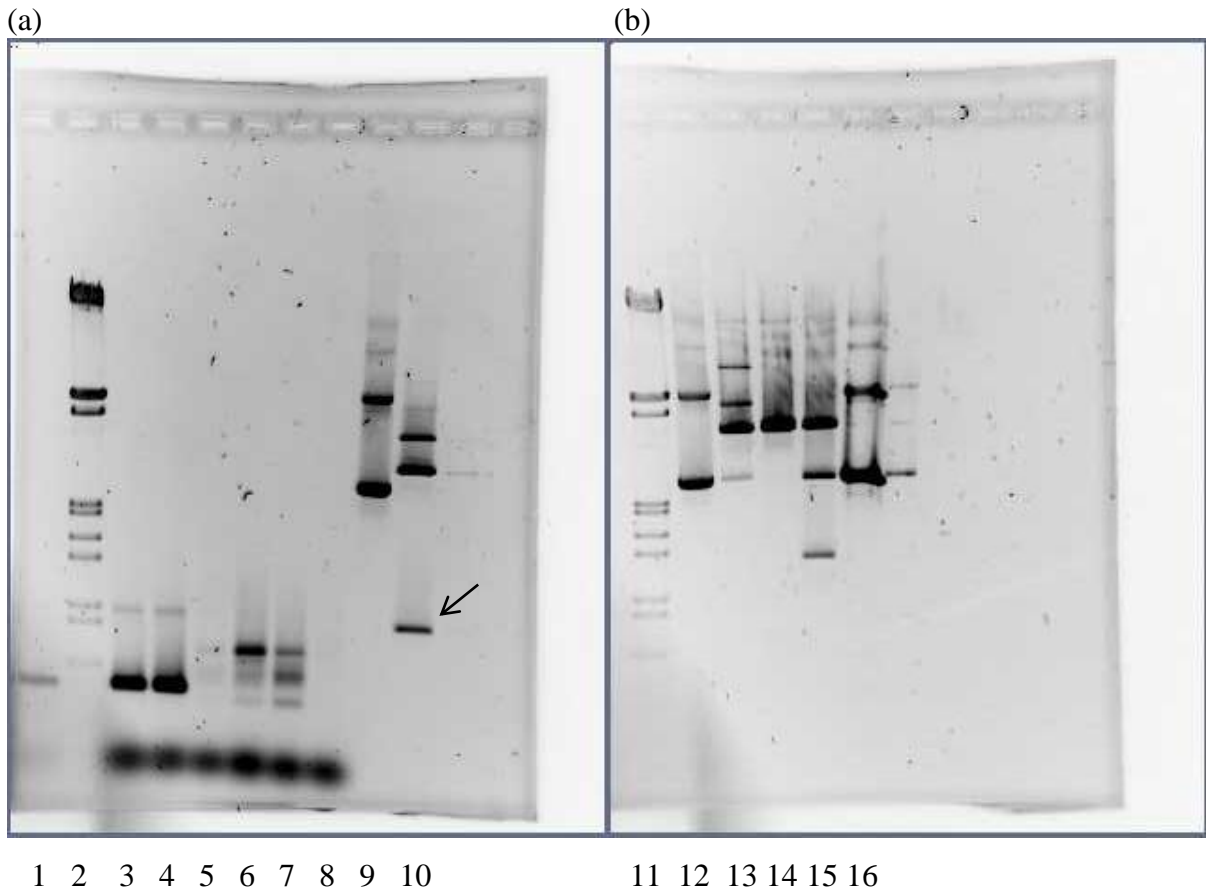


**Figure 5.7.: pENTR/D/hH1 Antisense Tel identification**

(a) 1% agarose-gel for examination if telomere fragment was inside (1) other experiment, (2)  $\lambda$ -marker, (3) – (8) other experiment, (9) pENTR/D/hH1 antisense Tel uncut, (10) pENTR/D/hH1 antisense Tel EcoRI cut. This partial cut showed a single clear band of telomere fragment with predicted size of 817bps (marked with arrow) and together with the detected size of 2768bps and 10bps of the vector backbone resulted size of 3595bps for the linear plasmid

(b) 1% agarose-gel to check-up orientation of insert, (11)  $\lambda$ -marker, (12) pENTR/D/hH1 antisense Tel uncut, (13) pENTR/D/hH1 antisense Tel ClaI cut resulted 3595bps, (14) pENTR/D/hH1 antisense Tel NruI cut resulted 3595bps, (15) pENTR/D/hH1 antisense Tel ClaI and NruI cut resulted 2350bps and 1245bps, (16) pENTR/D/hH1 antisense Tel uncut

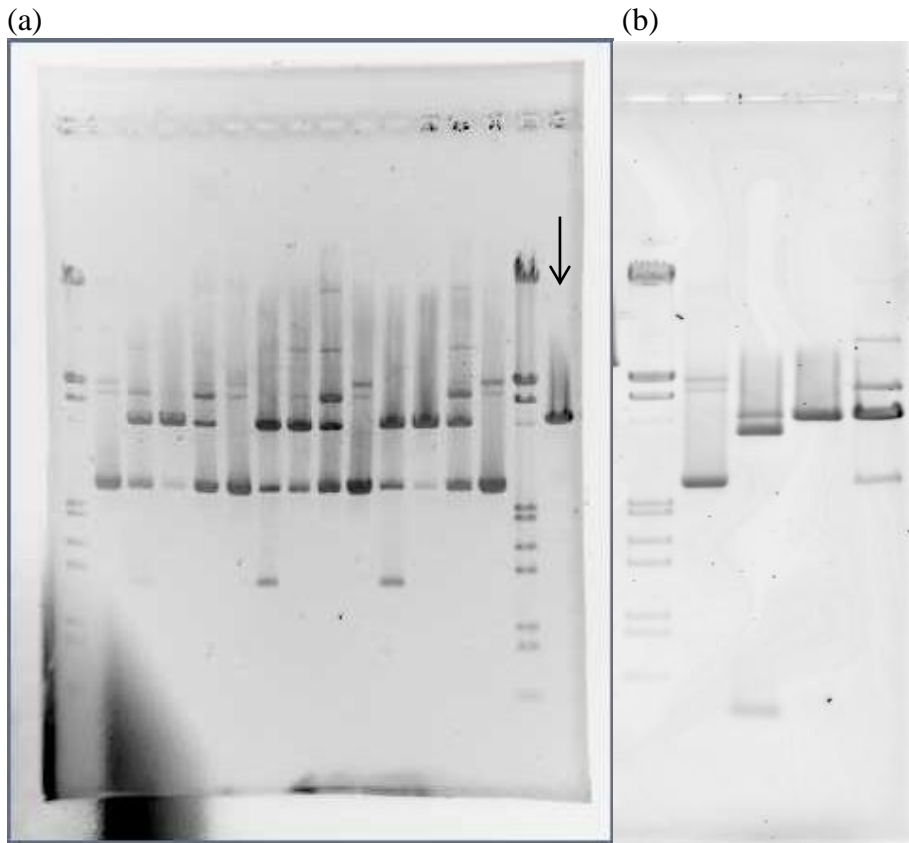
**5.1.3.2. pENTR/D/Linker sense Tel:**

Because of the low transformation efficiency results of the cloning strategy described under 5.1.3.1., other procedures were applied. For instance an EcoRI cut of the pENTR/D/Linker antisense Tel followed up by ligation was tried. This should lead to a vector with both, a

telomere fragment with sense and anti-sense orientation, but after transformation and investigation of some clones no vector with telomere fragment with sense orientation could be found (data not shown). Specific modifications of the cloning strategy and new experiments finally led to a more efficient procedure (Figure 5.9).

To produce a pENTR/D/Linker with a telomere fragment with a sense orientation the experimental application flow was changed as described in brief. Cut of pSP73 with telomere fragment with BamHI and BglII and pENTR/D/hH1 cut with SalI still remained the same. But then gel purification-step and Klenow fill in were flipped. This strategy finally resulted with a pENTR vector with a telomere fragment with sense orientation. SalI recut after ligation and transformation were the same as at producing of pENTR/Linker antisense Tel vector. Using this strategy four colonies were obtained. Plasmid DNA of clone IV showed expected size of 3595bps which is the size of the vector with Tel fragment (Figure 5.8.). Orientation was checked with NruI and ClaI restriction as it was done at pENTR/D/hH1 Antisense Tel. Clone IV showed banding patterns of 3192bps and 403bps which were predicted. This identified clone was termed pENTR/D/hH1 Sense Tel (supplement Figure 10.7).



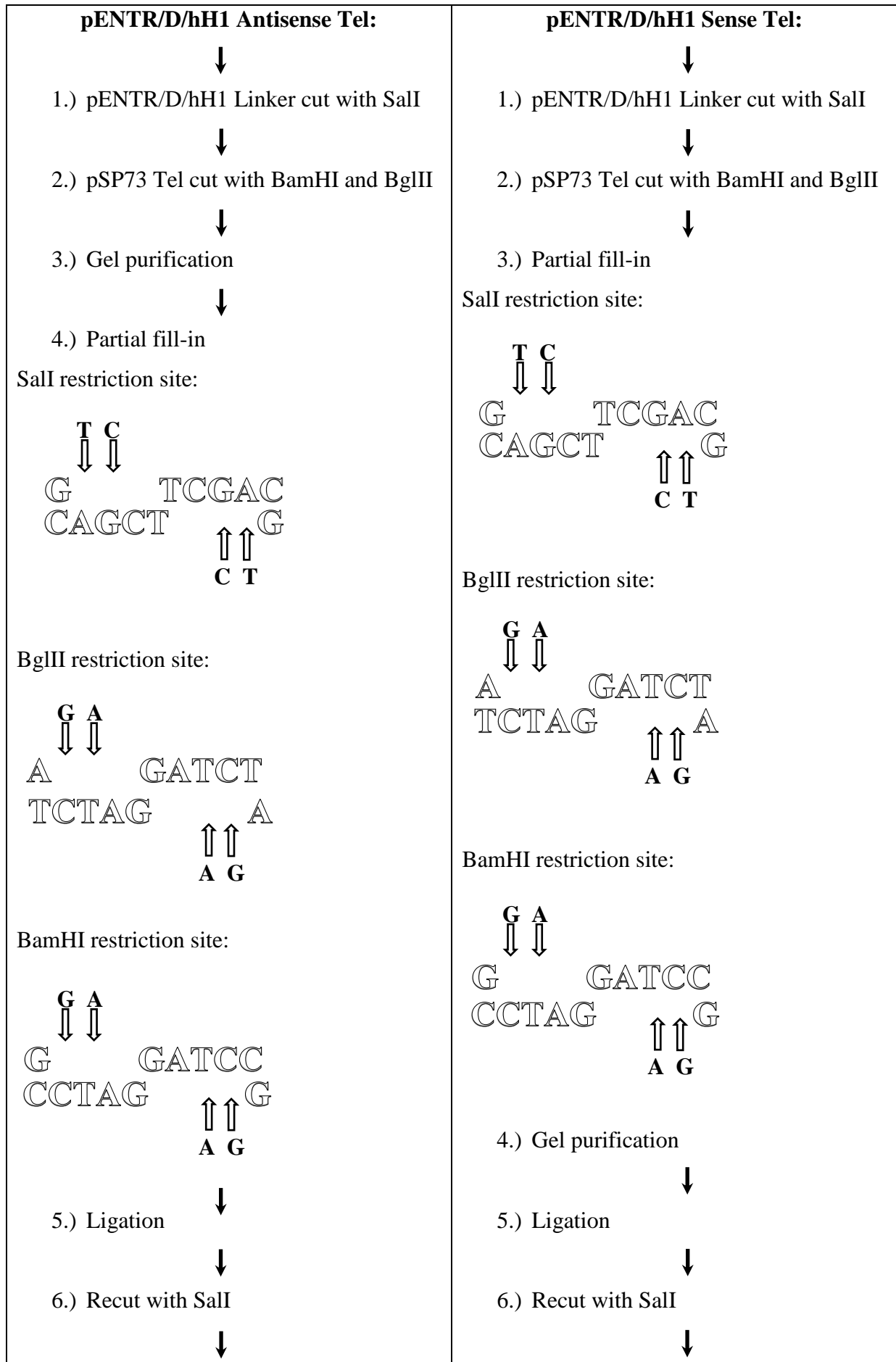


1 2 3 4 5 6 7 8 9 10 11 12 13 14 15 16 17 18 19 20 21  
**Figure 5.8.: pENTR/D/hH1 Sense Tel identification:**

(a): 1% agarose-gel for examination if telomere fragment was inside, (1)  $\lambda$ -marker, (2) clone I uncut, (3) clone I NruI and ClaI cut, (4) clone I NruI cut, (5) clone I ClaI cut, (6) clone II uncut, (7) clone II NruI and ClaI cut, (8) clone II NruI cut, (9) clone II ClaI cut, (10) clone III uncut, (11) clone III NruI and ClaI cut, (12) clone III NruI cut, (13) clone III ClaI cut, (14) clone IV uncut, (15)  $\lambda$ -marker, (16) clone IV BamHI cut. Clone IV showed correct size (marked with arrow)

(b): 1% agarose-gel to check-up orientation of insert, (17)  $\lambda$ -marker, (18) clone IV uncut, (19) clone IV NruI and ClaI cut resulted 3192bps and 403bps, (20) clone IV NruI cut resulted 3595bps, (21) clone IV ClaI cut resulted 3595bps

Schematic presentation of cloning steps (Figure 5.9.) gives an overview about the production of pENTR vectors with telomere fragments in sense and antisense orientation.



7.) Transformation into competent E.coli ↓	7.) Transformation into competent E.coli ↓
8.) pENTR/D/hH1 Antisense Tel	8.) pENTR/D/hH1 Sense Tel

**Figure 5.9.: Schematic illustration of strategy for production of pENTR/D/hH1 with telomere fragment in sense and anti-sense orientation:**

- 1.), 2.): Cut of the two provenience vectors pENTR/D/hH1 Linker with SalI and pSP73 Tel with BamHI and BglII
- 3.), 4.): These two steps were different between the constructions of the two vectors. At pENTR/D/hH1 Antisense Tel construction gel purification was first done and then Klenow fill-in. At pENTR/D/hH1 Sense Tel construction first Klenow fill-in was done and then gel purification. This resulted in a higher efficiency of resulting transformants. The pictures of Klenow fill-in show the partial fill-in assembly of the specific bases (black) into the 5'overhangs of the restriction sites (white)
- 5.) – 7.): These steps were done as usual like described into material and methods. Recut with SalI avoided self-ligation of outcome vector
- 8.) Vector maps of pENTR/D/hH1 Sense Tel and pENTR/D/hH1 Antisense Tel. Clamps show region of telomeric repeats. Arrows show restriction enzyme sites of NruI and ClaI for orientation check of telomeric region

#### **5.1.4. Creating promoter-less constructs:**

Deletion of hH1 promoter allows the use of constructs with promoters other than polymeraseIII in Gateway expression vectors with built in expression cassettes.

##### **5.1.4.1. Promoter deletion:**

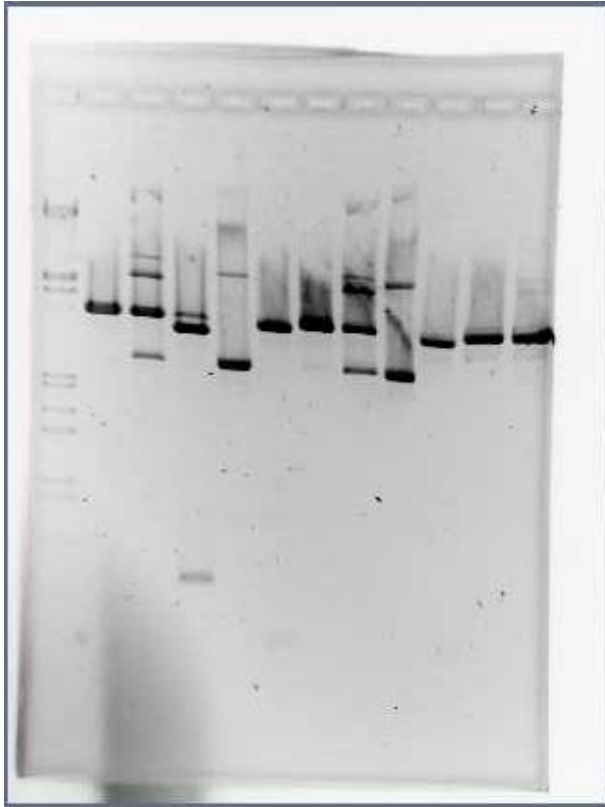
The hH1 promoter was cut out and the ends blunted. Religation, recut and transformation resulted into pENTR/D/linker with telomere fragments in both orientations and without functional promoter sequences.

#### **5.1.4.1.1. Deletion of hH1 in pENTR/D/Linker sense Tel:**

pENTR/D/Linker Sense Tel was cut with SacI and BamHI to cut out hH1 promoter and showed bands of 3464bps and 131bps (Figure 5.10). Because of the 3' overhang which resulted from SacI cut, exonucleolytic activity of Klenow fragment was used to create blunt ends. Fill in of BamHI 5' overhang with Klenow fragment, ligation and recut with SacI and BamHI were done to reduce original vector background. After transformation and plasmid DNA isolation from two colonies, clone 1 showed shift of estimated 131bps and no SacI or BamHI restriction site was found (Figure 5.11). This clone was termed pENTR/D/ Sense Tel  $\Delta$ hH1 (supplement Figure 10.8.).

#### **5.1.4.1.2. Deletion of hH1 in pENTR/D/Linker antisense Tel:**

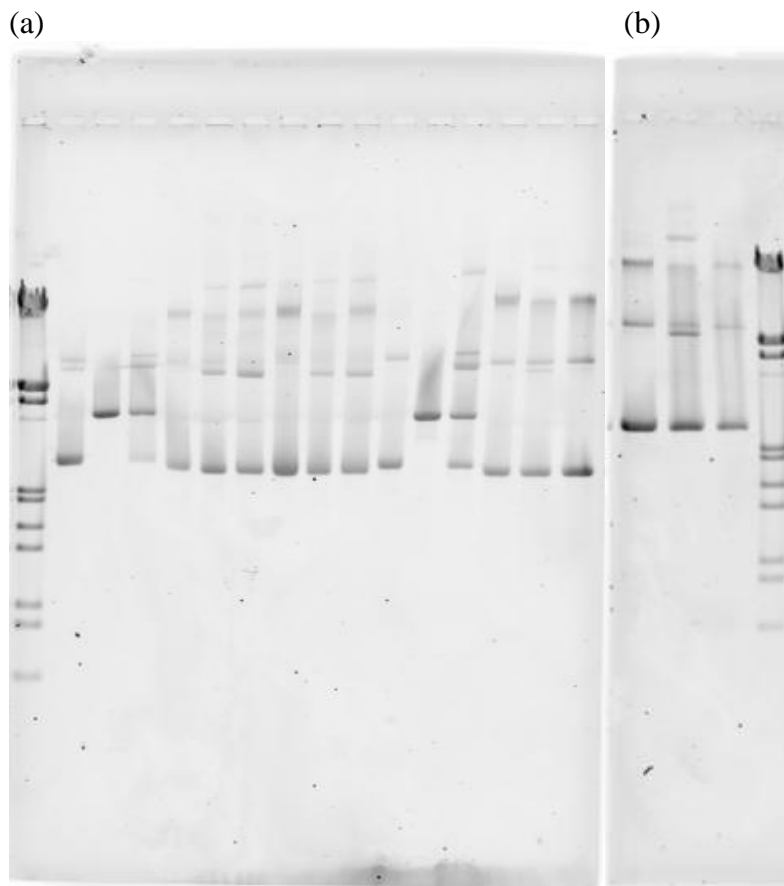
For creating the pENTR/D/Linker antisense Tel vector with deleted hH1 promoter, vector was cut with ClaI and BamHI and showed bands of 3470bps and 125bps (Figure 5.10.). Fill in with Klenow fragment, ligation and recut with ClaI and BamHI. After transformation and plasmid DNA isolation, clone 1 showed a shift of estimated 125bps and no BamHI or ClaI restriction site was found (Figure 5.11.). This clone was termed pENTR/D/ Antisense Tel  $\Delta$ hH1 (supplement Figure 10.9.).



1 2 3 4 5 6 7 8 9 10 11 12

**Figure 5.10.: Promotor deletion construction of pENTR/D/hH1 Tel plasmids:**

1% agarose-gel: (1)  $\lambda$ -marker, (2) pENTR/D/hH1 Sense Tel NruI cut resulted 3595bps, (3) pENTR/D/hH1 Sense Tel ClaI cut resulted 3595bps, (4) pENTR/D/hH1 Sense Tel NruI and ClaI cut resulted 3192bps and 403bps, (5) pENTR/D/hH1 Sense Tel uncut, (6) pENTR/D/hH1 Sense Tel BamHI and SacI cut resulted 3464bps and 131bps, (7) pENTR/D/hH1 Sense Tel BamHI cut resulted 3595bps, (8) pENTR/D/hH1 Sense Tel SacI cut resulted 3595bps, (9) pENTR/D/hH1 Antisense Tel uncut, (10) pENTR/D/hH1 Antisense Tel BamHI and ClaI cut resulted 3470bps and 125bps, (11) pENTR/D/hH1 Antisense Tel BamHI cut resulted 3595bps, (12) pENTR/D/hH1 Antisense Tel ClaI cut resulted 3595bps



1 2 3 4 5 6 7 8 9 10 11 12 13 14 15 16 17 18 19 20

**Figure 5.11.: Identification of promotor deletion of pENTR/D/hH1 Sense Tel and pENTR/D/hH1 Antisense Tel: 1% agarose-gels**

(a): (1)  $\lambda$ -marker, (2) pENTR/D/hH1 Antisense Tel uncut, (3) pENTR/D/hH1 Sense Tel BamHI cut, (4) pENTR/D/hH1 Sense Tel SacI cut, (5) clone 1 Sense Tel  $\Delta$ hH1 uncut, (6) clone 1 Sense Tel  $\Delta$ hH1 BamHI cut, (7) clone 1 Sense Tel  $\Delta$ hH1 SacI cut, (8) clone 2 Sense Tel  $\Delta$ hH1 uncut, (9) clone 2 Sense Tel  $\Delta$ hH1 BamHI cut, (10) clone 2 Sense Tel  $\Delta$ hH1 SacI cut, (11) pENTR/D/hH1 Antisense Tel uncut, (12) pENTR/D/hH1 Antisense Tel BamHI cut, (13) pENTR/D/hH1 Antisense Tel ClaI cut, (14) clone 1 Antisense Tel  $\Delta$ hH1 uncut, (15) clone 1 Antisense Tel  $\Delta$ hH1 BamHI cut, (16) clone 1 Antisense Tel  $\Delta$ hH1 ClaI cut

(b) (17) clone 2 Antisense Tel  $\Delta$ hH1 uncut, (18) clone 2 Antisense Tel  $\Delta$ hH1 BamHI cut, (19) clone 2 Antisense Tel  $\Delta$ hH1 ClaI cut, (20)  $\lambda$ -marker

### **5.1.5. Transfer telomere fragment into viral vectors:**

All used viral vectors are Gateway compatible destination vectors as described under material and methods.

### **5.1.5.1. Gateway system:**

For successful Gateway reactions the viral destination vectors had to be isolated with SNAP-plasmid DNA preparation as described under material and methods. Trying to execute the Gateway reaction with DNA isolated with Wizard<sup>®</sup> Plus SV Minipreps DNA Purification Systems did not work with adenoviral expression vectors (not shown).

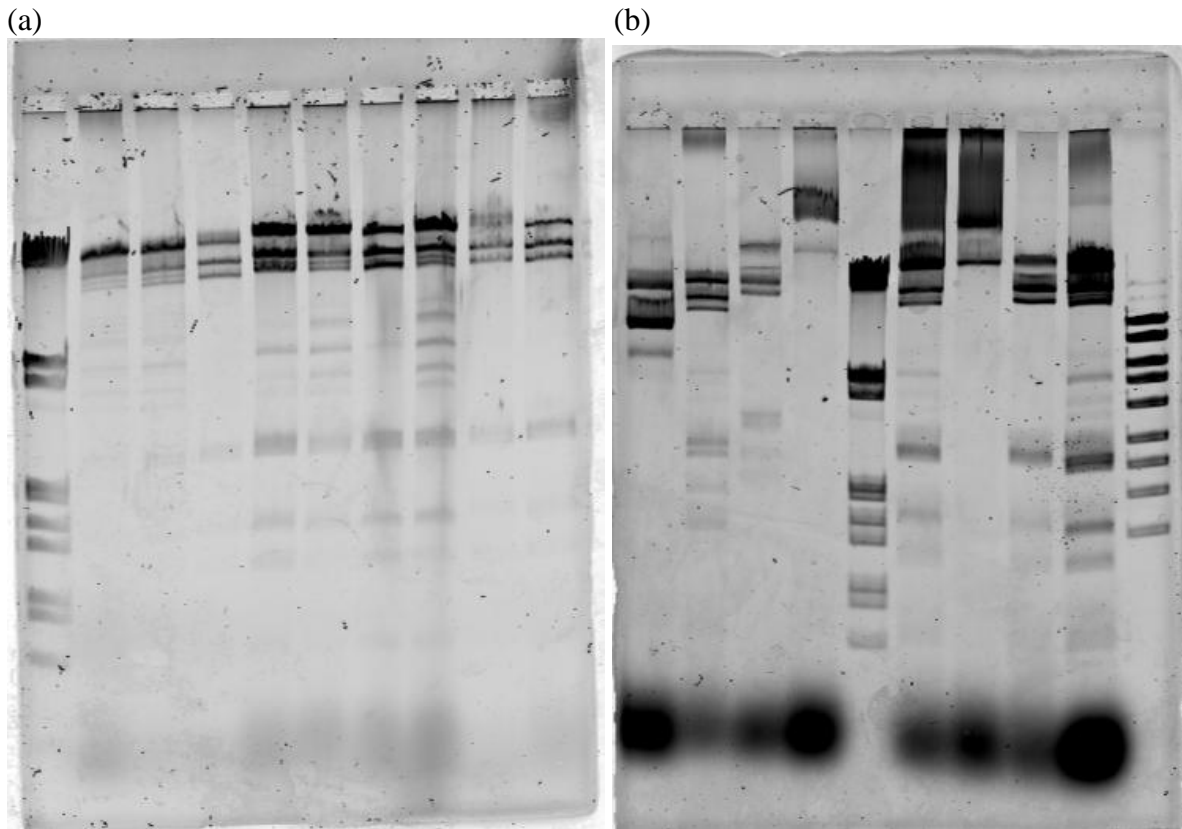
### **5.1.5.1.2. Producing recombinant adenoviral vectors:**

Three different adenoviral vectors were produced with the gateway-system as described under material and methods. pAd/CMV sense Tel, pAd/CMV antisense Tel and pAd/pl sense Tel  $\Delta$ hH1 constructs resulted from LR reactions between respective pENTR and pDEST plasmids. After, transformation into high competent E.coli cells ( $10^8$  transformants/ $\mu$ g) was conducted. Single colonies were further characterized with restriction enzymes. As controls, adenoviral vectors were cut with XhoI. All ten analyzed clones showed predicted banding patterns (Figure 5.12 and Table 5.1.).

**Table 5.1.: Banding patterns of adenoviral vectors after XhoI cut:** All counts are bps

<b>Vector</b>	<b>Banding pattern</b>
pAd/pL sense Tel	14502 + 11832 + 2466 + 2331 + 1445 + 1089 + 595
pAd/pl antisense Tel	14502 + 11832 + 2466 + 2331 + 1445 + 1089 + 595
pAd/CMV sense –hH1	14502 + 11832 + 2698 + 2466 + 1853 + 1445 + 595

Three of them, (clone III, IV and VI) were stored as reference stocks and termed pAd/pL sense Tel 1 to 3. Also clone B as pAd/CMV vector with sense –hH1 construct termed pAd/CMV sense –hH1 Tel and clone H as pAd/pl vector with antisense construct termed pAd/pl antisense Tel showed predicted banding patterns (Figure 5.12.) and were stored. The productions of the adenoviruses were taken over by Doris Mejri and Sandra Sampl due to lack of time.



1 2 3 4 5 6 7 8 9 10 11 12 13 14 15 16 17 18 19 20  
**Figure 5.12.: Identification of adenoviral vectors: 1% agarose gel**

(a) (1)  $\lambda$ -marker, (2) clone I XhoI cut, (3) clone II XhoI cut, (4) clone III XhoI cut, (5) clone IV XhoI cut, (6) clone V XhoI cut, (7) clone VI XhoI cut, (8) clone VII XhoI cut, (9) clone VIII XhoI cut, (10) clone IX XhoI cut

(b) (11) clone A XhoI cut, (12) clone B XhoI cut, (13) clone C XhoI cut, (14) clone D XhoI cut, (15)  $\lambda$ -marker, (16) clone E XhoI cut, (17) clone F XhoI cut, (18) clone G XhoI cut, (19) clone H XhoI cut, (20) mass ruler

Clone I to IX are pAd/pl vectors with sense constructs, clone A to D are pAd/CMV vectors with sense -hH1 constructs and clone E to H are pAd/pl vectors with antisense constructs.

#### **5.1.5.1.2. Producing recombinant lentiviral vectors:**

Although much effort was given, it was not possible to produce any lentiviral vectors. Gateway reactions were tried with lentiviral vectors pLenti6/BLOCK-iT<sup>TM</sup>-DEST and pLenti6/UbC/V5-DEST in combination with pENTR/D/hH1 with telomere fragment. However after transformation no clones with plasmid with telomere fragment could be found.



## **5.2. Pre-test for production of recombinant adenoviruses using HEK293 FT cells:**

### **5.2.1. Determining transfection efficiency of HEK293 FT by GFP transfection and FACS analyses:**

HEK293 FT cells were transfected with GFP-plasmid constructs isolated by different methods. Optical valuation via microscope and FACS analysis showed numbers of transfected and non-transfected cells. pEGFP-C1 was isolated with Wizard® Plus Midipreps DNA Purification System (Promega) or Wizard® Plus Minipreps DNA Purification System (Promega) and GFP-lentiviral vector was isolated with S.N.A.P.<sup>TM</sup> MidiPrep Kit (Invitrogen). These vectors were used as comparison for transfection efficiency.

#### **5.2.1.1. Optical valuation of transfection:**

Cells were settled well (Figure 5.13. a and b), but after lipofection they were accumulated to clusters (Figure 5.13. c-f).

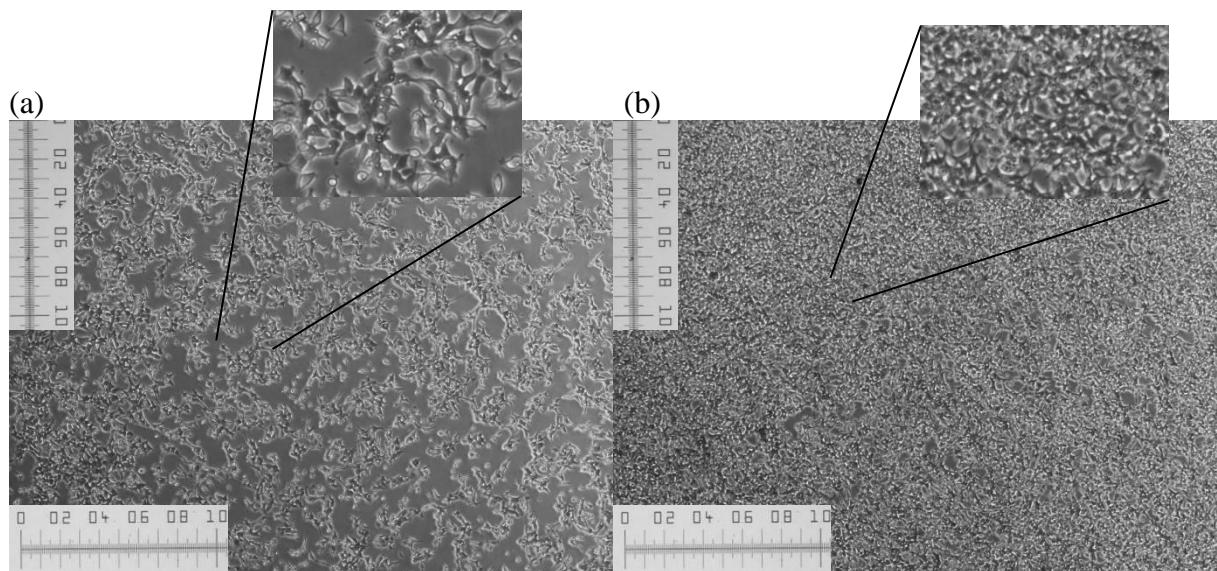


**Figure 5.13.: Lipofection of HEK293 FT with different isolated eGFPC1 vector: Microscopical investigation scale bar in  $\mu\text{m}$ . Only examples are shown.**

(a) Before lipofection, HEK293 FT with confluence 50%, 4x optical zoom. With an enlarged part

(b) Before lipofection, HEK293 FT with confluence 90%, 4x optical zoom. With an enlarged part

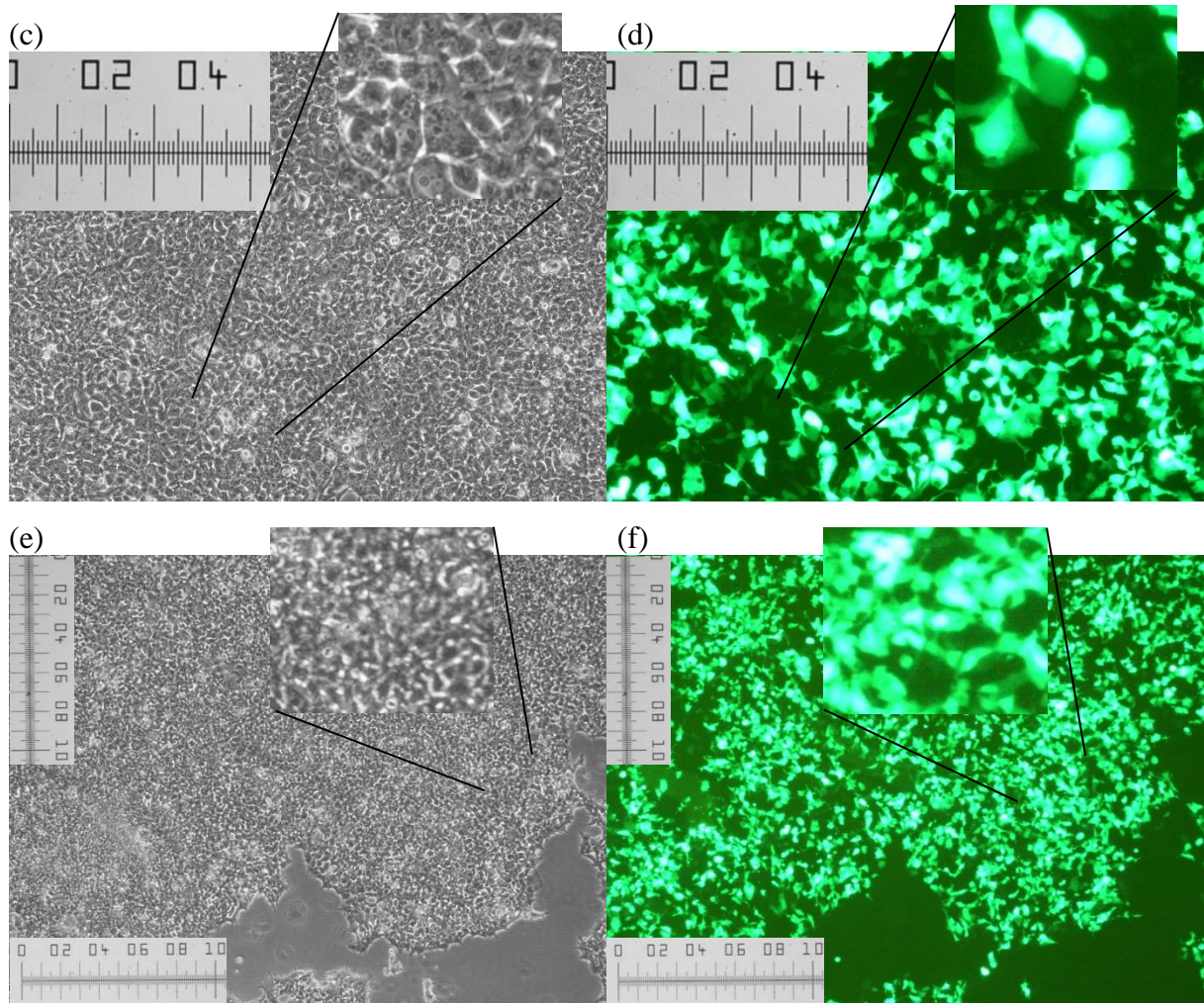


**Figure 5.13. (continued):** Microscopical investigation. Scale bar in  $\mu\text{m}$ . Only examples are shown

(c) After lipofection, HEK293 FT with 90% confluence, Wizard® *Plus* Midipreps DNA Purification System, 10x optical zoom. With an enlarged part

(d) After lipofection, HEK293 FT with 90% confluence, Wizard® *Plus* Midipreps DNA Purification System, phase, 10x optical zoom. With an enlarged part

(e) After lipofection, HEK293 FT with 50% confluence, Wizard® *Plus* Minipreps DNA Purification System, 4x optical zoom. With an enlarged part

(f) After lipofection, HEK293 FT with 50% confluence, Wizard® *Plus* Minipreps DNA Purification System, phase, 4x optical zoom. With an enlarged part

Lipofection was successful in every experiment with different efficiencies (Figure 5.13 c, d, e and f). To determine efficiency, GFP-FACSs were done.

### 5.2.1.2. FACS of GFP-transfection:

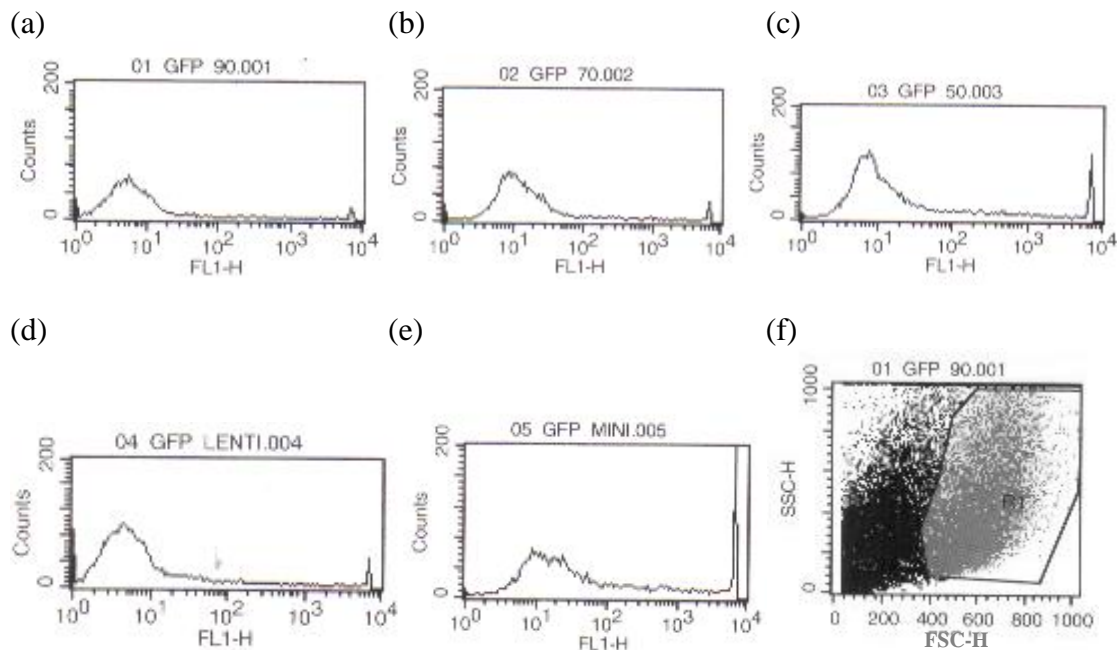


**Figure 5.14.: FACS analyses with differently isolated GFP-vectors, transfected into HEK293-FT cells with partwise different confluences:** Cells in the defined region (R1) (g)

were seen as fluorescing cells. FL1-H = height of fluorescence intensity

(a) Transfection rate of GFP C1 vector isolated with Wizard® *Plus* Midipreps DNA Purification System in HEK293-FT cells with 90% confluence

(b) Transfection rate of GFP C1 vector isolated with Wizard® *Plus* Midipreps DNA Purification System in HEK293-FT cells with 70% confluence

(c) Transfection rate of GFP C1 vector isolated with Wizard® *Plus* Midipreps DNA Purification System in HEK293-FT cells with 50% confluence

(d) Transfection rate of GFP-lenti vector isolated with Wizard® *Plus* Midipreps DNA Purification System in HEK293-FT cells with 50% confluence

(e) Transfection rate of GFP C1 vector isolated with Wizard® *Plus* Minipreps DNA Purification System in HEK293-FT cells with 50% confluence

(f) Gated cells (R1). SSC-H = Sideward scatter height (cell complexity or granularity), FSSC-H = Forward scatter height (cell size)

**Table 5.2.:** Transfection rates of different GFP vectors differently isolated:

Vector:	Transfection rate:
GFP Midi 90%	9.46%
GFP Midi 70%	15.48%
GFP Midi 95%	23.64%
GFP Lenti 50%	12.21%
GFP Mini 50%	41.63%

Percentage at vectors show confluence of cells, Midi stands for Wizard® *Plus* Midipreps DNA Purification System, Mini stands for Wizard® *Plus* Minipreps DNA Purification System, Lenti stands for GFP-lenti vector isolated with Wizard® *Plus* Midipreps DNA Purification System. The highest efficiency was shown by transfection of the GFP construct which was isolated by Wizard® *Plus* Minipreps DNA Purification System

Transfection rates were different between HEK293-FT cells with different confluences (Figure 5.14 and Table 5.2.). Transfection of cells with confluence of 50% showed the highest efficiency, 90% confluence the lowest. In comparison of different isolation methods Wizard® *Plus* Minipreps DNA Purification System showed the highest efficiency.

### **5.2.2. Blasticidin dose determination:**

Blasticidin as eukaryote antibiotic serves as selection marker for the lentiviral vectors of company Invitrogen. To determine the best concentration for selection of stable cells, a pretest had been conducted as described in material and methods. Cells were settled into 96 well plates in 5 biological repetitions.

#### **5.2.2.1. Optical estimation of blasticidin effects:**

With microscope the cytotoxic effect of blasticidin was seen and an estimation of the best concentration for further experiments was possible (Figure 5.15.).

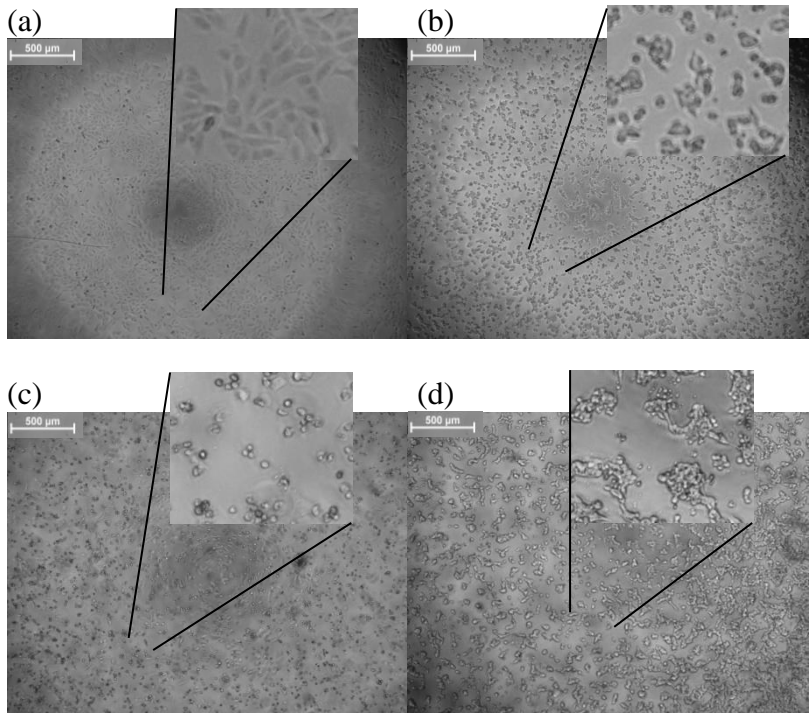


**Figure 5.15: Cell lines under blasticidin treatment for dosage determination:**

Microscopical investigation of treated cell lines in 96well plates

- (a) U2OS before blasticidin addition
- (b) SW480 B before blasticidin addition
- (c) U2OS, 10µg/ml blasticidin after two days
- (d) SW480 B, 10 µg/ml blasticidin after two days

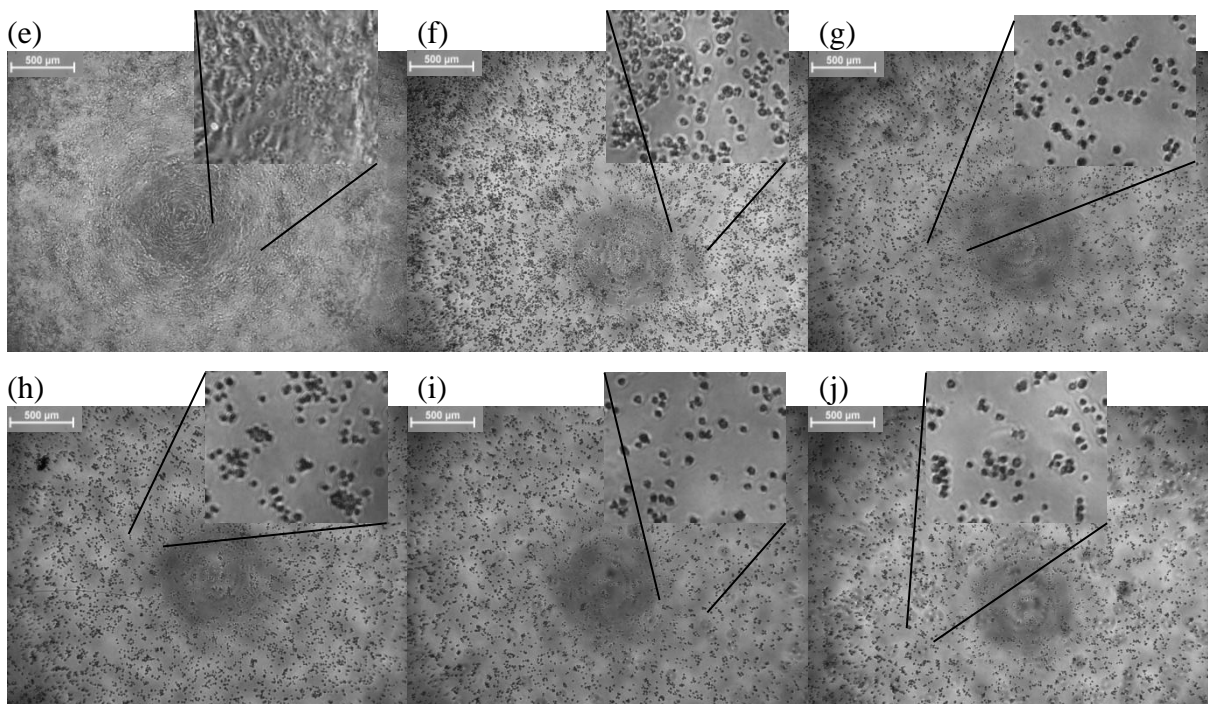


**Figure 5.15. (continued):** Microscopical investigation

(e) U2OS, 0 µg/ml blasticidin after six days. With an enlarged part

(f) U2OS, 3 µg/ml blasticidin after six days. With an enlarged part

(g) U2OS, 5 µg/ml blasticidin after six days. With an enlarged part

(h) U2OS, 6 µg/ml blasticidin after six days. With an enlarged part

(i) U2OS, 8 µg/ml blasticidin after six days. With an enlarged part

(j) U2OS, 10 µg/ml blasticidin after six days. With an enlarged part

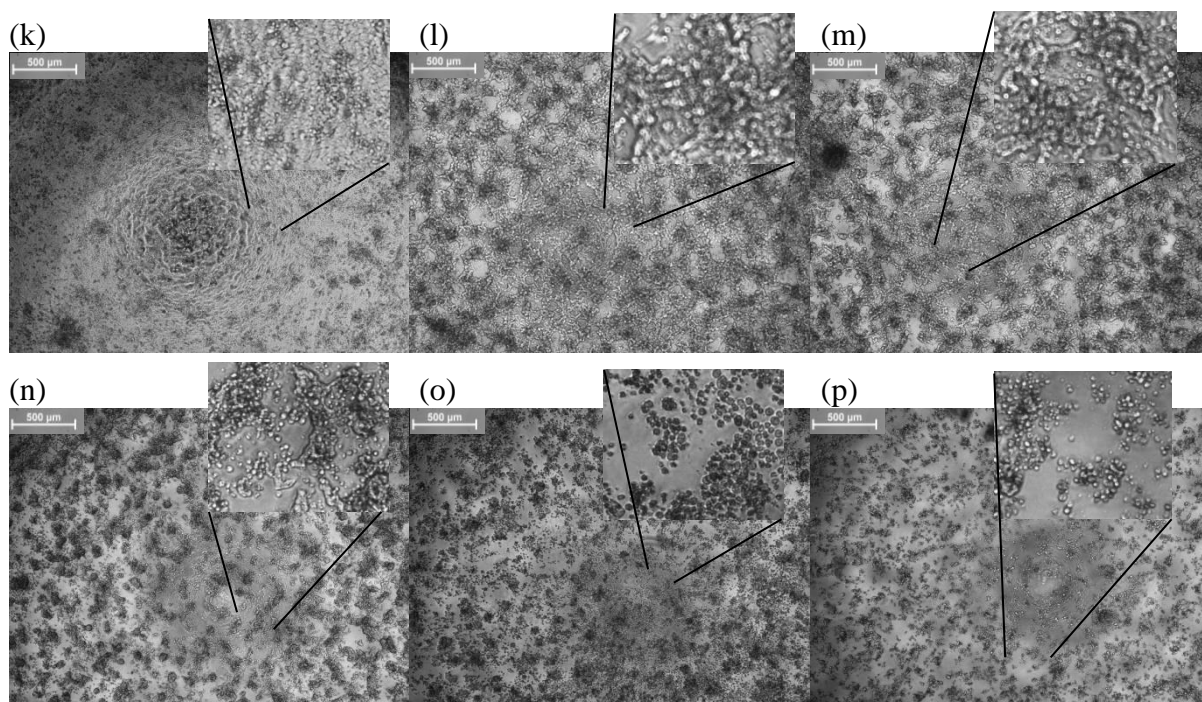


**Figure 5.15. (continued):** Microscopical investigation

(k) SW480 B, 0 µg/ml blasticidin after six days. With an enlarged part

(l) SW480 B, 3 µg/ml blasticidin after six days. With an enlarged part

(m) SW480 B, 5 µg/ml blasticidin after six days. With an enlarged part

(n) SW480 B, 6 µg/ml blasticidin after six days. With an enlarged part

(o) SW480 B, 8 µg/ml blasticidin after six days. With an enlarged part

(p) SW480 B, 10 µg/ml blasticidin after six days. With an enlarged part

First cytotoxic effects were visible after two days (Figure 5.15.). SW480B bore a higher blasticidin dosage than U2OS. After six days, neutral-red uptake was done.

### **5.2.2.2 Neutral-red uptake of blasticidin dosage determination:**

To determine the percentage of living cells after treatment neutral-red uptake as substantiation was also conducted. Fivefold repetition was done to enhance the significance.

U2OS showed a high sensitivity against blasticidin. For selection experiments a dose of 3µg/ml was considered sufficient. SW480 B showed a higher resistance against blasticidin. A dose of 10µg/ml was the only dose which resulted in an adequate selection pressure (Table 5.3.).

**Table 5.3.: Neutralred results of blasticidin dose experiments after 7 days of treatment:**  
(a)

<b>U2OS</b>							
<b>Blasticidin (µg/ml)</b>	<b>Absorption (562nm - 620nm)</b>					<b>Mean Abs.</b>	<b>SD</b>
0	0.196	0.155	0.149	0.153	0.164	0.163	0.017
3	0.003	0.003	0.003	0.002	0.003	0.003	0.001
5	0.002	0.003	0.004	0.004	0.002	0.003	0.001
6	0.003	0.003	0.003	0.003	0.003	0.003	0.000
8	0.003	0.003	0.003	0.011	0.003	0.005	0.003
10	0.004	0.003	0.003	0.004	0.003	0.003	0.001

(b)

<b>SW480B</b>							
<b>Blasticidin (µg/ml)</b>	<b>Absorption (562nm - 620nm)</b>					<b>Mean Abs.</b>	<b>SD</b>
0	0.079	0.262	0.207	0.213	0.223	0.197	0.062
3	0.207	0.237	0.202	0.258	0.184	0.218	0.026
5	0.166	0.126	0.128	0.179	0.187	0.157	0.026
6	0.220	0.140	0.086	0.084	0.144	0.135	0.050
8	0.088	0.069	0.018	0.030	0.007	0.031	0.031
10	0.009	0.003	0.003	0.004	0.004	0.005	0.002

Absorption at 562nm minus absorption at 620nm showed relative quantity of living cells.

Mean absorption (Mean Abs.) and standard deviation (SD) were calculated.

(a) Results of Blasticidin treatment of U2OS

(b) Results of Blasticidin treatment of SW480B

### **5.3. TERRA expression:**

#### **5.3.1. Cell cycle FACS:**

A cell cycle FACS of SW480 B and SW480 R showed unanticipated results (not shown). The reason was that confluence has influence on cell cycle state and also on expression. Due to this SW480 B and SW480 R settled with different confluences. Two different methods to detach cells were used, scratching and trypsin. FACS analysis showed the relative percentage of cells in different cell cycle phase.



### **5.3.1.1. Optical control of confluence:**

Confluences were controlled and estimated by microscope (Figure 5.16) and also measured with Casy Cellcounter (data not shown).

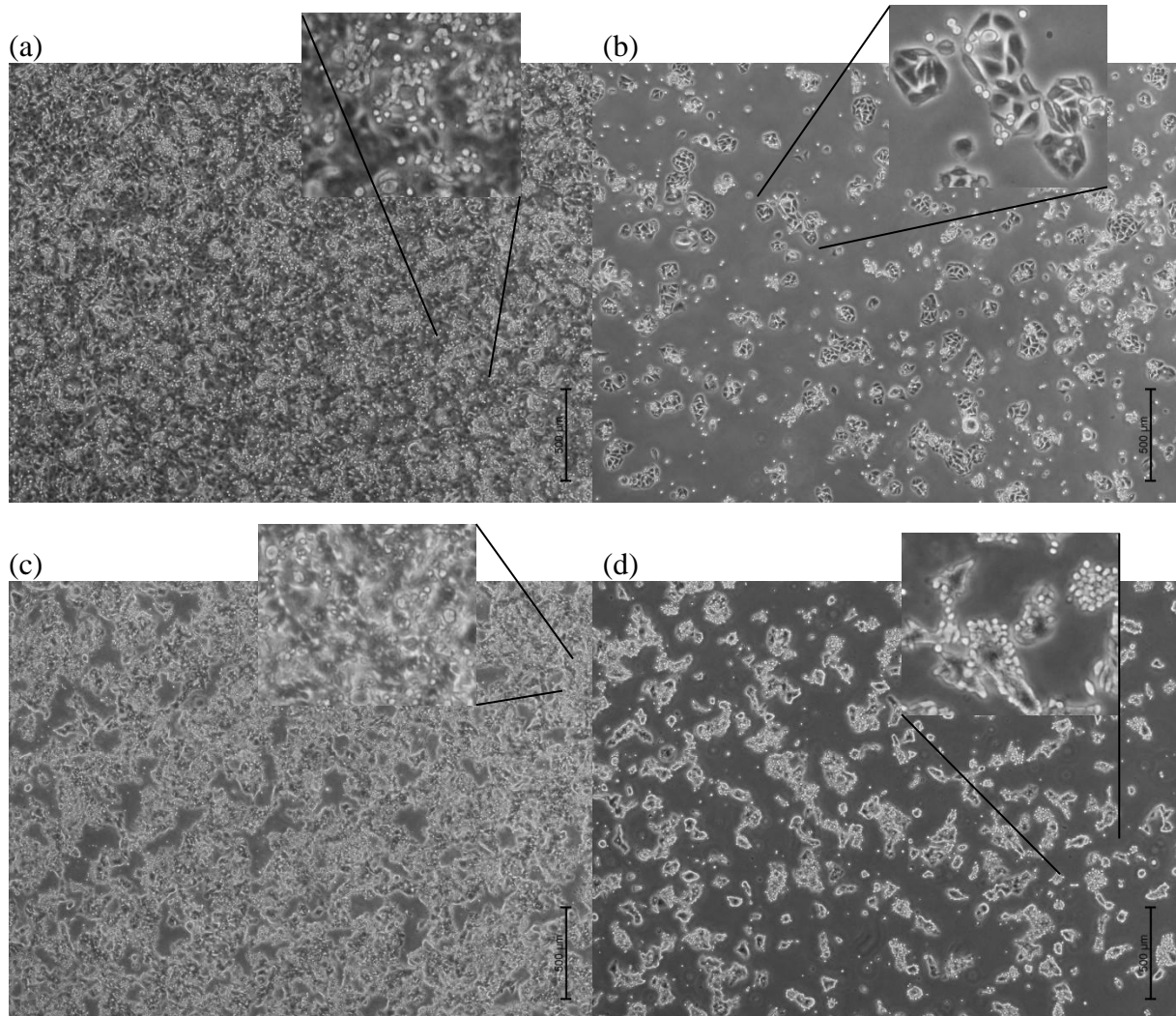


**Figure 5.16.: Examples of cells used for cell cycle FACS analyses under microscopical investigation:**

- (a) SW480R with 100% confluence. With enlarged part
- (b) SW480R with 25% confluence. With enlarged part
- (c) SW480B with 80% confluence. With enlarged part
- (d) SW480B with 25% confluence. With enlarged part

### 5.3.1.2. Cell cycle FACS analyses of cell line with different confluences:

Nuclear disposal was controlled by microscope (example: Figure 5.17). The efficiencies were calculated and were between 96 and 100% (not shown) which were sufficient for cell cycle FACS.

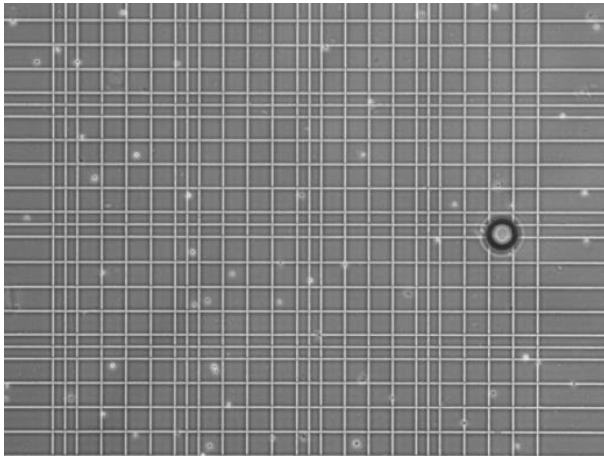


**Figure 5.17.: Example of nuclear disposal:** Blue dots are cell nuclei

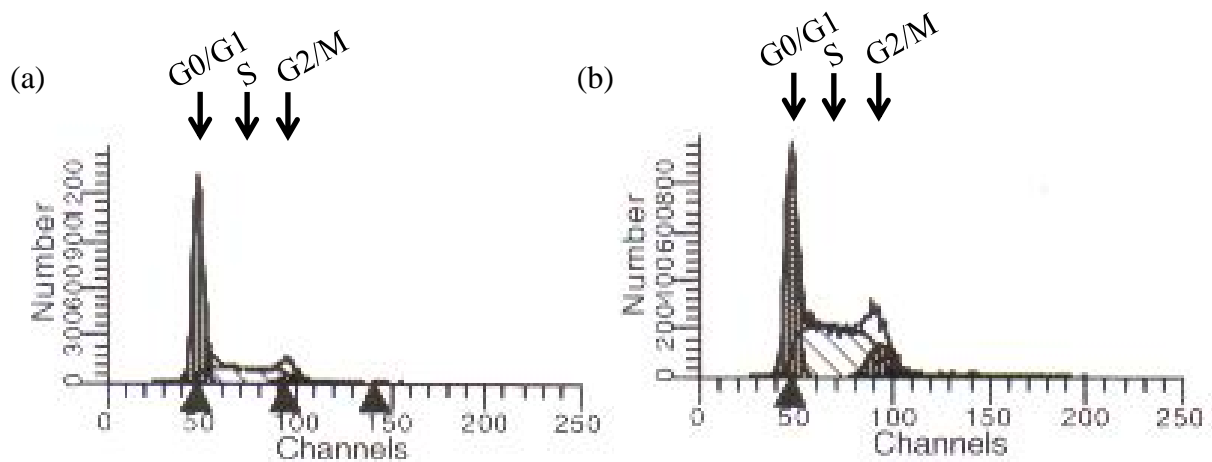


**Figure 5.18: Examples of cell cycle FACS results of SW480 B and SW480 R detached by scratching or by Trizol:** Percentage of cells in different cell cycle state was shown. Distinction between G0/G1, G2/M and S phase was done. Arrows at channel about 50 (2n state) showed G0/G1 cell cycle state, arrows at channel about 100 (4n state) showed G2/M cell cycle state. Cell cycle state S is detected between 50 and 100. Y-axis showed the number of measured cells

(a) SW480 B 80% confluence, detached by trypsin

(b) SW480 B 5% confluence, detached by trypsin

Raw data of FACS analysis (Figure 5.18.) were summarized into diagrams (Figure 5.19.) and tables (Table 5.4.).

**Table 5.4.: Cell cycle FACS results of SW480 B and SW480 R with different confluences and differently detached:** Cell cycle states in percentage

(a) SW480 B scratched

Confluence:	G0/G1:	S:	G2/M:
80%	38.23	50.01	11.76
50%	38.16	55.21	6.63
25%	29.70	57.44	12.86
10%	25.62	61.00	13.38
7%	23.11	57.41	19.48
<5%	26.26	40.92	32.82

(b) SW480 B detached with trypsin

Confluence:	G0/G1:	S:	G2/M:
80%	60.48	34.16	5.36
50%	53.90	37.47	8.63
25%	48.43	43.92	7.64
15%	45.60	46.03	8.37
10%	40.87	48.64	10.49
5%	36.61	52.03	11.36

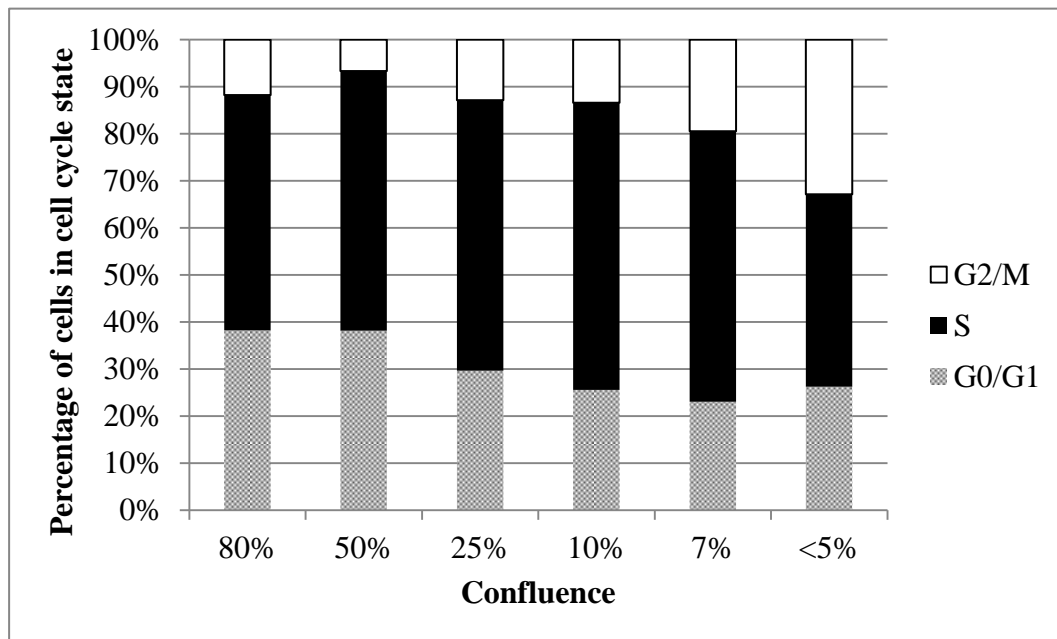
(c) SW480R scratched

Confluence:	G0/G1:	S:	G2/M:
100%	73.71	21.32	4.97
80%	66.14	24.13	9.72
50%	61.12	30.04	8.84
25%	58.83	26.86	14.31
15%	61.47	27.17	11.36
8%	63.49	29.66	6.86

(d) SW480 B detached with trypsin

Confluence:	G0/G1:	S:	G2/M:
100%	79.70	15.36	4.94
80%	72.20	23.68	4.12
50%	70.48	24.70	4.81
30%	61.70	32.10	6.20
15%	53.59	38.23	8.18
10%	49.85	46.72	3.43

(a)



(b)

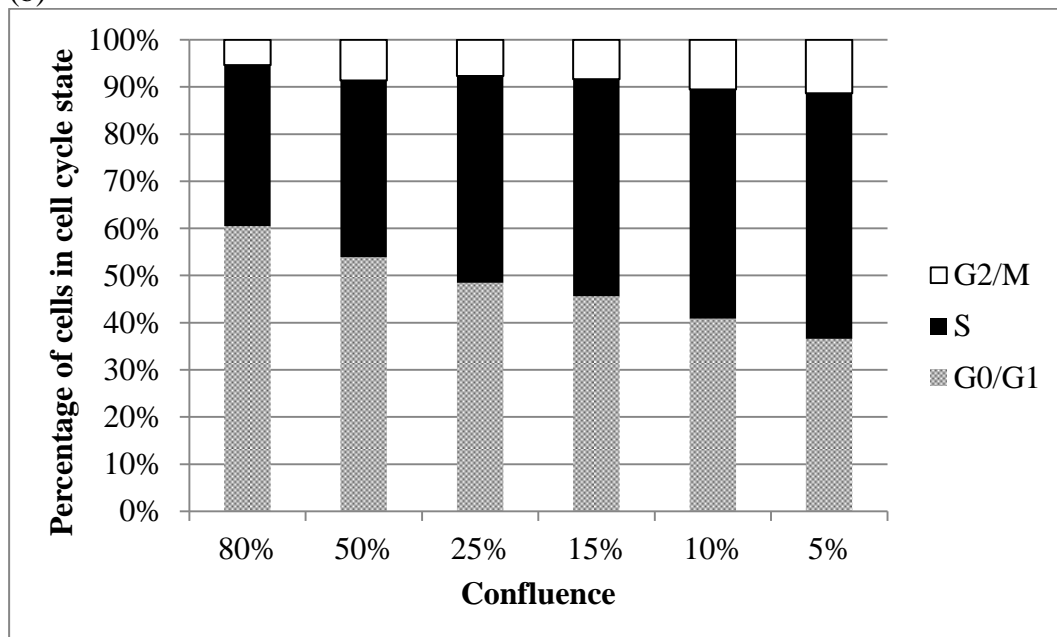


**Figure 5.19.: Cell cycle state of SW480 B and SW480 R with different confluences and differently isolated:**

(a) Diagram of cell cycle state of SW480 B scratched in percentage

(b) Diagram of cell cycle state of SW480 B detached by trypsin in percentage

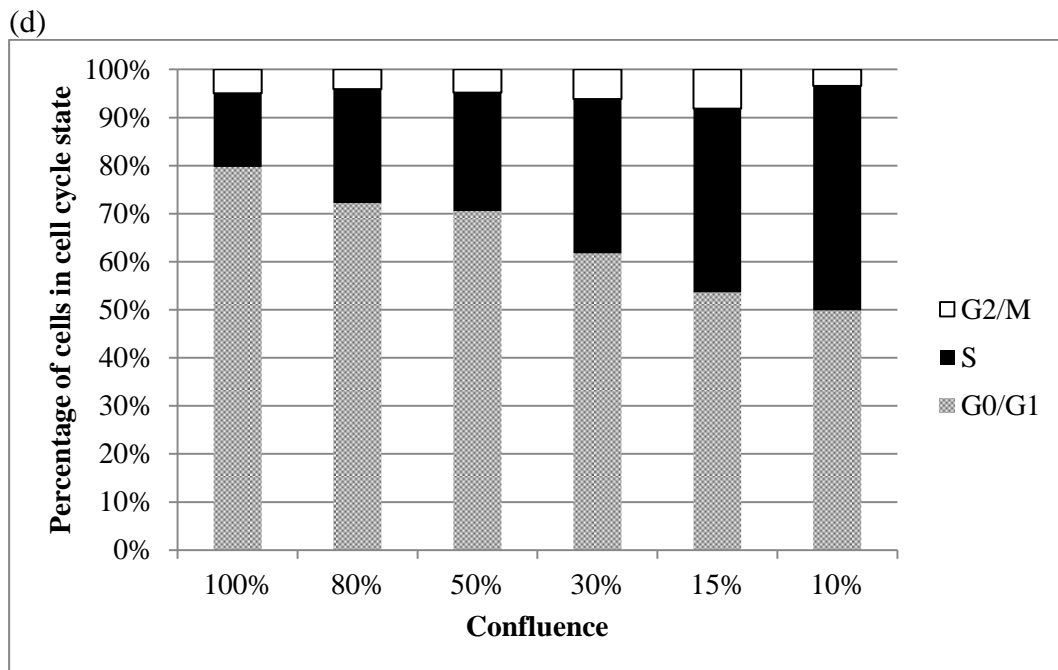
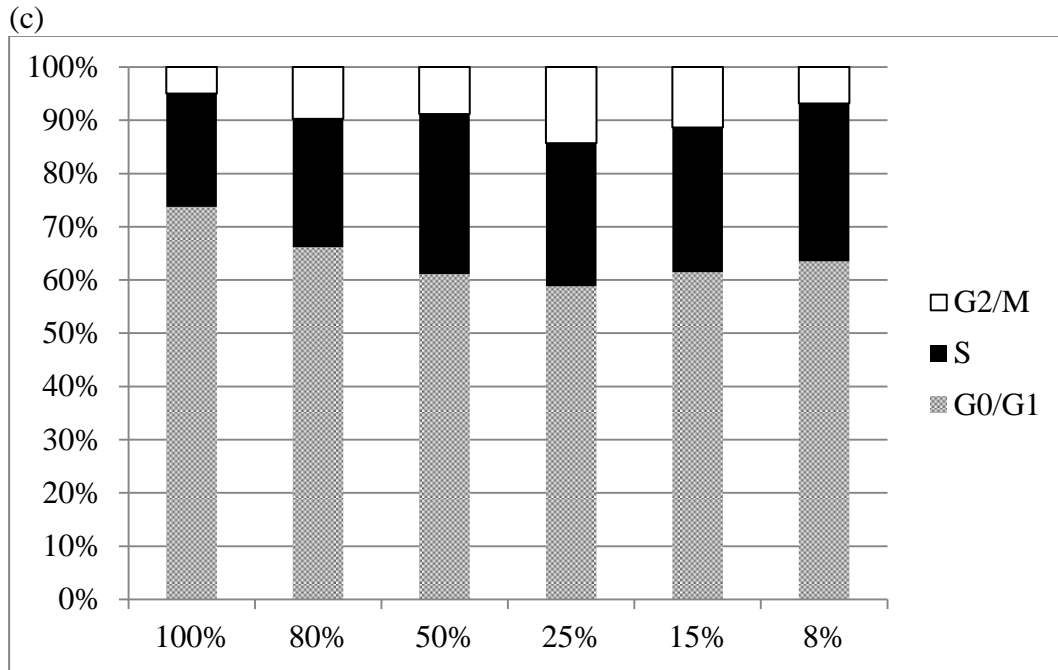


**Figure 5.19. (continued):**

(c) Diagram of cell cycle state of SW480 R scratched in percentage

(d) Diagram of cell cycle state of SW480 R detached by trypsin in percentage

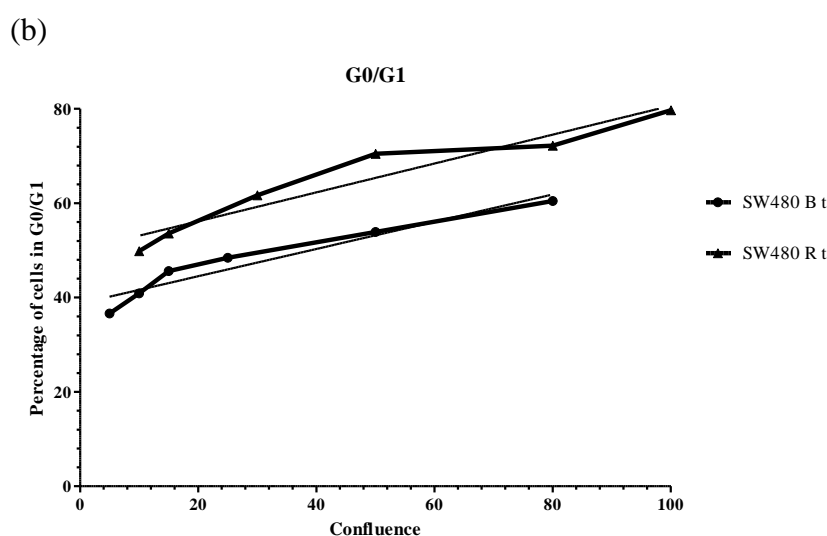
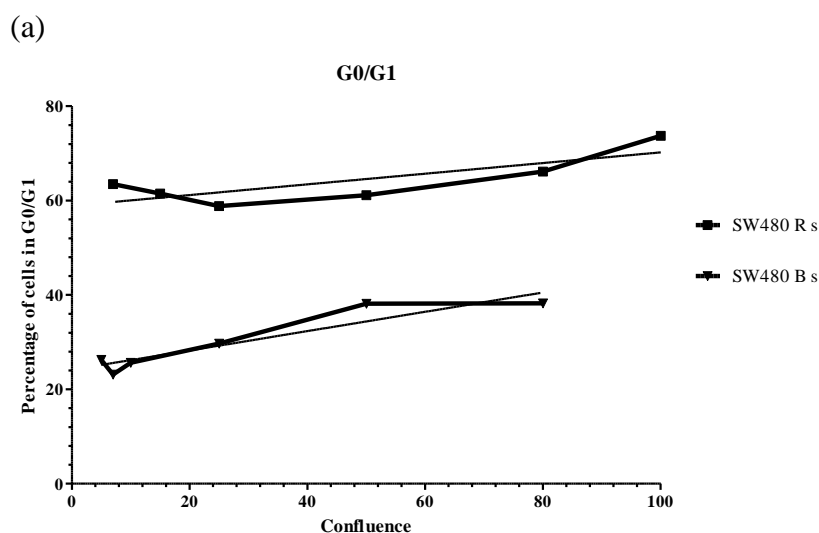


**Figure 5.20.: Percentage of SW480 B and SW480 R with different confluences in cell cycle state G0/G1:** Detached by s(cratching) or with t(rypsin). Confluence in percentage.  
 (a) Percentage of SW480 B and SW480 R detached by scratching in cell cycle state G0/G1  
 (b) Percentage of SW480 B and SW480 R detached with trypsin in cell cycle state G0/G1

**Table 5.5.: Trendlines G0/G1 cell cycle state of SW480 B and SW480 R differently detached:**

Cell line	Trendline	R <sup>2</sup>	P-value
SW480 B s	$y = 0.2046x + 24.143$	0.8728	0.0063
SW480 B t	$y = 0.2889x + 38.741$	0.925	0.0022
SW480 R s*	$y = 0.1142x + 58.836$	0.6437	0.0568
SW480 R t	$y = 0.3061x + 50.049$	0.9244	0.0022

Formula of trendline, goodness of fit (R<sup>2</sup>) and P-value of slope deviation from zero are mentioned. P-value below 5% (0.0500) was seen as significant different to zero. Cell lines with no significant difference were marked with an \*. Detached by s(cratching) or with t(rypsin).

By comparison SW480 R cells showed a higher percentage from about 8% to 30% of cells in G0/G1 phase than SW480B cells (Table 5.4. and Figure 5.19.). Cell detached with trypsin showed a higher percentage from about 6% to 22% of G0/G1 than scratched cell lines, except SW480 R at 15% confluence. The percentage of cells in G0/G1 phase increased with confluence in both cell lines. SW480R detached by scratching show no significant trend (0.0558), but it's very close to significance and a low trend is visible (Table 5.5. and Figure 5.20.).

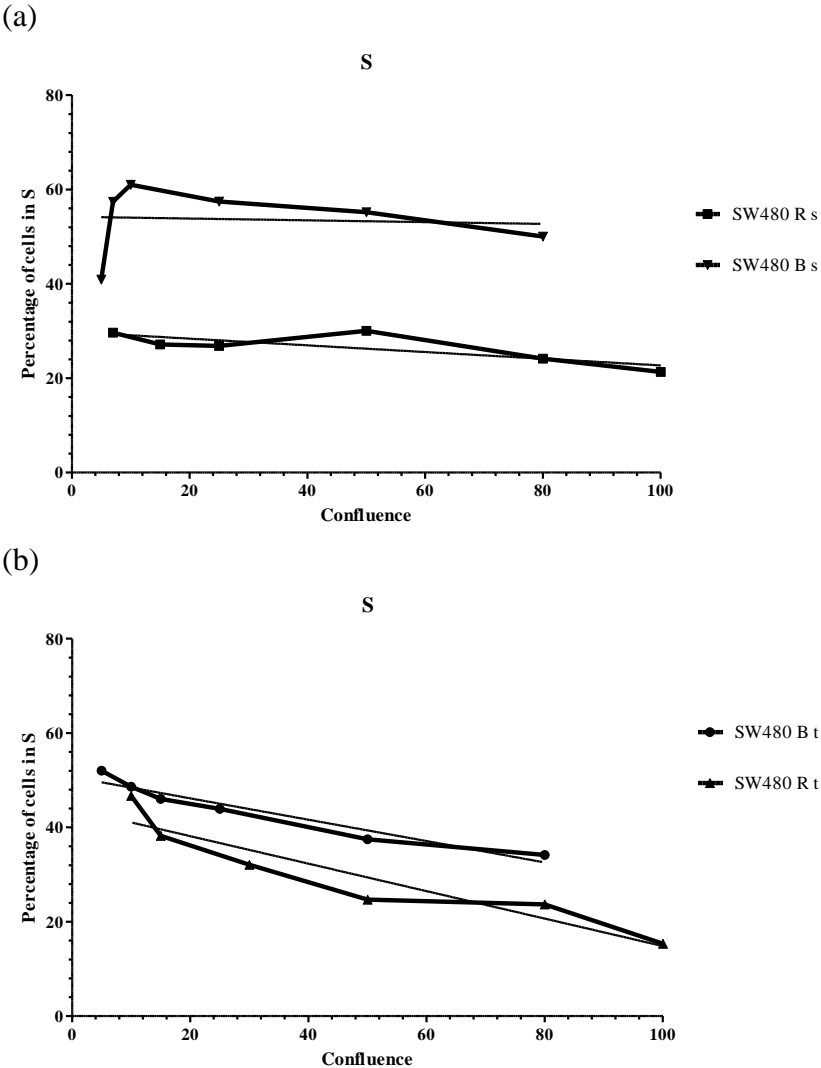


**Figure 5.21.: Percentage of SW480 B and SW480 R with different confluences in cell cycle state S:** Detached by s(cratching) or with t(rypsin). Confluence in percentage.

(a) Percentage of SW480 B and SW480 R detached by scratching in cell cycle state S

(b) Percentage of SW480 B and SW480 R detached with trypsin in cell cycle state S

**Table 5.6.: Trendlines S cell cycle state of SW480 B and SW480 R differently detached:**

Cell line	Trendline	R <sup>2</sup>	P-value
SW480 B s*	$y = -0.019x + 54.225$	0.0062	0.8822
SW480 B t	$y = -0.2265x + 50.692$	0.9341	0.0017
SW480 R s*	$y = -0.0713x + 29.835$	0.6353	0.0573
SW480 R t	$y = -0.2912x + 43.965$	0.8813	0.0055

Formula of trendline, goodness of fit (R<sup>2</sup>) and P-value of slope deviation from zero are mentioned. P-value below 5% (0.0500) was seen as significant different to zero. Cell lines with no significant difference were marked with an \*. Detached by s (scratching) or with t (trypsin).

SW480B cells showed a higher percentage from about 2% to 25% of cells in S phase than SW480R cells (Table 5.4. and Figure 5.20). Percentage of cells in S cell cycle state decreased with increasing confluence (Figure 5.21.). Cells detached with trypsin showed a significant trend, cell lines detached by scratching show no significant trend, but SW480 R with a P-value of 0.0573 was very close to significance (Table 5.6.).

(a)

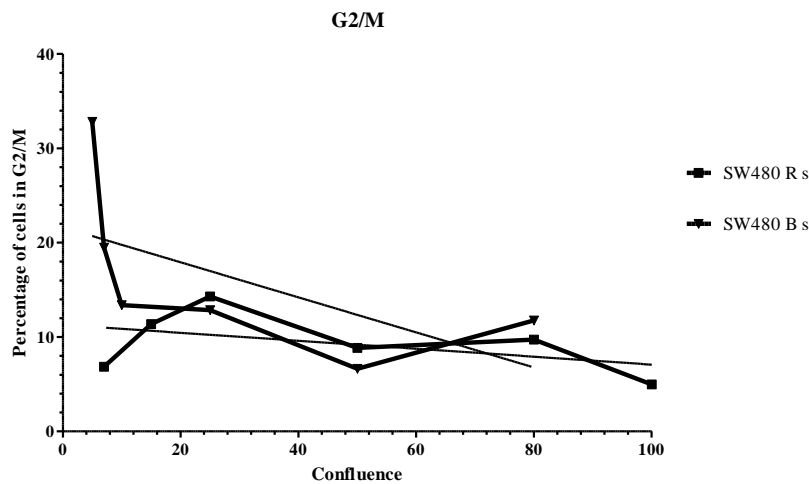


**Figure 5.22.: Percentage of SW480 B and SW480 R with different confluences in cell cycle state G2/M:** Detached by s (scratching) or with t (trypsin). Confluence in percentage.

(a) Percentage of SW480 B and SW480 R detached by scratching in cell cycle state S



(b)

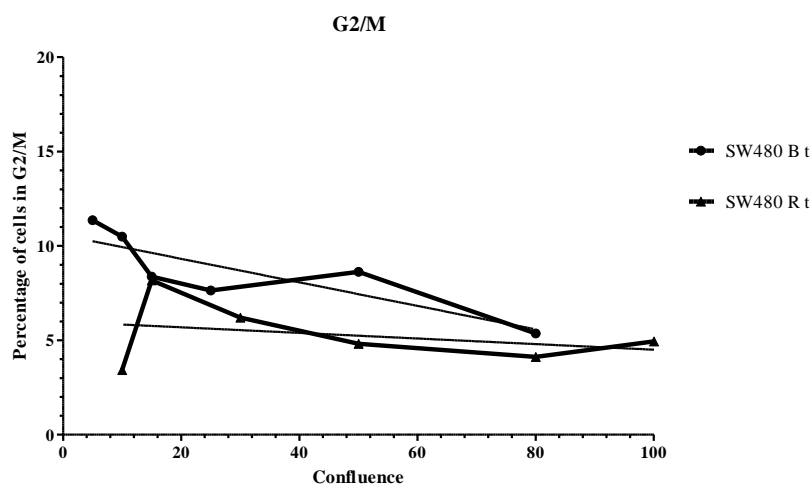


**Figure 5.22. (continued):**

(b) Percentage of SW480 B and SW480 R detached with trypsin in cell cycle state S

**Table 5.7.: Trendlines G2/M cell cycle state of SW480 B and SW480 R differently detached:**

Cell line	Trendline	R <sup>2</sup>	P-value
SW480 B s*	$y = -0.1857x + 21.633$	0.3699	0.2002
SW480 B t	$y = -0.043x + 11.334$	0.2351	0.0336
SW480 R s*	$y = -0.0148x + 5.9845$	0.1009	0.3375
SW480 R t*	$y = -0.043x + 11.334$	0.2351	0.5396

Trendline, goodness of fit (R<sup>2</sup>) and P-value of slope deviation from zero are mentioned. P-value below 5% (0.0500) was seen as significant different to zero. Cell lines with no significant difference were marked with an \*. Detached by s(scraping) or with t(trypsin).

Only SW480B detached with trypsin showed a significant trend (Table 5.7.) by decreasing phase G2/M at increasing confluence (Table 5.4., Figure 5.19. and Figure 5.22.).

### **5.3.2. Best Keeper:**

Best Keeper analysis housekeeping genes of confluence dependent TERRA expression (Table 5.9.) and determined betaactin as more stable in comparison to 36B4 (Table 5.8.). All samples were related to betaactin.

**Table 5.8.: Best Keeper analysis of 36B4 and beatActin:** p-value = level of significance, SE = Standard error

	<b>36B4</b>	<b>betaActin</b>
coefficient of correlation [r]	0,98	0,99
coefficient of detection [r <sup>2</sup> ]	0,95	0,98
intercept [CP]	4,25	-3,56
slope [CP]	0,87	1,10
SE [CP]	±0,42	±0,36
p-value	0,001	0,001
Power [x-fold]	<b>1,83</b>	<b>2,15</b>

### **5.3.2. Confluence dependent totalTERRA expression level:**

Total TERRA expression level was measured by Real Time-PCR (Figure 5.23.). The isolated RNA (Table 10.1.) showed a 28S to 18S ratio between 1.5-2:5:1 (Supplement Figure 10.10. and Table 10.2.). Different confluences should be in correlation with cell cycle state influence expression of TERRA.

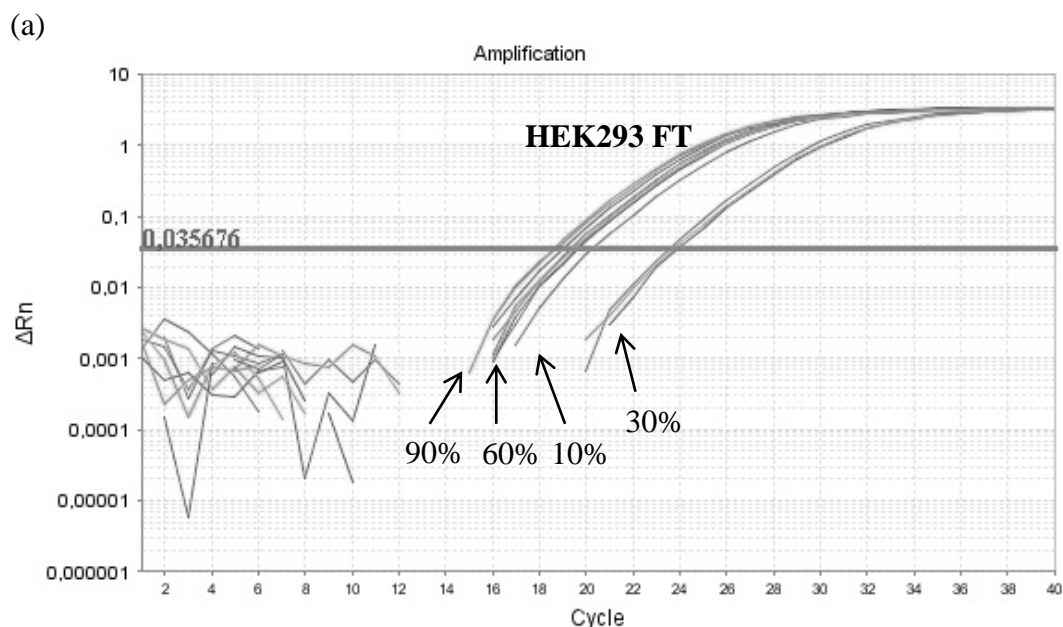


**Figure 5.23: Amplification plots of TERRA expression of HEK293 FT and Saos-2 as examples:** 0.035676 = threshold for TERRA.  $\Delta Rn$  = normalized fluorescence. Percentages = confluences

(a): Amplification plot of HEK293 FT

(b)

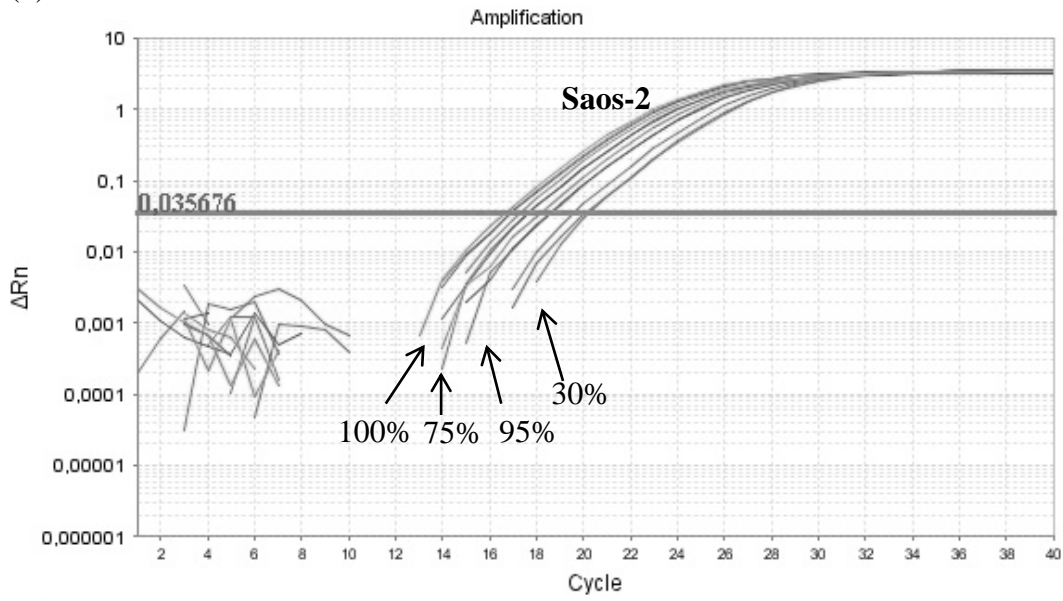


**Figure 5.23 (continued):**

(b): Amplification plot of Saos2

Raw data and RQ-values were summarized into diagrams (Table 5.9. and Figure 5.24.).

**Table 5.9.: Real-Time PCR results of total TERRA expression of different cell lines and different confluences:**

Cell line	Confluence	C <sub>T</sub>			C <sub>T</sub> Mean	SD	RQ	RQ Min	RQ Max
<b>T98G</b>	100%	18.98	19.20	19.47	19.22	0.20	1.000	0.754	1.327
	70%	20.70	20.20	20.49	20.46	0.20	0.263	0.195	0.355
	35%	19.51	19.55	19.96	19.67	0.20	0.710	0.496	1.018
	20%	20.46	20.26	20.83	20.52	0.23	0.158	0.114	0.220
<b>HEK293</b>	95%*	26.52	25.43	26.74	26.23	0.57	0.018	0.008	0.040
	75%	22.14	22.52	22.67	22.44	0.22	0.128	0.090	0.184
	30%	23.87	23.37	24.17	23.80	0.33	0.060	0.036	0.101
	10%	24.37	23.67	24.51	24.18	0.37	0.030	0.017	0.054
<b>HEK293 FT</b>	90%	19.10	18.66	19.38	19.05	0.30	1.393	0.929	2.090
	60%	19.67	19.49	20.37	19.84	0.38	0.945	0.558	1.601
	30%	23.97	23.79	23.62	23.79	0.14	0.099	0.081	0.121
	10%	19.66	18.72	19.47	19.28	0.41	0.556	0.320	0.967
<b>Saos-2</b>	100%	16.94	16.72	16.93	16.86	0.10	2.602	2.258	2.998
	95%	18.64	18.22	18.66	18.51	0.20	91.541	67.796	123.601
	75%	17.71	17.37	17.70	17.60	0.16	1.394	1.075	1.807
	30%	19.65	20.22	20.31	20.06	0.29	0.248	0.166	0.372
<b>U2OS</b>	100%	18.33	18.19	19.27	18.60	0.48	0.619	0.323	1.189
	75%	14.24	14.38	15.01	14.54	0.33	8.931	5.629	14.170
	70%*	15.89	15.68	16.89	16.16	0.53	2.259	1.101	4.634
	35%	16.13	16.14	16.68	16.31	0.26	1.802	1.271	2.556
	20%	14.45	14.10	14.58	14.38	0.20	13.546	10.298	17.817
<b>SW480 B</b>	100%	20.45	20.82	20.57	20.61	0.15	3.721	2.906	4.765
	75%*	20.23	19.80	20.14	20.06	0.19	4.953	3.703	6.625
	40%	23.61	23.66			0.03	0.739	0.636	0.859
	35%	20.39	20.63	21.09	20.70	0.29	0.355	0.232	0.543
	10%	24.48	24.33	24.68	24.50	0.14	0.462	0.364	0.587
<b>SW480 R</b>	80%	20.24	20.43	20.81	20.49	0.24	6.394	4.554	8.978
	80%(2)	22.21	21.92	22.65	22.26	0.30	2.704	1.739	4.205
	40%	18.73	18.66	19.28	18.89	0.28	8.881	6.105	12.919
	20%	21.54	20.55	20.84	20.98	0.42	4.651	2.640	8.194
	10%	25.99	26.48	26.56	26.35	0.25	0.113	0.080	0.160
<b>SW620</b>	70%	25.51	25.17	25.61	25.43	0.19	0.249	0.158	0.394
<b>LT97</b>	100%	27.21	27.54		27.37	0.17	0.197	0.124	0.314
<b>Vaco</b>	50%	24.96	25.20	24.98	25.05	0.11	0.567	0.488	0.659
<b>Caco</b>	100%	26.93	26.75	27.21	26.96	0.19	0.154	0.112	0.211
<b>HTC116</b>	60%	26.44	25.44	25.97	25.95	0.41	0.342	0.196	0.598
<b>HT29</b>	70%	24.13	23.52	23.63	23.76	0.26	1.032	0.717	1.485

As reference cell line T98G 100% confluence and gene  $\beta$ -actin were used. Triplicates were measured. If no third value for cycle threshold (CT) is mentioned, it was omitted. Samples with standard deviation (SD) over 0.5 are seen as not valid and marked with \*.

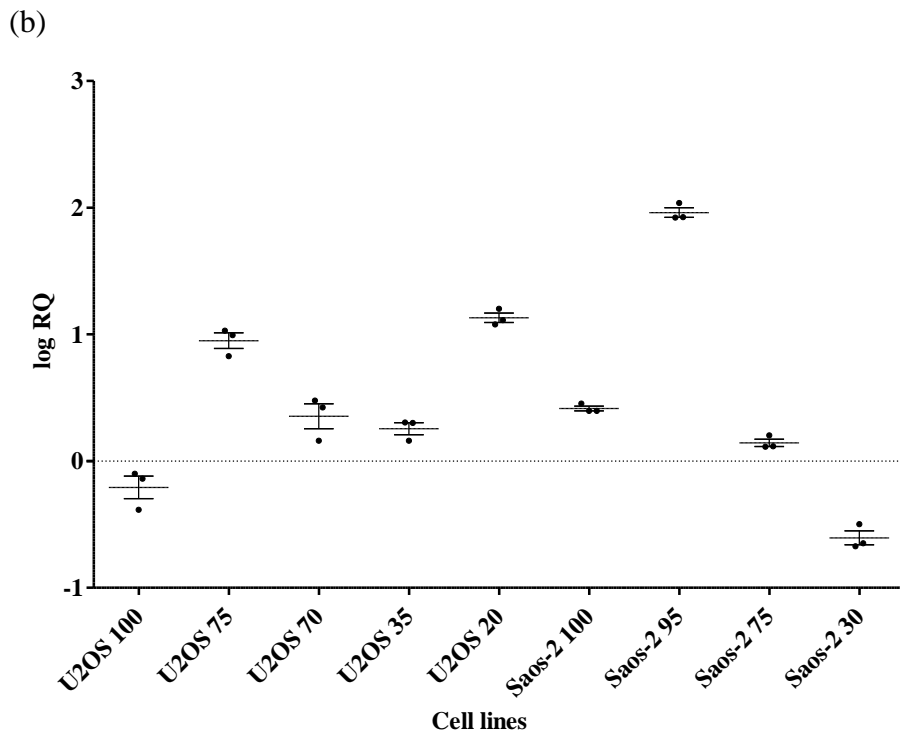
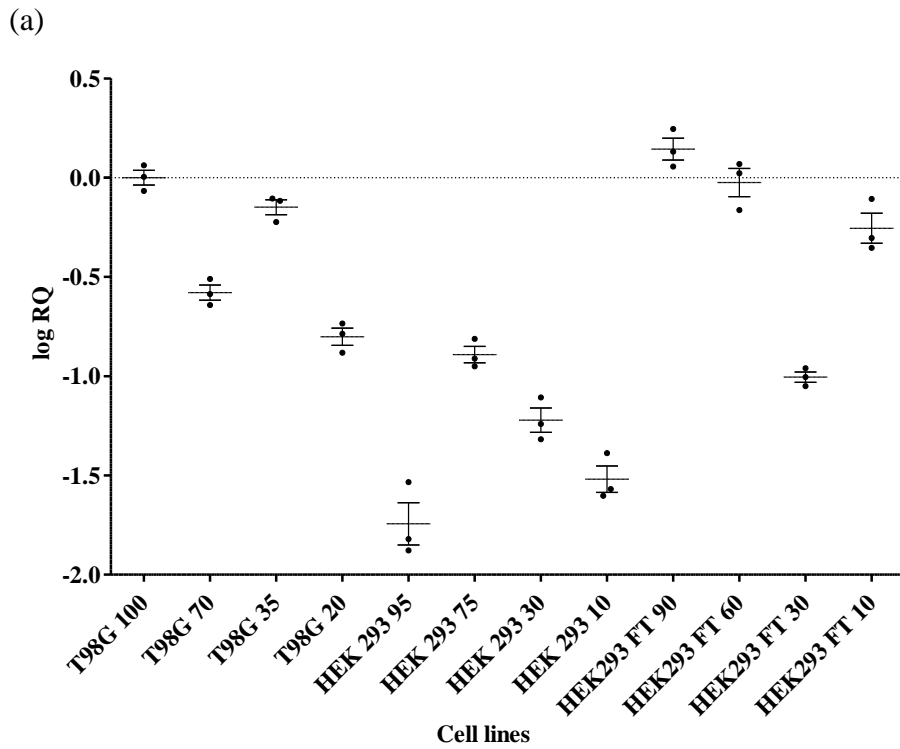


**Figure 5.24.: Scattered dot plot of confluence dependend total TERRA levels of different cell lines:** Points show single values, middle bar shows mean, upper and lower bar show SEM (standard error of the mean). Values at cell lines are percentage of confluence.

(a) Cell lines: T98-G, HEK293 and HEK293 FT

(b) Cell lines: U2OS and Saos-2

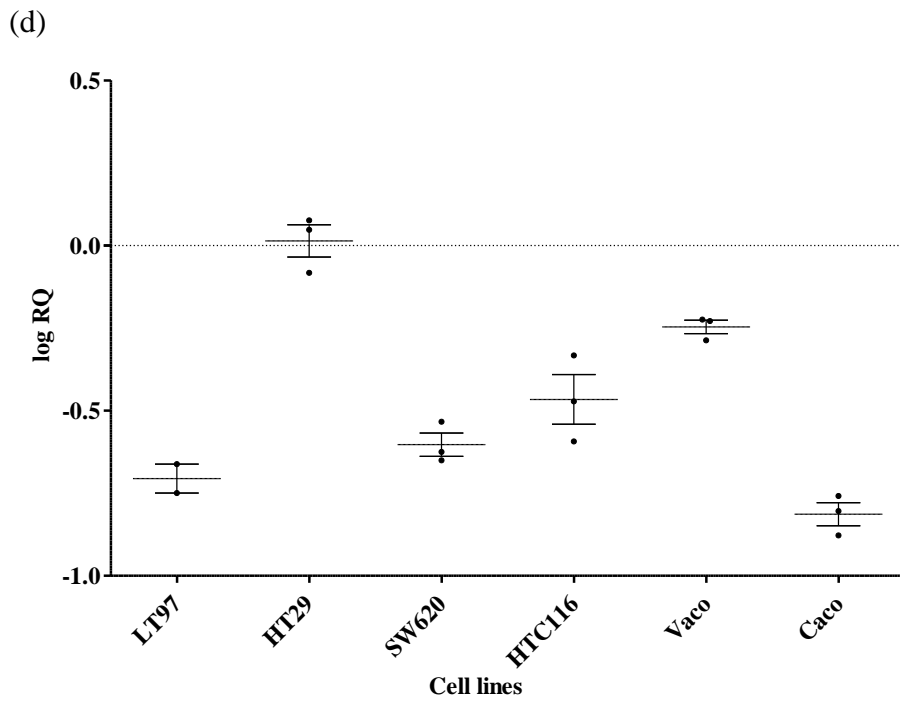
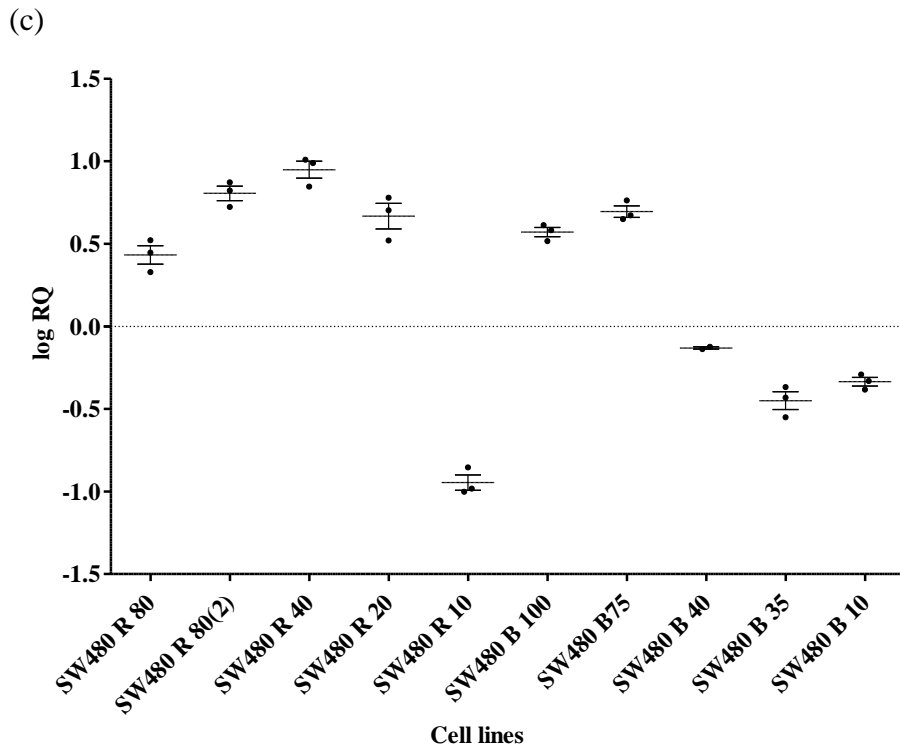


**Figure 5.24. (continued):**

(c) Cell lines: SW480 R and SW480 B

(d) Cell lines: LT97, HT29, SW620, HTC116, Vaco, Caco

**Table 5.10.: Trend analysis of confluence dependent TERRA expression:**

Cell lines	One-way analysis of variance		Post test for linear trend	
	P value		P value	R <sup>2</sup>
T98G	< 0.0001		< 0.0001	0.4447
HEK293*	< 0.0001		0.4142	0.0067
HEK293 FT	0.0005		0.0003	0.5361
Saos-2	< 0.0001		0.0008	0.0757
U2OS	< 0.0001		< 0.0001	0.2644
SW480B	< 0.0001		< 0.0001	0.6788
SW480R	< 0.0001		0.0073	0.0949

Cell lines with a P-value for linear trend excess 5% (0.0500) are marked with \*

Except HEK293 with 95% confluence, U2OS with 70% confluence and SW480 B with 75% confluence all cycle thresholds (Ct) showed a standard deviation below 0.5 and are seen as valid (Table 5.9.). Trend analysis of confluence dependent TERRA expression show in all cell lines a statistical trend except HEK293 cells (Table 5.10.) TERRA expression increases with increasing confluence in all cell lines (Table 5.9.). Saos-2, U2OS, SW480 B and SW480 R showed the highest TERRA expression levels (Table 5.9., Figure 5.24.). Lowest TERRA expression levels were reached by HEK293.

### **5.3.3. Subtelomer specific TERRA-level:**

From different cell lines subtelomere specific TERRA-level were measured with primer for subtelomeric region of chromosome 2p, 18p, 10p and 10q. Confluences of the samples were not known.

**Table 5.11.: Subtelomere specific TERRA expression:** CT = Cycle threshold. SD = standard deviation, Samples with standard deviation over 0.5 are not valid and are marked with \*

(a) Chromosome 10p TERRA

Cell line	Ct			Ct Mean	SD	RQ	RQ Min	RQ Max
T98G	23.47	23.41	23.43	23.44	0.02	1.000	0.855	1.169
HEK293	24.40	24.75	24.77	24.64	0.17	0.908	0.544	1.514
HEK293 FT	22.58	22.56	22.55	22.56	0.01	11.829	0.881	158.791
U2OS	25.42	25.34	25.47	25.41	0.05	0.177	0.152	0.206
Saos-2	23.94	24.38	24.39	24.24	0.21	0.577	0.498	0.667
SW480R	23.45	23.58	23.72	23.58	0.11	27.003	21.142	34.487
SW480B	29.95	29.69	30.28	29.97	0.24	0.182	0.124	0.268

**Table 5.11. (continued):****(b) Chromosome 10q TERRA**

<b>Cell line</b>	<b>C<sub>T</sub></b>			<b>C<sub>T</sub> Mean</b>	<b>SD</b>	<b>RQ</b>	<b>RQ Min</b>	<b>RQ Max</b>
T98G	25.75	25.82	25.78	25.78	0.03	1.000	0.853	1.173
HEK293	27.52	27.49	27.50	27.50	0.01	0.632	0.408	0.979
HEK293 FT*	28.89	25.17		27.03	1.86	2.713	0.004	1933.482
U2OS	27.29	27.07	27.29	27.22	0.10	0.257	0.209	0.316
Saos2	26.44	26.38	26.41	26.41	0.03	0.650	0.639	0.662
SW480R	25.51	25.25	25.51	25.42	0.12	38.290	29.578	49.568
SW480B	31.75	31.50	31.40	31.55	0.15	0.310	0.243	0.395

**(c) Chromosome 18p TERRA**

<b>Cell line</b>	<b>C<sub>T</sub></b>			<b>C<sub>T</sub> Mean</b>	<b>SD</b>	<b>RQ</b>	<b>RQ Min</b>	<b>RQ Max</b>
T98G	27.97	28.30	28.42	28.23	0.19	1.000	0.715	1.398
HEK293	28.62	28.38	29.23	28.74	0.36	1.461	0.717	2.974
HEK293 FT	26.60	26.55	27.09	26.75	0.24	18.002	1.305	248.413
U2OS	31.57	31.75	31.18	31.50	0.24	0.072	0.048	0.108
Saos2	27.32	27.74	27.54	27.53	0.17	1.629	1.445	1.837
SW480R	26.81	26.69	26.58	26.70	0.09	86.513	68.978	108.507
SW480B*	31.27	32.31	34.64	32.74	1.41	0.743	0.082	6.700

**(d) Chromosome 2p TERRA**

<b>Cell line</b>	<b>C<sub>T</sub></b>			<b>C<sub>T</sub> Mean</b>	<b>SD</b>	<b>RQ</b>	<b>RQ Min</b>	<b>RQ Max</b>
T98G	27.56	27.62	27.55	27.58	0.03	1.000	0.852	1.174
HEK293	27.85	27.73		27.79	0.06	1.797	0.972	3.321
HEK293 FT	25.96	25.92	25.92	25.93	0.02	20.121	1.499	270.158
U2OS*	30.22	31.21	29.75	30.39	0.61	0.099	0.038	0.258
Saos2	28.70	28.71	28.99	28.80	0.13	0.429	0.391	0.471
SW480R	26.35	26.44	25.98	26.26	0.20	74.394	52.171	106.082
SW480B*	32.42	31.78	33.07	32.42	0.53	0.587	0.256	1.345

10q subtelomeric TERRA level of HEK293 FT, 18p subtelomeric TERRA level of SW480 B and 2p subtelomeric TERRA levels of U2OS and SW480 B showed standard deviation over 0.5 and are determined as not valid. The highest RQ-values were measured in cell lines SW480R and HEK293 FT which showed a 2.7 to 86 times higher RQ level than T98G in all measured subtelomeric TERRA levels (Table 5.11. and Figure 5.25.). The lowest reached subtelomeric TERRA levels were reached by U2OS and SW480 B (till 1/10 of T98G). TERRA levels of chromosome 18p showed the highest level in comparison with other measured subtelomeric TERRA levels in cell lines Saos-2, SW480B and SW480R (Table



5.11. and Figure 5.25.). TERRA levels of chromosome 2p showed the highest level in comparison to other subtelomeric TERRAs in cell lines HEK293 and HEK293 FT. TERRA level of chromosome 10q TERRA showed the highest level in comparison to other subtelomeric TERRAs in cell line U2OS.

Statistic analysis with one-way ANOVA showed that means differ significantly (Table 5.12.)

(a)

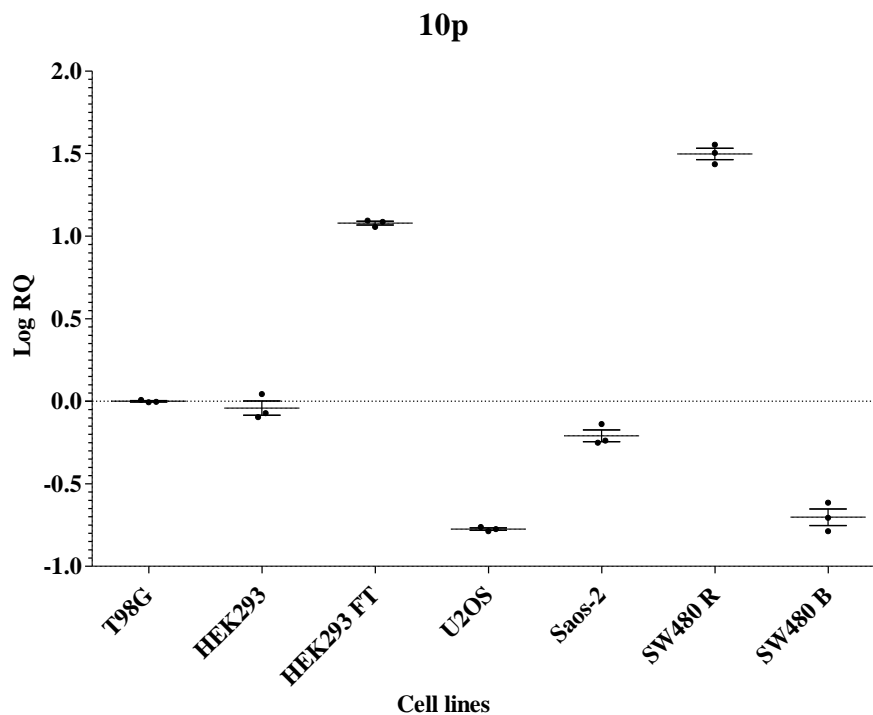
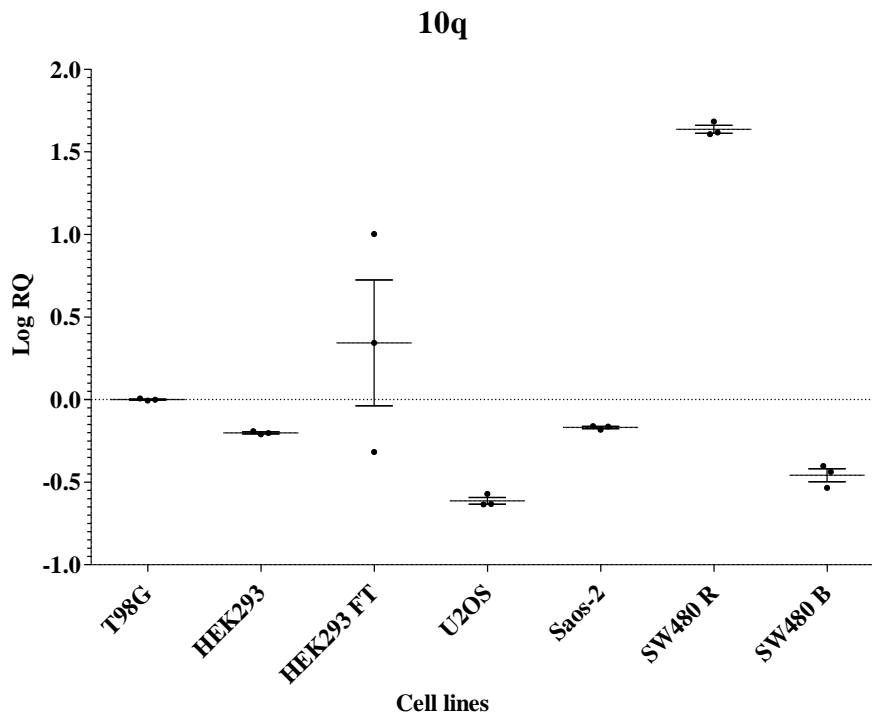


**Figure 5.25.: Scattered dot plot of logRQ subtelomeric TERRA levels:** Points show single values, middle bar shows mean, upper and lower bar show SEM (standard error of the mean)

(a) Scatter dot plot of chromosome 10p subtelomeric TERRA expression

(b)



(c)

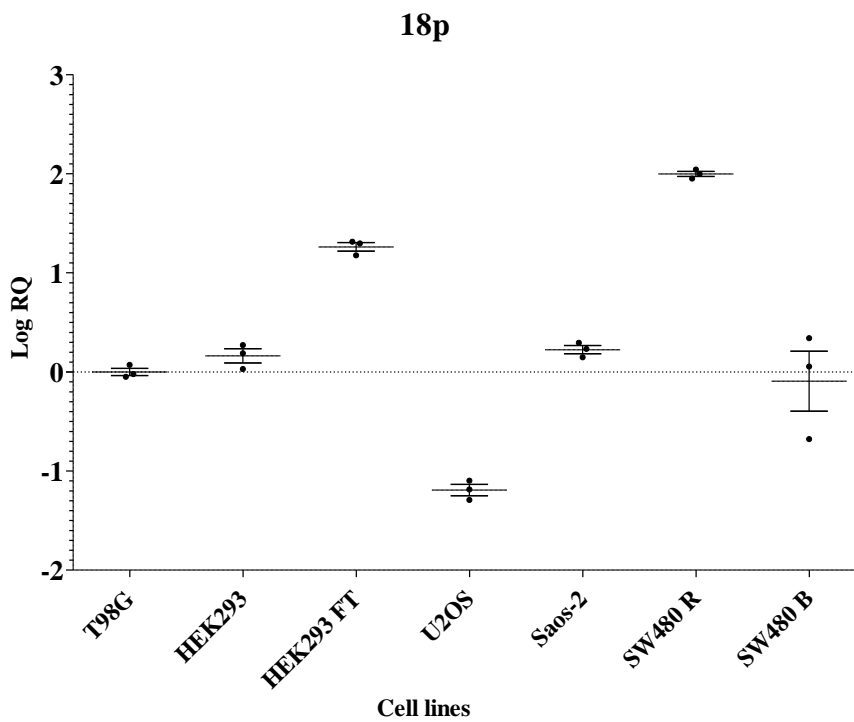


**Figure 5.25. (continued):**

(b) Scatter dot plot of chromosome 10q subtelomeric TERRA expression

(c) Scatter dot plot of chromosome 18p subtelomeric TERRA expression

(d)

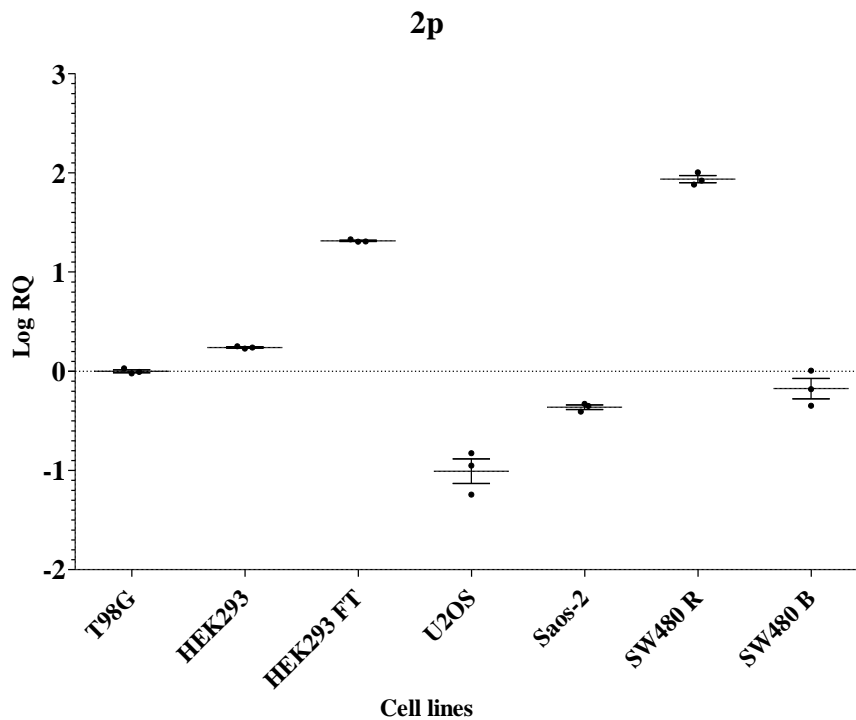


**Figure 5.25. (continued):**

(d) Scatter dot plot of chromosome 18p subtelomeric TERRA expression

**Table 5.12.: One-way ANOVA of subtelomere specific TERRA expression: P-values below 0.0500 (=5%) shows a statistically significant difference.**

Gene	One way analysis of variance
	P-value
10p	< 0.0001
10q	< 0.0001
18p	< 0.0001
2p	< 0.0001

#### **5.4. Relative telomere length by Real Time-PCR:**

Telomere lengths were also determined by RT-PCR. This method only gives information about relative length but not about absolute length. For absolute length determination TRF must be conducted. For telomere length genomic DNA isolated with Maxwell® DNA Purification Kit from Promega as described in material and methods were used.

**Table 5.13.: Relative quantities of telomere length:** As reference sample T98G and gene  $\beta$ -actin were used. Samples were measured in duplicates. Two measurements were done (a) 1<sup>st</sup> measurement, (b) 2<sup>nd</sup> measurement, CT = Cycle threshold. SD = Standard deviation, SD over 0.5 were seen as not valid and are marked with \*

(a)

**1st Measurement**

Cell line	CT		CT mean	SD	RQ	RQmin	RQmax
T98G	23,21	22,44	22,83	0,38	1,000	0,349	2,867
HEK293 FT*	16,64	14,66	15,65	0,99	0,121	0,008	1,784
U2OS	16,57	16,10	16,34	0,24	42,837	23,081	79,504
Saos2	21,37	21,12	21,25	0,13	3,936	3,626	4,249
SW480R	22,68	22,45	22,56	0,12	0,554	0,381	0,807
SW480B	21,97	21,29	21,63	0,34	2,352	0,849	6,517
HT29	11,98	12,77	12,38	0,39	1,118	0,338	3,692
HTC116	13,71	13,88	13,80	0,08	0,800	0,293	2,184
LT97	15,08	15,81	15,45	0,37	0,281	0,045	1,765
Vaco	25,87	25,63	25,75	0,12	0,179	0,122	0,264
YTBO*	14,38	12,84	13,61	0,77	0,658	0,066	6,533
Fibroblasten*	24,75	22,81	23,78	0,97	2,710	0,209	35,119

(b)

**2nd Measurement**

Cell line	CT		CT mean	SD	RQ	RQmin	RQmax
T98G	23,72	23,76	23,74	0,02	1,000	0,773	1,293
HEK293 FT*	16,19	17,28	16,74	0,55	0,123	0,029	0,530
U2OS	16,27	16,98	16,62	0,36	56,598	22,322	143,508
Saos2	22,05	22,92	22,49	0,43	2,952	0,954	9,134
SW480R	22,87	23,66	23,26	0,40	0,652	0,191	2,221
SW480B	21,41	21,14	21,27	0,13	3,708	2,193	6,269
HT29	12,87	12,72	12,79	0,08	1,346	0,959	1,890
HTC116	15,49	15,30	15,40	0,09	0,332	0,227	0,486
LT97	14,53	15,20	14,87	0,34	0,285	0,090	0,904
Vaco	26,67	26,74	26,70	0,04	0,182	0,137	0,243
YTBO	13,93	14,22	14,07	0,15	0,769	0,181	3,265
Fibroblasten	23,98	23,87	23,92	0,05	1,338	0,008	228,012

(a) First measurement of relative telomere length by Real-Time PCR

(b) Second measurement of relative telomere length by Real-Time PCR

Cell line HEK293 FT showed no valid values adverted to SDs, but both measured RQs are very similar (0.121 and 0.123), so it could be seen as valid data (Table 5.13.). YTBO and fibroblasts showed each one not valid value adverted to SDs. Values of both measurements were calculated to an RQ mean (Table 5.13.c).

**Table 5.13. (continued):** RQ means of RQs of first and second measurement. SD RQ = Standard deviation of RQs of first and second measurement, %SD RQ = percentage of standard deviation in reference to RQ mean

(c)

Cell line	RQ mean	SD RQ	%SD RQ
T98G	1.000	0.000	0.00
HEK293 FT	0.122	0.001	1.16
U2OS	49.718	6.881	13.84
Saos2	3.444	0.492	14.30
SW480R	0.603	0.049	8.08
SW480B	3.030	0.678	22.36
HT29	1.232	0.114	9.28
HTC116	0.566	0.234	41.30
LT97	0.283	0.002	0.71
Vaco	0.181	0.002	0.93
YTBO	0.714	0.056	7.82
Fibroblasten	2.024	0.686	33.90

(c) Mean RQ of first and second measurement

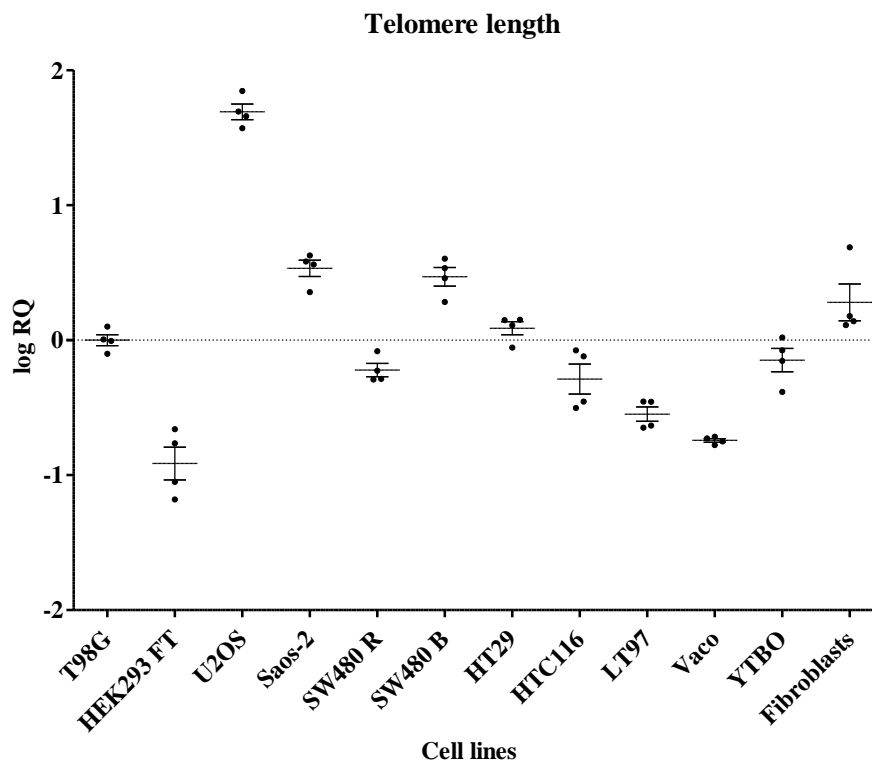


**Figure 5.26.:** Scattered dot plot of telomere lengths of both measurements. Points show single values, middle bar shows mean, upper and lower bar show SEM (standard error of the mean)

The ALT cell lines U2OS and Saos-2 reached a 3.4 to 49.7 times higher RQ than T98-G and also SW480 B reached a 3 times higher RQ than T98-G (Figure 5.26. and Table 5.12.c). Lowest RQ values were reached in HEK293-FT (0.112), Vaco (0.181) and LT97 (0.283) in comparison to T98-G.

### **5.5. Chromosome 2p subtelomeric methylation specific RT-PCR:**

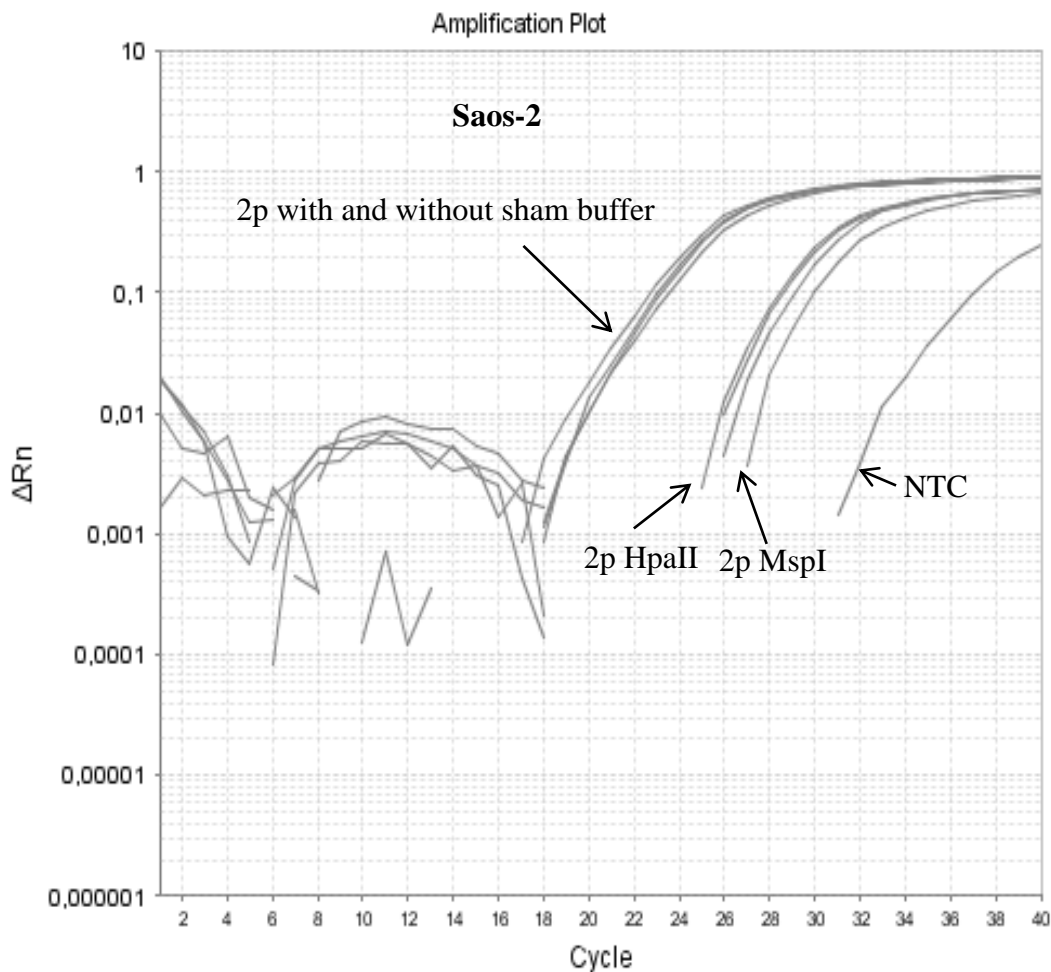


**Figure 5.27: Amplification plot of 2p subtelomeric methylation specific Real Time-PCR pretesting:** Test if sham buffer influences PCR-reaction. Samples have the same cycle threshold regardless if buffer was added or not

No difference was detectable between PCR with sham buffer, which was used as control for samples which were not cut by restriction enzymes and without this buffer. Due to this further studies with sham buffer were omitted (Figure 5.27).

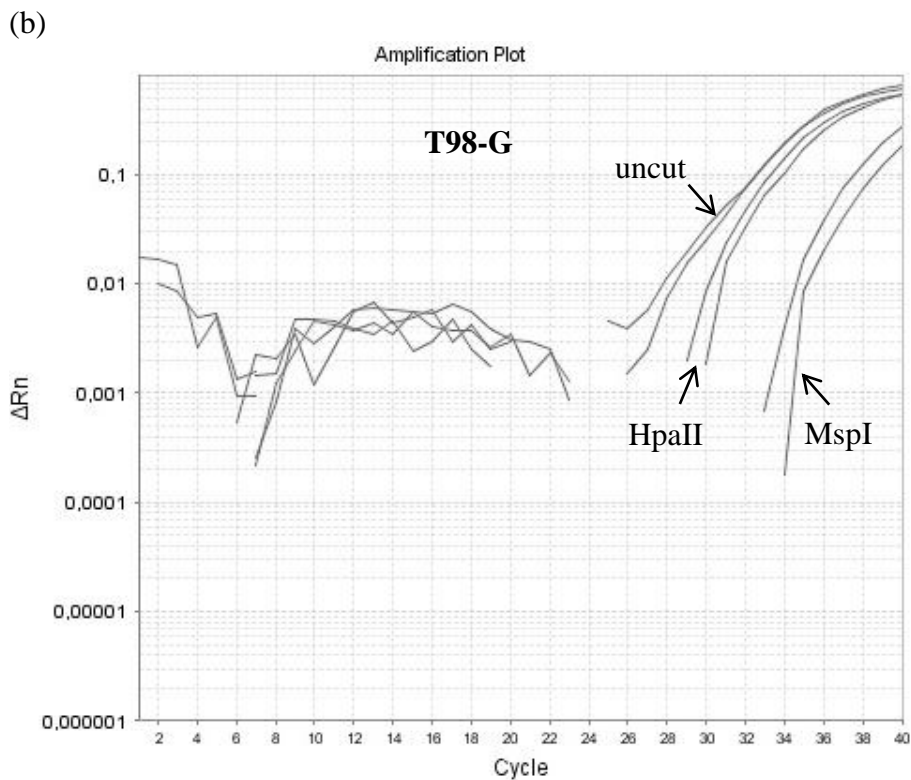
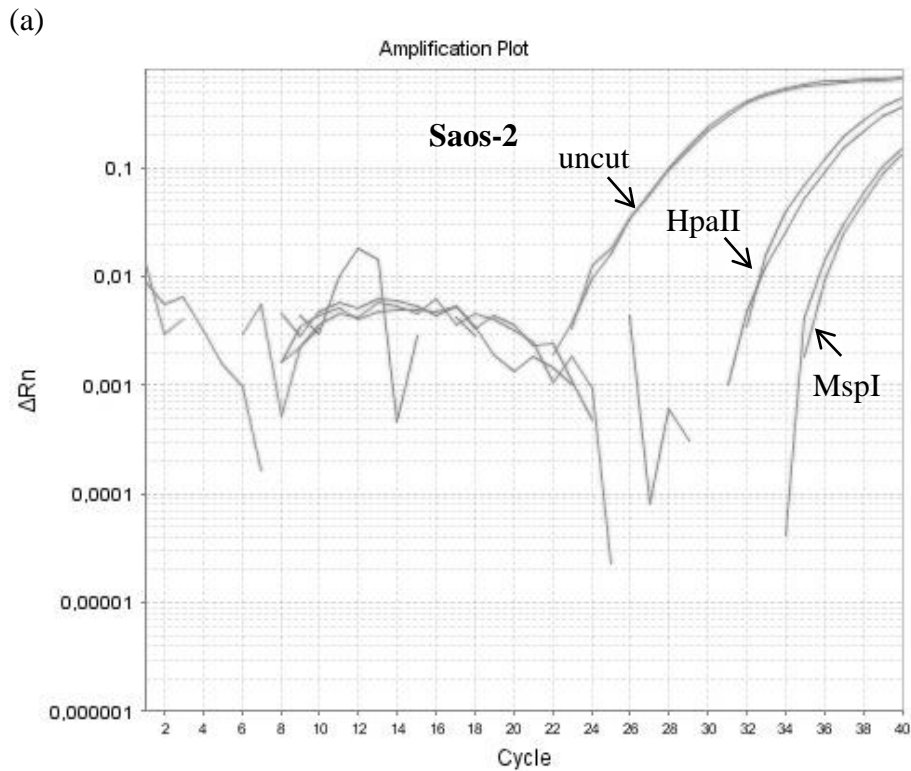


**Figure 5.28: RQ values of 2p subtelomeric methylation specific Real Time-PCR: Saos2** was used as references sample. Saos2 and T98G were cut with MspI, HpaII or stayed uncut to check up methylation state.

(a): Amplification plot of Saos-2

(b): Amplification plot of T98-G

Chromosome 2p subtelomeric methylation specific RT-PCR of Saos-2 and T98-G (Figure 5.28.) allowed to calculate cut and methylation percentages.

Cut percentages were calculated with fomula:

Saos-2:

- CFTR: 100%
- Chromosome 2p TERRA: 100%

T98-G:

- CFTR: 99.9%
- Chromosome 2p TERRA: 98.5%

Methylation percentages were calculated with formula:

Saos-2:

- CFTR: 7.7%
- Chromosome 2p TERRA: 0.4%

T98-G:

- CFTR: 25.8%
- Chromosome 2p TERRA: 34.4%

Efficiency of cut was very high, 100% at Saos-2 and 98.5% for chromosome 2p TERRA and 99.9% for CFTR at T98-G. T98-G showed a more than 3 times higher methylation percentage at CFTR and an 86 times higher methylation percentage at chromosome 2p TERRA promoter region.



## **6. Discussion:**

The inhibitory function of the non-coding RNA called TERRA [70, 71] at telomerase activity was recently demonstrated [73, 78] and rises the possibility for a new anticancer mechanism. One of the major aims of this thesis was to develop expression vectors for telomere sequences.

Cloning of the telomere fragment showed some difficulties. Different modifications were necessary to transfer the telomere fragment into the pENTR- vector. Reason for these difficulties at cloning steps could be the intramolecular G-quadruplex structure that is adopted by telomeric repeats [9]. It is known, that this special structure could influence potency on very different targets. G-quadruplex structures show an inhibitory function against telomerase [99] and in a few eukaryotic promoter regions it was found that it could influence transcription activity [100]. It is possible that this structure could also have more effects on a variety of different targets, but this is not investigated. Due to examples with known functions of this special DNA-structure, I would speculate that enzyme functions important for cloning in bacteria are hindered acting near the telomere sequence.

We reasoned that transferring the telomere fragment between plasmids or vectors by recombination would be easier and more efficient than using standard cloning techniques. Using promoters, other than RNA polymerase II was also an aim of my diploma thesis. It is not clear that RNA polymerase II is responsible for TERRA transcription [71]. The known association of only non polyadenylated TERRA with telomeres was one reason behind my decision to use a different RNA polymerase than RNA polymerase II [73].

The 0.8kbp telomere fragment was finally successfully cloned with standard techniques into pENTR plasmids, in sense and anti-sense orientation, with and without hH1 promoter and terminator for RNA-polymerase III. With gateway recombination adenoviral vectors pAd/pl Sense Tel, pAd/pl Antisense Tel and pAd/CMV Sense  $\Delta$ hH1 with the deleted hH1 but under control of CMV promoter and Herpes Simplex Virus thymidine kinase (TK) polyadenylation sequence termination signal were produced.

In first attempts I tried to create lentiviral vectors via the same gateway recombination reaction, but it did not work with telomere fragments. The used vector pLenti6/UbC/V5-DEST worked in a gateway reaction with another fragment for another project. The reasons for this failed attempt are not clear however it may be that the telomere fragment and its structure interfered with the lentiviral vector backbone and inhibited the gateway reaction.

Unfortunately there was not enough time to repeat these experiments and discover the reasons for this problem. In the near future replications of experiments using lentiviral vectors will arise if a general problem does indeed exist. However, my results demonstrate that with the gateway recombination system adenoviral expression vectors for telomere sequences can be constructed.

The production of recombinant adenoviruses was performed with HEK293 FT, transfected with adenoviral plasmid constructs. To optimize this transfection, I first performed experiments with pEGFP expression vectors. The efficiency was measured with FACS and microscopy. The GFP-FACS showed that the highest efficiency for transfection with lipofectamine 2000 was with 50% confluence and with Wizard® *Plus* Minipreps DNA Purification System. HEK293 FT cells settled well with a good distribution and confluence but after treatment with lipofectamine they built up agglomerates. This could influence uptake efficiency. The reason for this agglomerates were, that the cells stayed too long at room temperature and together with the lipofectamine treatment they detached and settled down again. This temperature sensitivity is also known in literature [101].

With the produced constructs the level of TERRA in cells should be altered. The endogenous ground level has to be determined. Recent publication showed that TERRA level is influenced by cell cycle state [73]. Different confluences showed influence on cell cycle. Detaching with trypsin led in both cell lines to a higher percentage of cells in G0/G1 and a lower percentage of cells in S cell cycle state in comparison to detaching by scratching. Treatment with Trypsin required a few minutes of treatment, maybe this could influence the cell cycle state. SW480 R showed more cells in G0/G1 cell cycle state than SW480 B, regardless of detaching technique. In both cell lines higher confluences showed less cells in S and G2/M cell cycle state (up to 3 times lower). Detaching with trizol showed also a clear trend of increasing percentage of cells in S phase by decreasing confluence state.

Real-Time PCR of total TERRA expression in dependency of confluence was done. TERRA expression increased up to 10 times with increasing confluence in all measured cell lines except U2OS. But also U2OS showed a significant trend of increasing TERRA expression level by increasing confluence. A relationship between confluence and cell cycle state was shown. These results accompany with literature, that during S phase TERRA level decreases and reached the lowest level at the transition state between S and G2 [73]. TERRA level in U2OS and Saos-2 were about 1 to 450 times higher than in T98-G. In general, higher TERRA levels in ALT cell lines like U2OS and Saos-2 are in agreement with literature [77].

Interestingly, two of the studied telomerase positive cells, SW480 B and SW480 R showed in nearly all confluence states higher TERRA expression levels in comparison to T98-G of about 0.5 to 3 and 0.7 up to 10 fold, respectively. Why these elevated TERRA levels occurred at these two telomerase positive cell lines is not yet clear. Maybe in these cell lines both telomere maintain mechanism (TMM), telomerase activity (TA) and ALT, are active as known in literature [67]. At least for SW480 B, extreme long telomeres could be detected by TRF southern blotting and the existence of c-circles within the cells, both indicating the existence of ALT (S.Sampl, personal communication). Telomerase positive cell lines like HEK293 showed about 2 to 50 times lower TERRA expression levels and HEK293 FT showed nearly similar TERRA expression levels than T98-G as in accordance with literature [77]. These results were investigated, because lack of time only by a single experiment and were not repeated. So the results should not be overestimated and repeating is necessary. We demonstrated in a further study, that a correlation of TERRA levels and TMM in astrocytomas [103]. Further planned in vitro experiments with TERRA expression constructs may demonstrate if a functional correlation between TERRA expression and TMM may exist in tumor cells. Such results may have implication for anti-telomerase tumor therapy concepts. Collaboration with Geron Corporation, which has the telomerase inhibitor drug Imetelstat (GRN162L), currently in clinical phase II trials [102] is already in progress and further experiments are planned.

It can be estimated from literature that a large part of TERRA molecules consist of subtelomeric sequences [72, 73]. It could be an interesting point which chromosome ends expresses TERRA and how strong these chromosome-end specific expressions are. Measurements showed differences between subtelomeric expression levels in different cell lines. HEK293 and HEK293 FT showed both the highest RQs at chromosome 2p subtelomeric TERRA and SW480 R and SW480 B showed both the highest RQs at chromosome 18p subtelomeric TERRA. Because this cell lines have respectively the same origin, it could be that the ratios of chromosome end specific TERRAs stay constant, but this hypothesis needs validation. Between telomerase positive and negative cell lines, no relation is visible. Reasons for these different levels of subtelomeric TERRA expression levels are not clear. In our further study we investigated chromosome end 18p and 2p TERRA expressions among other samples [103]. In our further study chromosome end 18p was similar expressed in Saos-2 as in T98-G, in this study Saos-2 showed a 1.6 higher expression as T98-G, which are not quiet different. Chromosome end 2p was expressed 2.5 to 5 times higher in Saos-2 as in T98-G and our further study, in this study T98-G showed about 2 times higher expression in

comparison to Saos-2. Why this difference at chromosome end 2p expression level exists is not known, but the results of this study are based on a single experiment and were not repeated, so the validity is not very high and a repeating should be done.

Due to TMM tumor cells retain a constant telomere length. Treatment with TERRA which acts as telomerase inhibitor [78] should decrease telomere length in telomerase positive tumor cells. U2OS and Saos-2, two known ALT cell lines reached about 49.7 and 3.4 times higher relative high telomere length as T98-G, respectively. Heterogeneous and high telomere lengths of ALT tumor cell lines are known in literature [66], and in our further study we also mentioned an about 3.2 times higher Saos-2 relative telomere length in comparison to T98-G. Telomere length of fibroblasts depends on time grown in cell culture, because they have not got the ability to maintain their telomere length. In further experiments telomere lengths of treated and untreated cells have to be compared. SW480-B also showed an about 3 times higher telomere length in comparison to T98-G. This was also mentioned in further studies in our lab and enforces the assumption that long time passaging of SW480 led to a change of TMM maintenance.

Expression of TERRA depends strongly on methylation of CpG islands of their promoters [72]. Based on the publication of Kanel et al. [98], my colleague Sandra Sampl and I established a one-step methylation specific Real-Time PCR assay for one CpG loci of the TERRA promoter on chromosome end 2p. The methylation sensitive restriction endonuclease HpaII cuts at this defined CpG position if it is not methylated. MspI cuts at the same position, but isn't methylation sensitive so it is always cut and serves as a control. The cutting efficiencies were 98.5% to 100% and so the DNA should be restrictable. With HpaII methylation percentage of this CpG-position is ascertainable. T98-G showed a more than 3 times higher methylation percentage at CFTR (25.8% to 7.7%) and an 86 times higher methylation percentage at the chromosome 2p TERRA promoter region (34.4% to 0.4%) as Saos-2. This methylation results correlates with our former study based on epigenetic allelic sequencing which determined, a higher methylation grade of T98-G in comparison to Saos-2 [103]. In this study we measured a mean methylation grade of subtelomeric region 2p of 95.8% in T98-G and 17.3% in Saos-2. To optimize this assay further experiments have to be done, including other tumor cell lines and tissues. Investigation of other subtelomeric regions, more CpG islands of TERRA promoter regions with the right sequence for restriction enzyme cuts could be found and allows extension of this assay. This would be an easy and fast way to compare different subtelomeric methylation state.

The TERRA expressing constructs of this study should now be tested in vitro. TERRA and antisense TERRA could be produced to increase TERRA concentration or to inhibit endogenous TERRA in cells. They may grant the ability to learn more about the function and potential of TERRA in tumor cell suppression. My data about cell cycle state dependency of TERRA expression and the connection with confluences of cell growth on monolayer will be a starting point for detailed in vitro studies. The expression system developed in this study can be used to express chromosome-end specific TERRA transcripts. With such a strategy the chromosome end specific effects of subtelomeric TERRA and TMM may be studied. In connection with qTelo-FISH (quantitative telomere fluorescent-in-situ-hybridization) for cells with normal karyotype and STELA (single telomere length analyses) for tumor cell the effects of subtelomeric TERRA on individual telomere lengths may be investigated. Furthermore, as anti-telomerase tumor therapies with small molecules like Imetelstat [102] reach the clinics, it may be interesting to see if TERRA interferes with the success of anti-telomerase treatments. Summing up, TERRA expression systems will be an important starting point for research of TERRA function, anti-telomerase potency and may be helpful to investigate new important anti-cancer mechanism.

## 7. Curriculum Vitae:

Währingerstrasse 126/6

A-1180 Vienna

+43650/3018600

[christianstern@gmx.at](mailto:christianstern@gmx.at)



### Personal data:

Date of birth: 30.01.1986  
Place of birth: Bad Eisenkappel  
Citizenship: Austria

### Education:

1992-1994 Öffentliche Volksschule 6 Klagenfurt (Elementary school)  
1994-1996 Volksschule 2 Süd Ferlach (Elementary school)  
1996-2004 Bundesgymnasium und Bundesrealgymnasium Klagenfurt  
Lerchenfeldstrasse (secondary school)  
2004 June 21<sup>st</sup>, school leaving examination with first rate success  
2005 Start of study biology on the university of vienna  
2007 Specialization into genetics/microbiology and furthermore into  
immunology  
2010 Start of diploma thesis under mentoring of A.o. Univ. Prof. Dr. Klaus  
Holzmann (Division of Cancer, Department of Medicine I,  
Comprehensive Cancer Center, medical university vienna)

### Scientific Experiences:

From 12/2010 - 02/2011: Practical at Division of Cancer, Department of Medicine I, Comprehensive Cancer Center, medical university vienna at the laboratory of Klaus Holzmann PH.D

From 02/2010 - 04/2011: Practical work on the diploma thesis at Division of Cancer, Department of Medicine I, Comprehensive Cancer Center, medical university vienna at the laboratory of Klaus Holzmann PH.D

From 04/2010: Collaboration at the co-operation project: „Anti-cancer-therapy using anti-viral drugs” between Division of Cancer, Department of Medicine I, Comprehensive Cancer Center, medical university vienna (Klaus Holzmann PH.D) and the division of surgical research, general surgery (Michael Bergmann MD)

From 12/2010: Collaboration at the project: „Expression of telomeres as therapeutic target for colon cancers“. (Project-team: Stefan Stättner MD, Klaus Holzmann PH.D, Brigitte Marian PH.D)

From 04/2011: Tutor at the vienna open lab

### Posters for congresses and publications:

Sandra Sampl, Christian Stern, Johannes Hainfellner, Matthias Preusser, Christine Marosi, and Klaus Holzmann (2010) „Expression of telomeres in astrocytic brain tumors and correlation with telomerase activity, telomere length and malignancy grade.“

Posterpresentation at the AACR-Special Conference 2010: The Role of Telomeres and Telomerase in Cancer Research, February 27 - March 2. 2010. Fort Worth, Texas

Sandra Sampl, Christian Stern, Johannes Hainfellner, Matthias Preusser, Christine Marosi, and Klaus Holzmann (2010) “Expression studies of telomerase and telomeres in brain tumors: Correlation with malignancy grade and prognoses.” Invited speech of Dr. Klaus Holzmann at 2nd Asian Conference on Environmental Mutagens, December 15 to 18. 2010. Pattaya, Thailand

Sandra Sampl<sup>1</sup>, Sibylle Pramhas<sup>1</sup>, Christian Stern<sup>1</sup>, Johannes Hainfellner<sup>3</sup>, Matthias Preusser<sup>2</sup>, Christine Marosi<sup>2</sup> and Klaus Holzmann<sup>1</sup>: “Expression of telomeres in astrocytoma WHO grade II to IV: high TERRA level correlates to telomere length and negatively to telomerase activity and advanced clinical stage”, Translational oncology (in press)

Authors Affiliations:

<sup>1</sup>Division of Cancer Research and <sup>2</sup>Division of Medical Oncology, Department of Medicine I, Comprehensive Cancer Center;

<sup>3</sup>Institute of Neurology; Medical University Vienna, Austria

Sandra Sampl, Christian Stern, Klaus Holzmann (2011) „Die Chromosomenlänge ist entscheidend.“ Article for the magazine: Krebs:hilfe! 2:2011

Nonscientific activities:

2005	Military Service
2008	Organisation work for the sport union „Studentensport“
2009	Sportadvisor for children for „WAT – Wiener Arbeiter-, Sport- und Turnverein“
02/2010	Chairman of the sport union „Studentensport“
07/2010	Working for „Manpower Hospitality“ as waiter
02/2011	Apprenticeship as group leader for “Manpower Hospitality”

Hobbies:

Floorball, Football, Volleyball, Reading

Special skills:

EMT at the Red Cross

State-certified Instructor for Fitsport/youths

Basic informatic knowledge (microsoft office, databases research, internet research, ...)

Driver’s license



## **8. Acknowledgment:**

Ich danke a.o. Univ. Prof. Dr. Klaus Holzmann für die Unterstützung und Hilfestellung während meiner Diplomarbeit. Für viele Gespräche die mir immer wieder neue Sichtweisen und Gedanken aufzeigten. Dafür das ich meine Diplomarbeit in seiner Arbeitsgruppe durchführen konnte und für die Tipps und Ratschläge beim Schreiben dieser Arbeit.

Univ. Prof. Dr. Manuela Baccarini für die Betreuung meiner Diplomarbeit.

Doris Mejri und Mag. Sandra Sampl danke ich für die Zusammenarbeit im Labor, für Hilfe bei Problemen und aufbauenden Gesprächen in Phasen in denen die Arbeit nicht wie geplant funktioniert hat. Nur mit Ihrer Hilfe konnte ich meine Diplomarbeit zu einem Abschluss führen.

Große Dankbarkeit gilt auch meinen Eltern, die mich immer finanziell unterstützt haben und mir auch immer die Möglichkeit gaben mich selbst zu verwirklichen.

Weiterer Dank gilt meiner Freundin Barbara, die immer für mich da war. Sie war mir der Rückhalt den ich immer wieder brauchte. Für diese Unterstützung bin ich über alles dankbar.

**9. Supplement:**

pENTR/D/hH1 shRNA NMP265

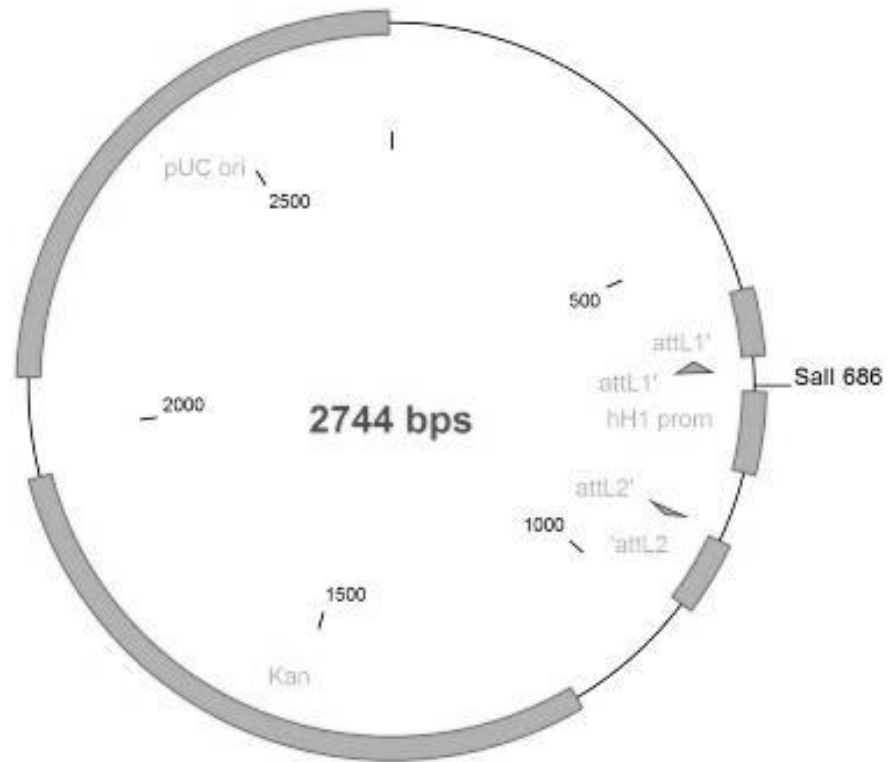


**Figure 10.1.:**

Start vector for cloning strategy. pENTR/D/hH1 vector with an shNMP265 insert.

pENTR/D/hH1 shNMP265 Delta SalI

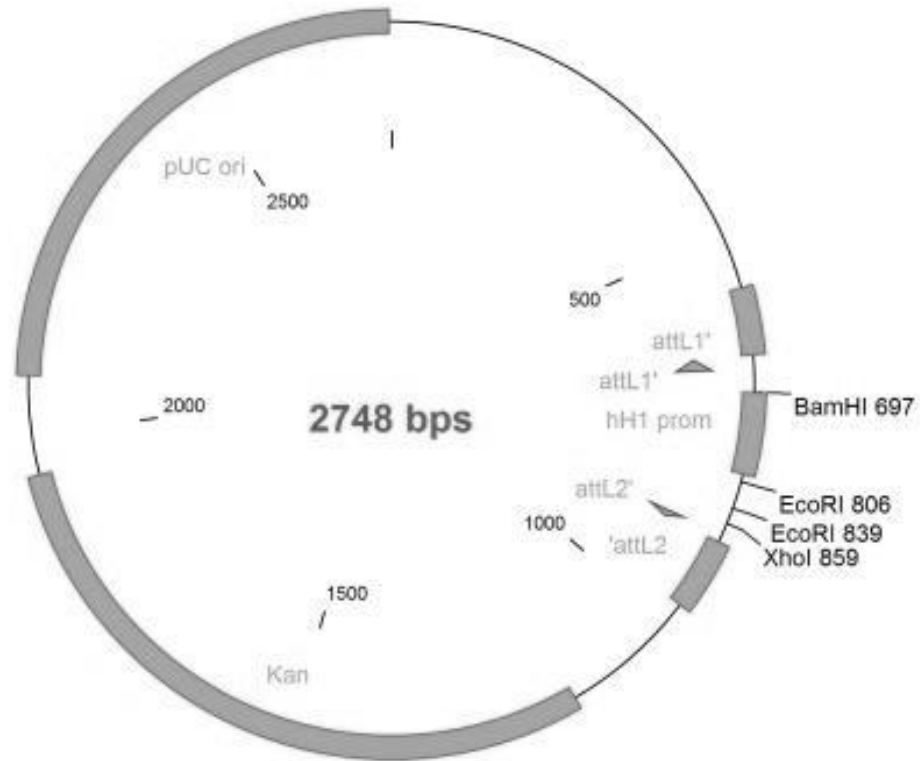


**Figure 10.2.:**

Deletion of SalI restriction site of pENTR/D/hH1 shRNA NMP265. Cut with SalI, fill in of overhangs with Klenow fragment and relegation were done.

pENTR/D/hH1 delta shNMP265

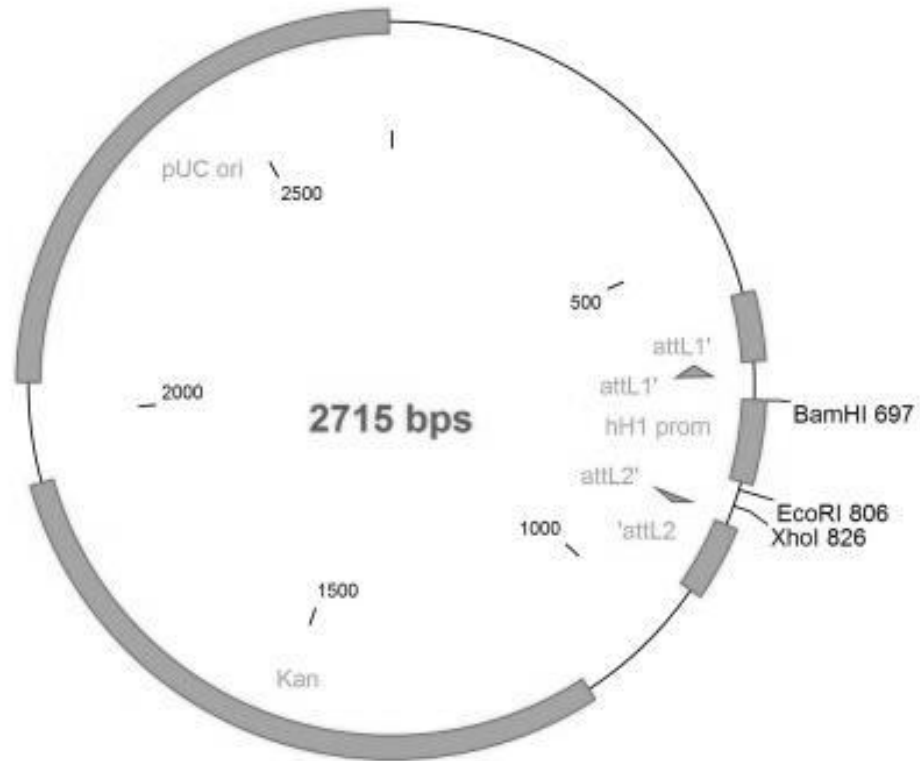


**Figure 10.3.:**

Elimination of shRNA NMP265 gene from vector pENTR/D/hH1 shNMP265 delta SalI. Cut with EcoRI and relegation eliminated gene for shRNA NMP265 were done.

### pENTR/D/hH1 Linker

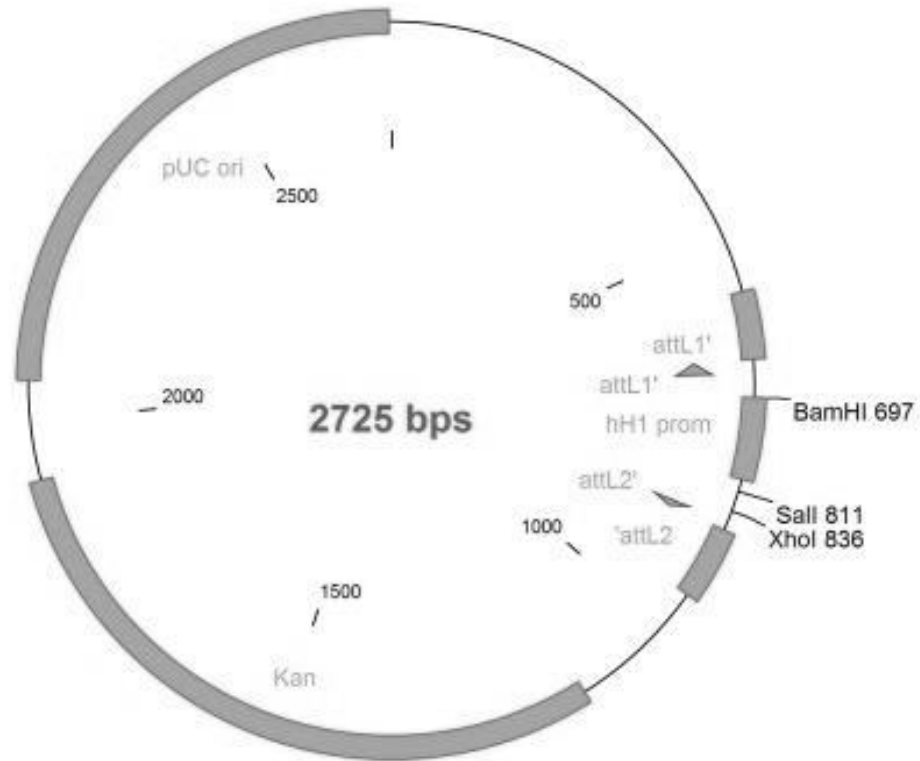


#### Figure 10.4.:

Insert of linker into pENTR/D/hH1delta shNMP265. Cut with EcoRI and annealing of pre-phosphorylated linker were done.

pSP73 with 0.8kb telomere fragment



**Figure 10.5.:**

pSP73 with Tel fragment

### pENTR/D/hH1 Antisense Tel

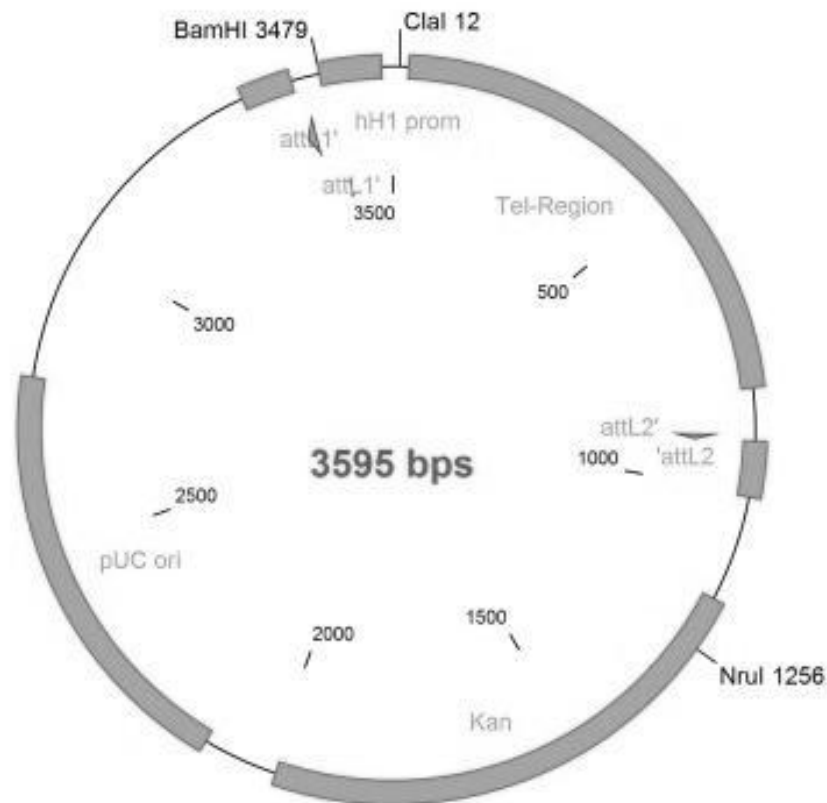


**Figure 10.6.:**

Integration of telomere fragment into pENTR/D/hH1 linker in anti-sense orientation. Cut of pENTR/D/hH1 linker with Sall and cut of pSP73 Tel with BamHI and BglII were done. Then gel purification, partial fill-in (Fill in with dTTP and dCTP at Sall overhangs and with dATP and dGTP at BamHI and BglII overhangs) and ligation were done.

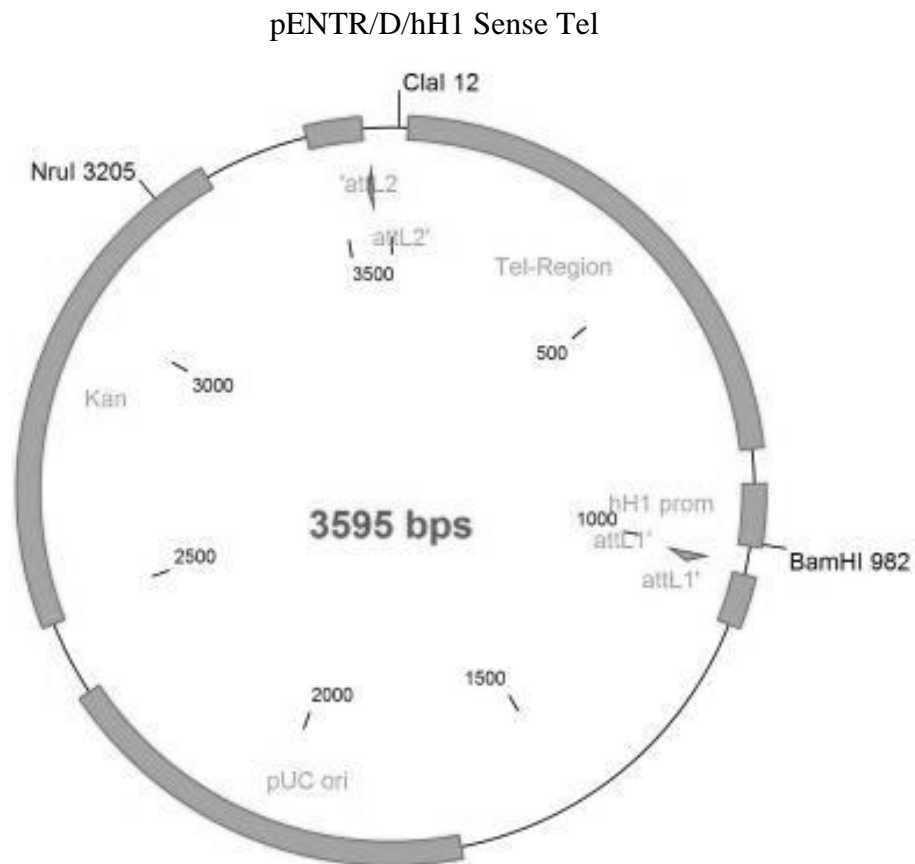


**Figure 10.7.:**

Integration of telomere fragment into pENTR/D/hH1 linker in sense orientation. Cut of pENTR/D/hH1 linker with SalI and cut of pSP73 Tel with BamHI and BglII were done. Then partial fill-in (Fill in with dTTP and dCTP at SalI overhangs and with dATP and dGTP at BamHI and BglII overhangs), gel purification and ligation were done.



pENTR/D/ Sense Tel delta hH1

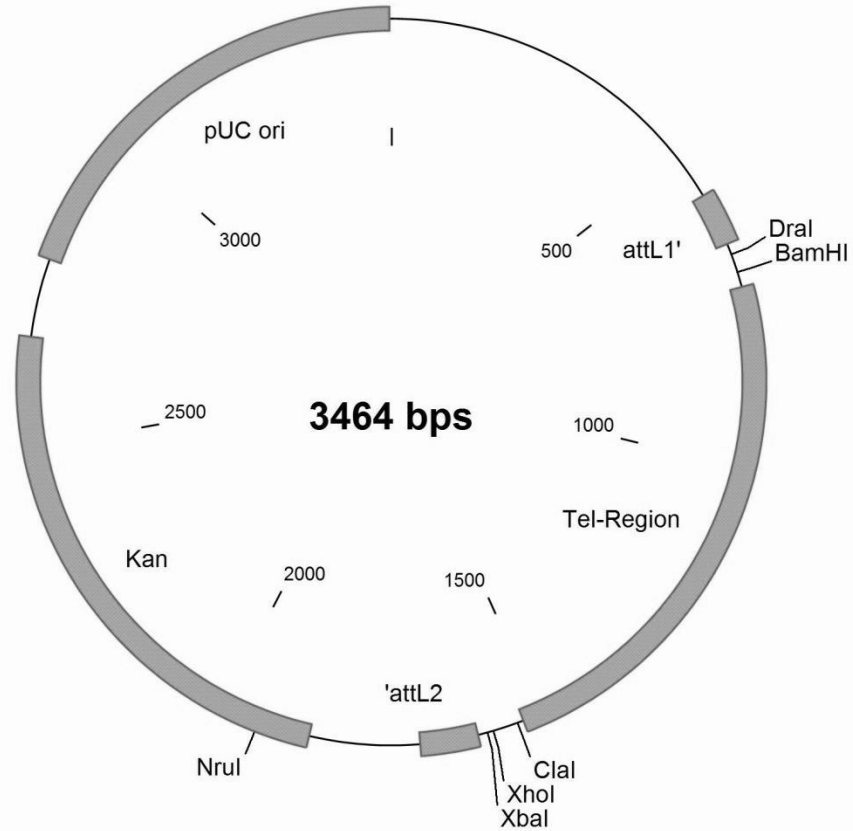


**Figure 10.8.:**

Deletion of hH1 promoter of pENTR/D/hH1 Sense Tel. Cut of pENTR/D/hH1 Sense Tel with SacI and BamHI, exonucleolytic activity at SacI overhang, fill-in at BamHI overhang and religation.

### pENTR/D/Antisense Tel delta hH1

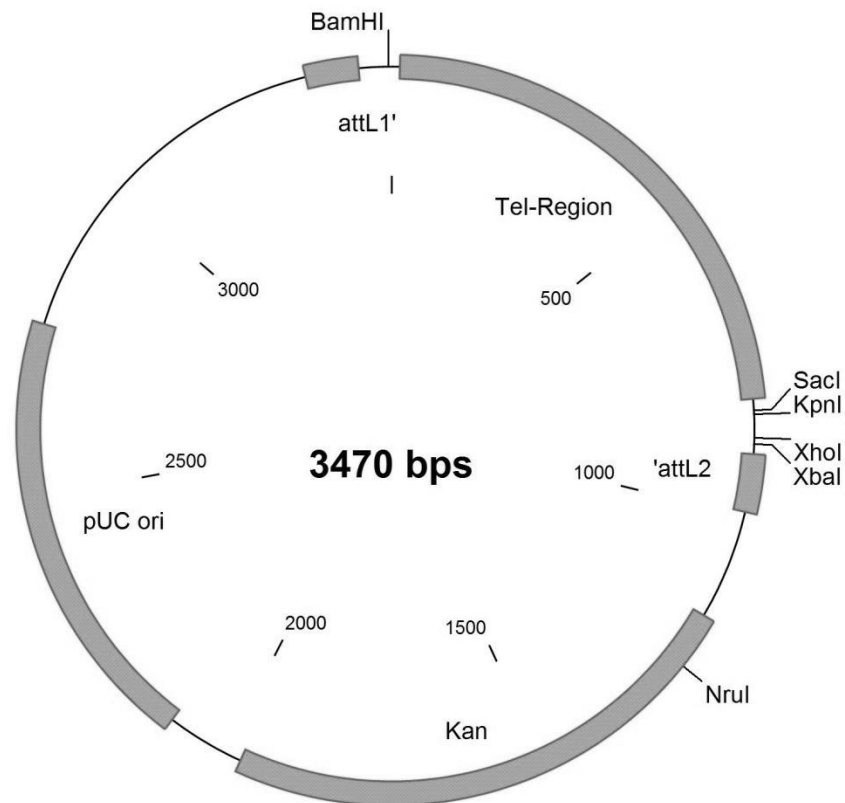


**Figure 10.9.:**

Deletion of hH1 promoter of pENTR/D/hH1 Antisense Tel. Cut of pENTR/D/hH1 Antisense Tel with BamHI and ClaI, fill-in and religation.

#### **10.1. RNA isolation efficiency and RNA quality for TERRA expression analysis:**

Cell pellets of cell lines were produced as described in material and methods. These pellets were used for expression studies.

RNA-isolation by Trizol was done for TERRA expression determination (Figure 10.10.). cDNA, synthesized as described in material and methods were used for Real Time-PCR.

RNA concentration of cell lines with different confluences, isolated by trizol:

Cell line:	ng/μl	total RNA (μg)	260/280	μl/500ng	Cell line:	ng/μl	total RNA (μg)	260/280	μl/500ng
U2OS 35%	91.2	2.7	1.86	5.5	HEK293 FT 10%	62.9	1.9	1.77	7.9
U2OS 70%	201.0	6.0	1.94	2.5	SW480R 80%	1122.9	33.7	2.07	0.5
U2OS 100%	830.0	24.9	2.04	0.6	SW480R 10%	112.9	3.4	1.78	4.4
U2OS 75%	298.4	9.0	1.92	1.7	SW480R 40%	785.6	23.6	2.05	0.6
U2OS 20%	28.5	0.9	1.86	17.5	SW480R 20%	115.1	3.5	1.95	4.4
T98G 100%	696.0	20.9	2.00	0.7	SW480R_2 80%	917.0	27.5	2.11	0.6
T98G 70%	455.5	13.7	1.98	1.1	SW480R 35%	80.3	2.4	1.84	6.2
T98G 35%	106.9	3.2	1.75	4.7	SW480B 75%	577.0	17.3	2.08	0.9
T98G 20%	47.3	1.4	1.79	10.6	SW480B 40%	301.7	9.1	1.91	1.7
Saos2 100%	138.2	4.1	1.92	3.6	SW480B 10%	108.4	3.3	1.96	4.6
Saos2 75%	59.6	1.8	1.92	8.4	SW480B 100%	1010.8	30.3	2.04	0.5
Saos2 30%	49.8	1.5	1.57	10.0	SW480B 35%	51.6	1.5	1.81	9.7
HEK293 95%	1548.8	46.5	2.03	0.3	Caco 100%	4294.1	128.8	1.67	0.1
HEK293 75%	549.5	16.5	2.03	0.9	HT29 70%	3909.8	117.3	1.81	0.1
HEK293 30%	153.5	4.6	2.02	3.3	HCT 116 60%	4592.8	137.8	1.40	0.1
HEK293 10%	73.6	2.2	1.83	6.8	LT97 100%	4549.4	136.5	1.28	0.1
HEK293 FT 60%	442.4	13.3	1.95	1.1	SW620 70%	4140.4	124.2	1.79	0.1
HEK293 FT 90%	1022.2	30.7	2.03	0.5	Vaco 50%	4471.8	134.2	1.40	0.1
HEK293 FT 30%	125.9	3.8	1.80	4.0					

**Table 10.1.: RNA concentration of cell lines with different confluences isolated by trizol:** Concentrations were measured by Nanodrop1000. All samples with a μl/500ng value below 0.5 were diluted 1:10 before use. Percentage show confluences of cell lines

### **10.1.1. Quality check with RNA-Gel:**

28S and 18S bands are clearly visible at the RNA-agarosegel (Figure 10.11.). Smear and slight bands corresponding to 5S rRNAs, tRNAs and mRNAs.

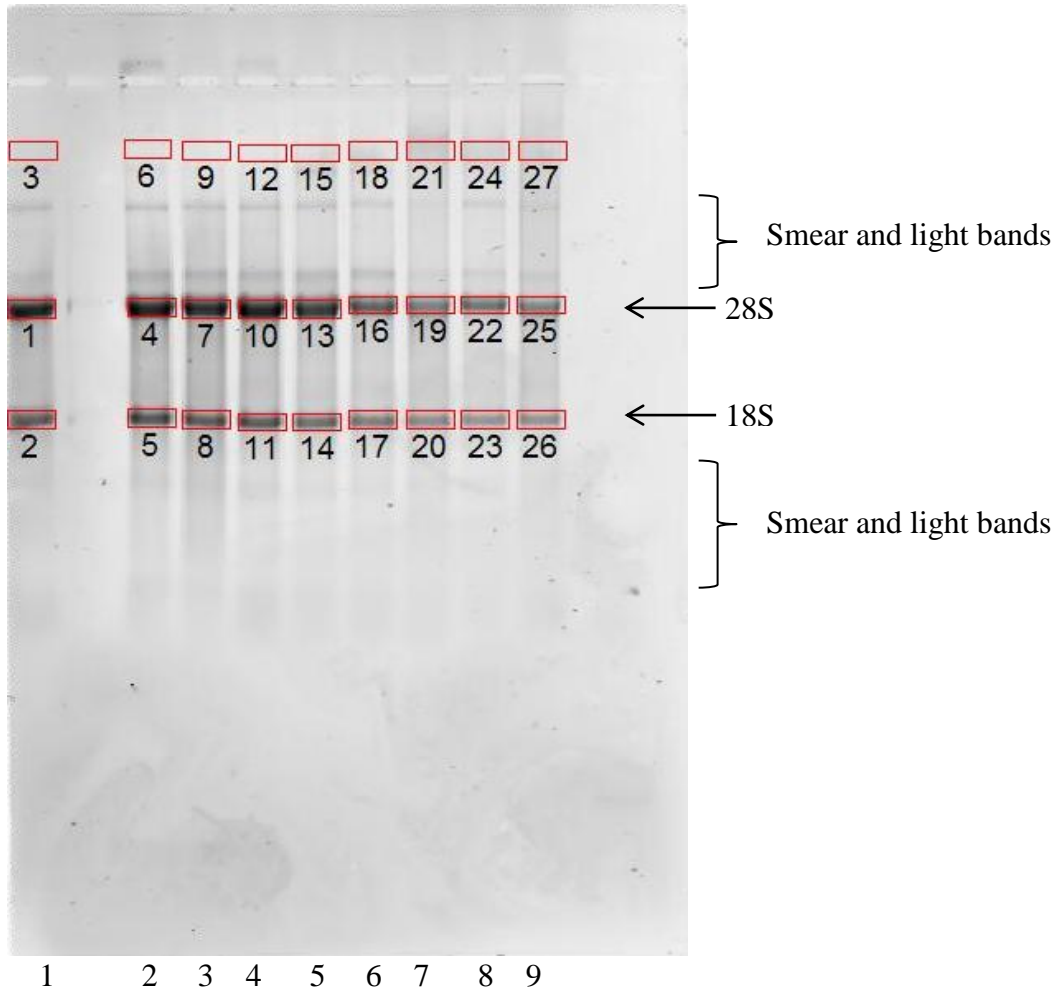


**Figure 10.10.: RNA-agaosegel for quality check-up:**

Denaturing RNA-agarosegel. 28S RNAs and 18S RNAs are visible as two big bands. Ratio should be 1.5-2.5:1

(1)HT29. (2) Caco, (3) Vaco, (4) LT97. (5) HCT116. (6) SW620. (7) T98G 70%, (8) SW480 B 75%, (9) HEK293 FT 90%

All tested RNAs showed a sufficient ratio between 1.5-2:1 of 28S and 18S (Table 10.1.). Because of this they were used for cDNA synthesis and expression studies.

**Table 10.2.:** Ratio between 28S and 18S of RNA-agarosegel

<b>Lane</b>	<b>28S/18S</b>
Lane 1:	2.05
Lane 2:	2.07
Lane 3:	2.01
Lane 4:	2.30
Lane 5:	2.48
Lane 6:	1.90
Lane 7:	1.77
Lane 8:	2.24
Lane 9:	1.88

## **10. References:**

1. Muller H The remaking of chromosomes, *The Collecting Net-Woods Hole*13: 182-98
2. Wellinger RJ, Sen D (1997), The DNA structures at the ends of eukaryotic chromosomes, *Eur J Cancer* 33: 735-49
3. Beltina.org. *Telomere*
4. Blackburn EH (1991), Structure and function of telomeres, *Nature* 350: 569-73
5. Oeseburg H, et al (2010), Telomere biology in healthy aging and disease, *Pflugers Arch* 459: 259-68
6. Griffith JD, et al (1999), Mammalian telomeres end in a large duplex loop, *Cell* 97: 503-14
7. McElligott R, Wellinger RJ (1997), The terminal DNA structure of mammalian chromosomes, *EMBO J* 16: 3705-14
8. Linger BR, Price CM (2009), Conservation of telomere protein complexes: shuffling through evolution, *Crit Rev Biochem Mol Biol* 44: 434-46
9. Ambrus A, et al (2006), Human telomeric sequence forms a hybrid-type intramolecular G-quadruplex structure with mixed parallel/antiparallel strands in potassium solution, *Nucleic Acids Res* 34: 2723-35
10. Mergny JL, Helene C (1998), G-quadruplex DNA: a target for drug design, *Nat Med* 4: 1366-7
11. Dejardin J, Kingston RE (2009), Purification of proteins associated with specific genomic Loci, *Cell* 136: 175-86
12. Liu D, et al (2004), Telosome, a mammalian telomere-associated complex formed by multiple telomeric proteins, *J Biol Chem* 279: 51338-42
13. Bianchi A, et al (1997), TRF1 is a dimer and bends telomeric DNA, *EMBO J* 16: 1785-94
14. Griffith J, et al (1998), TRF1 promotes parallel pairing of telomeric tracts in vitro, *J Mol Biol* 278: 79-88
15. Sfeir A, et al (2009), Mammalian telomeres resemble fragile sites and require TRF1 for efficient replication, *Cell* 138: 90-103
16. Stansel RM, et al (2001), T-loop assembly in vitro involves binding of TRF2 near the 3' telomeric overhang, *EMBO J* 20: 5532-40
17. Amiard S, et al (2007), A topological mechanism for TRF2-enhanced strand invasion, *Nat Struct Mol Biol* 14: 147-54

18. Benetti R, et al (2008), Role of TRF2 in the assembly of telomeric chromatin, *Cell Cycle* 7: 3461-8
19. Li B, de Lange T (2003), Rap1 affects the length and heterogeneity of human telomeres, *Mol Biol Cell* 14: 5060-8
20. Houghtaling BR, et al (2004), A dynamic molecular link between the telomere length regulator TRF1 and the chromosome end protector TRF2, *Curr Biol* 14: 1621-31
21. Ye JZ, et al (2004), TIN2 binds TRF1 and TRF2 simultaneously and stabilizes the TRF2 complex on telomeres, *J Biol Chem* 279: 47264-71
22. Ye JZ, et al (2004), POT1-interacting protein PIP1: a telomere length regulator that recruits POT1 to the TIN2/TRF1 complex, *Genes Dev* 18: 1649-54
23. Xin H, et al (2007), TPP1 is a homologue of ciliate TEBP-beta and interacts with POT1 to recruit telomerase, *Nature* 445: 559-62
24. Wang F, et al (2007), The POT1-TPP1 telomere complex is a telomerase processivity factor, *Nature* 445: 506-10
25. d'Adda di Fagagna F, et al (2003), A DNA damage checkpoint response in telomere-initiated senescence, *Nature* 426: 194-8
26. Herbig U, et al (2004), Telomere shortening triggers senescence of human cells through a pathway involving ATM, p53, and p21(CIP1), but not p16(INK4a), *Mol Cell* 14: 501-13
27. Smogorzewska A, et al (2002), DNA ligase IV-dependent NHEJ of deprotected mammalian telomeres in G1 and G2, *Curr Biol* 12: 1635-44
28. de Lange T (2009), How telomeres solve the end-protection problem, *Science* 326: 948-52
29. Watson JD (1972), Origin of concatemeric T7 DNA, *Nat New Biol* 239: 197-201
30. Hayflick L, Moorhead PS (1961), The serial cultivation of human diploid cell strains, *Exp Cell Res* 25: 585-621
31. Levy MZ, et al (1992), Telomere end-replication problem and cell aging, *J Mol Biol* 225: 951-60
32. de Lange T, et al (1990), Structure and variability of human chromosome ends, *Mol Cell Biol* 10: 518-27
33. Magalhães J. *Sensescence*
34. Karlseder J, et al (2002), Senescence induced by altered telomere state, not telomere loss, *Science* 295: 2446-9

35. Rubio MA, et al (2004), Telomere length mediates the effects of telomerase on the cellular response to genotoxic stress, *Exp Cell Res* 298: 17-27
36. von Zglinicki T, et al (2000), Accumulation of single-strand breaks is the major cause of telomere shortening in human fibroblasts, *Free Radic Biol Med* 28: 64-74
37. Takai H, et al (2003), DNA damage foci at dysfunctional telomeres, *Curr Biol* 13: 1549-56
38. Gire V, et al (2004), DNA damage checkpoint kinase Chk2 triggers replicative senescence, *EMBO J* 23: 2554-63
39. Nabetani A, et al (2004), Localization of hRad9, hHus1, hRad1, and hRad17 and caffeine-sensitive DNA replication at the alternative lengthening of telomeres-associated promyelocytic leukemia body, *J Biol Chem* 279: 25849-57
40. Zou Y, et al (2004), Does a sentinel or a subset of short telomeres determine replicative senescence?, *Mol Biol Cell* 15: 3709-18
41. Guo X, et al (2007), Dysfunctional telomeres activate an ATM-ATR-dependent DNA damage response to suppress tumorigenesis, *EMBO J* 26: 4709-19
42. Shay JW, et al (1991), A role for both RB and p53 in the regulation of human cellular senescence, *Exp Cell Res* 196: 33-9
43. Baur JA, et al (2001), Telomere position effect in human cells, *Science* 292: 2075-7
44. Smogorzewska A, de Lange T (2002), Different telomere damage signaling pathways in human and mouse cells, *EMBO J* 21: 4338-48
45. Prives C, Hall PA (1999), The p53 pathway, *J Pathol* 187: 112-26
46. Chin L, et al (1999), p53 deficiency rescues the adverse effects of telomere loss and cooperates with telomere dysfunction to accelerate carcinogenesis, *Cell* 97: 527-38
47. Fu W, et al (2009), MDM2 acts downstream of p53 as an E3 ligase to promote FOXO ubiquitination and degradation, *J Biol Chem* 284: 13987-4000
48. Schultz LB, et al (2000), p53 binding protein 1 (53BP1) is an early participant in the cellular response to DNA double-strand breaks, *J Cell Biol* 151: 1381-90
49. Lee JH, Paull TT (2005), ATM activation by DNA double-strand breaks through the Mre11-Rad50-Nbs1 complex, *Science* 308: 551-4
50. Misri S, et al (2008), Telomeres, histone code, and DNA damage response, *Cytogenet Genome Res* 122: 297-307
51. Kim NW, et al (1994), Specific association of human telomerase activity with immortal cells and cancer, *Science* 266: 2011-5



52. Greider CW, Blackburn EH (1985), Identification of a specific telomere terminal transferase activity in Tetrahymena extracts, *Cell* 43: 405-13
53. Cohen SB, et al (2007), Protein composition of catalytically active human telomerase from immortal cells, *Science* 315: 1850-3
54. Occidental-College-Los-Angeles. *Action of telomerase*
55. Bryan TM, et al (1997), Evidence for an alternative mechanism for maintaining telomere length in human tumors and tumor-derived cell lines, *Nat Med* 3: 1271-4
56. Cesare AJ, Griffith JD (2004), Telomeric DNA in ALT cells is characterized by free telomeric circles and heterogeneous t-loops, *Mol Cell Biol* 24: 9948-57
57. Nabetani A, Ishikawa F (2009), Unusual telomeric DNAs in human telomerase-negative immortalized cells, *Mol Cell Biol* 29: 703-13
58. Wang RC, et al (2004), Homologous recombination generates T-loop-sized deletions at human telomeres, *Cell* 119: 355-68
59. Pickett HA, et al (2009), Control of telomere length by a trimming mechanism that involves generation of t-circles, *EMBO J* 28: 799-809
60. Henson JD, et al (2009), DNA C-circles are specific and quantifiable markers of alternative-lengthening-of-telomeres activity, *Nat Biotechnol* 27: 1181-5
61. Yeager TR, et al (1999), Telomerase-negative immortalized human cells contain a novel type of promyelocytic leukemia (PML) body, *Cancer Res* 59: 4175-9
62. Murnane JP, et al (1994), Telomere dynamics in an immortal human cell line, *EMBO J* 13: 4953-62
63. Londono-Vallejo JA, et al (2004), Alternative lengthening of telomeres is characterized by high rates of telomeric exchange, *Cancer Res* 64: 2324-7
64. Blagoev KB, Goodwin EH (2008), Telomere exchange and asymmetric segregation of chromosomes can account for the unlimited proliferative potential of ALT cell populations, *DNA Repair (Amst)* 7: 199-204
65. Henson JD, et al (2002), Alternative lengthening of telomeres in mammalian cells, *Oncogene* 21: 598-610
66. Cesare AJ, Reddel RR (2010), Alternative lengthening of telomeres: models, mechanisms and implications, *Nat Rev Genet* 11: 319-30
67. Johnson JE, et al (2005), Multiple mechanisms of telomere maintenance exist in liposarcomas, *Clin Cancer Res* 11: 5347-55
68. Garcia-Cao M, et al (2004), Epigenetic regulation of telomere length in mammalian cells by the Suv39h1 and Suv39h2 histone methyltransferases, *Nat Genet* 36: 94-9

69. Gonzalo S, et al (2006), DNA methyltransferases control telomere length and telomere recombination in mammalian cells, *Nat Cell Biol* 8: 416-24
70. Azzalin CM, et al (2007), Telomeric repeat containing RNA and RNA surveillance factors at mammalian chromosome ends, *Science* 318: 798-801
71. Schoeftner S, Blasco MA (2008), Developmentally regulated transcription of mammalian telomeres by DNA-dependent RNA polymerase II, *Nat Cell Biol* 10: 228-36
72. Nergadze SG, et al (2009), CpG-island promoters drive transcription of human telomeres, *RNA* 15: 2186-94
73. Porro A, et al (2010), Molecular dissection of telomeric repeat-containing RNA biogenesis unveils the presence of distinct and multiple regulatory pathways, *Mol Cell Biol* 30: 4808-17
74. Solovei I, et al (1994), The arrangement and transcription of telomere DNA sequences at the ends of lampbrush chromosomes of birds, *Chromosome Res* 2: 460-70
75. Vrbsky J, et al (2010), siRNA-mediated methylation of Arabidopsis telomeres, *PLoS Genet* 6: e1000986
76. Rhee I, et al (2002), DNMT1 and DNMT3b cooperate to silence genes in human cancer cells, *Nature* 416: 552-6
77. Ng LJ, et al (2009), Telomerase activity is associated with an increase in DNA methylation at the proximal subtelomere and a reduction in telomeric transcription, *Nucleic Acids Res* 37: 1152-9
78. Redon S, et al (2010), The non-coding RNA TERRA is a natural ligand and direct inhibitor of human telomerase, *Nucleic Acids Res* 38: 5797-806
79. Zhang LF, et al (2009), Telomeric RNAs mark sex chromosomes in stem cells, *Genetics* 182: 685-98
80. Marion RM, et al (2009), Telomeres acquire embryonic stem cell characteristics in induced pluripotent stem cells, *Cell Stem Cell* 4: 141-54
81. Chawla R, Azzalin CM (2008), The telomeric transcriptome and SMG proteins at the crossroads, *Cytogenet Genome Res* 122: 194-201
82. Ciaudo C, et al (2006), Nuclear mRNA degradation pathway(s) are implicated in Xist regulation and X chromosome inactivation, *PLoS Genet* 2: e94
83. Schoeftner S, Blasco MA (2010), Chromatin regulation and non-coding RNAs at mammalian telomeres, *Semin Cell Dev Biol* 21: 186-93

84. Isken O, Maquat LE (2008), The multiple lives of NMD factors: balancing roles in gene and genome regulation, *Nat Rev Genet* 9: 699-712
85. Bagasra O, Prilliman KR (2004), RNA interference: the molecular immune system, *J Mol Histol* 35: 545-53
86. Fire A, et al (1998), Potent and specific genetic interference by double-stranded RNA in *Caenorhabditis elegans*, *Nature* 391: 806-11
87. NCBI. *Probe Reagents For Functional Genomics, RNA INTERFERENCE (RNAi)*
88. Kanoh J, et al (2005), Telomere binding protein Taz1 establishes Swi6 heterochromatin independently of RNAi at telomeres, *Curr Biol* 15: 1808-19
89. Ho CY, et al (2008), Telomeres acquire distinct heterochromatin characteristics during siRNA-induced RNA interference in mouse cells, *Curr Biol* 18: 183-7
90. Flynn RL, et al (2011), TERRA and hnRNPA1 orchestrate an RPA-to-POT1 switch on telomeric single-stranded DNA, *Nature* 471: 532-6
91. Caslini C, et al (2009), MLL associates with telomeres and regulates telomeric repeat-containing RNA transcription, *Mol Cell Biol* 29: 4519-26
92. Inoue H, et al (1990), High efficiency transformation of *Escherichia coli* with plasmids, *Gene* 96: 23-8
93. Holmes DS, Quigley M (1981), A rapid boiling method for the preparation of bacterial plasmids, *Anal Biochem* 114: 193-7
94. Invitrogen. *Gateway® Recombination Cloning Technology*
95. Promega. *Technical Manual, Maxwell® 16 DNA Purification Kits*
96. Atlas. *Atlas® Pure Total RNA Labeling System User Manual*
97. O'Callaghan N, et al (2008), A quantitative real-time PCR method for absolute telomere length, *Biotechniques* 44: 807-9
98. von Kanel T, et al (2010), Quantitative 1-step DNA methylation analysis with native genomic DNA as template, *Clin Chem* 56: 1098-106
99. Zahler AM, et al (1991), Inhibition of telomerase by G-quartet DNA structures, *Nature* 350: 718-20
100. Yang D, Okamoto K (2010), Structural insights into G-quadruplexes: towards new anticancer drugs, *Future Med Chem* 2: 619-46
101. ATCC. *CRL-1573™*
102. Geron-Corporation. *Telomerase Inhibitor Drug - Imetelstat (GRN163L)*

103. Sampl S, et al. *Expression of telomeres in astrocytoma WHO grade II to IV: high TERRA level correlates to telomere length and negatively to telomerase activity and advanced clinical stage*